HIGH-ENERGY SCATTERING PROCESSES WITH CUTS IN THE ANGULAR MOMENTUM PLANE

Thesis by

John D. Reichert

In Partial Fulfillment of the Requirements

For the Degree of

Doctor of Philosophy

California Institute of Technology

Pasadena, California

1966

(Submitted July 1, 1965)

ACKNOWLEDGEMENTS

It is a pleasure to thank Dr. Steven Frautschi for his kind interest and his guidance of this work. I am also indebted to my friend, Dr. William G. Wagner, for many helpful discussions and suggestions. I also want to express my appreciation to Miss Yvonne Dawson for typing the manuscript and to my wife Linda, for reading proof. The National Science Foundation and the California Institute of Technology provided financial assistance for this work.

I dedicate this dissertation to Linda for all the many things she has done to make my life more pleasant, to Dad, Mother, and David for their continuing faith and encouragement, to Judge and Dot for their interest and their daughter, and to Mrs. Edna Boon, Dr. Kuan Sun, and Dr. Wilson Stone for their help along the way and their continuing inspiration.

ABSTRACT

The experimental consequences of Regge cuts in the angular momentum plane are investigated. The principle tool in the study is the set of diagrams originally proposed by Amati, Fubini, and Stanghellini. Mandelstam has shown that the AFS cuts are actually cancelled on the physical sheet, but they may provide a useful guide to the properties of the real cuts. Inclusion of cuts modifies the simple Regge pole predictions for high-energy scattering data. As an example, an attempt is made to fit high energy elastic scattering data for pp, $\bar{p}p$, $\pi^{\pm}p$, and $K^{\pm}p$, by replacing the Igi pole by terms representing the effect of a Regge cut. The data seem to be compatible with either a cut or the Igi pole.

TABLE OF CONTENTS

I. INTRODUCTION

In a lecture several years ago when Regge pole theory was new, Professor Richard Feynman stated that, on the basis of his knowledge of the cuts present in field theory, he believed there must be cuts in the angular momentum plane. As he put it,"the cuts are not going to go away just because we now choose to view the world through a piece of twisted, colored glass."

It appeared in 1962 that these cuts had been explicitly found in the multiperipheral model of Amati, Fubini, and Stanghellini[1]. This model put the inelastic scattering amplitude in the form of a Regge pole. The effects of elastic scattering were then estimated by iterating this pole in a unitarity equation. Diagrams of the form

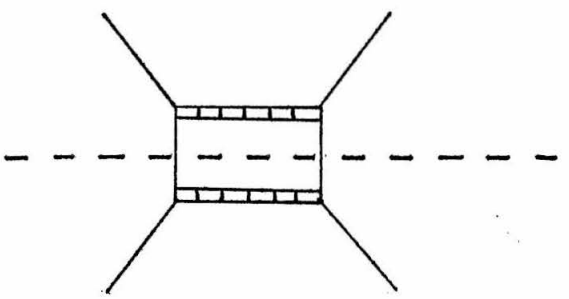

Two particle unitarity cut ,

when evaluated using only the unitarity condition for two particle intermediate states, give rise to a term of the type characteristic of a cut in the angular momentum plane.

Mandelstam[2] has shown, however, that the cut from this diagram is not on the physical sheet of the angular momentum plane. Mandelstam actually considered diagrams of the form

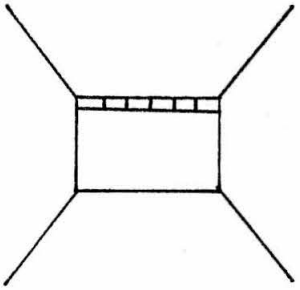

Such diagrams also indicate a cut in the angular momentum plane when only two particle unitarity cuts are considered. Mandelstam chopped up these diagrams with all possible unitarity cuts through the rungs of the ladder. The resulting mincemeat led to explicit cancellation of the terms which had indicated a cut in the angular momentum plane, i.e., the discontinuity across the cut is zero. This result was confirmed by Polkinghorne[3] from a study of Feynman integrals in field theory.

Even though the diagrams proposed by Amati, Fubini, and Stanghellini failed to give a cut on the physical sheet, they offered a clue to the mechanism by which physical cuts might arise. Using this clue, Mandelstam[2] proposed a study of diagrams of the form

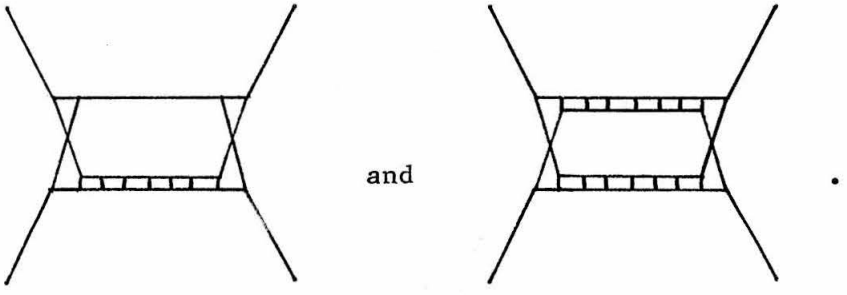

The third double spectral function, A_{tu}, is non-zero for these diagrams. Mandelstam[2] and Polkinghorne[3] both demonstrated that these diagrams produce a moving cut on the physical sheet of the

angular momentum plane, and furthermore, that the position of the branch point coincided with the "unphysical" branch point found by Amati, Fubini, and Stanghellini (AFS).

Mandelstam has an independent argument for the existence of a cut. When the third double spectral function is non-zero, Gribov and Pomeranchuk[6] have demonstrated the existence of essential singularities in the partial wave amplitudes at $\ell = -1, -2, ---$. A crisis arises if the total spin, J, includes intrinsic spin in addition to ℓ. The essential singularity at $\ell = -1$ may rise to $J = 0$ or 1 or even higher, violating the Froissart[7] limit. The presence of a cut in the angular momentum plane allows the essential singularities to pass onto an unphysical sheet before violating the Froissart limit. Thus Mandelstam argues that a cut is actually needed in the theory.

At the moment the cuts seem to be well established as part of a Regge pole theory. Since pole models have had considerable difficulty giving a detailed fit to the available high-energy scattering data, it is of interest to examine physical consequences of the evidence of Regge cuts. Gatland and Moffat[8] have attempted to fit the pp, $\bar{p}p$, $\pi^+ p$, and $\pi^- p$ scattering data at small momentum transfer, t, with expressions of the form

$$\frac{d\sigma}{dt} = \left| g(t) \left(\frac{s}{s_0}\right)^{\alpha_p(t) - 1} + \frac{f(t)}{\log \frac{s}{s_0}} \right|^2 .$$

Granted the freedom of obtaining g(t), $\alpha_p(t)$, and f(t) from the data, this model can give qualitative agreement with the data. A fixed cut

was used in order to simplify the expressions. Although this approach is purely phenomenological, the results do suggest that it is worthwhile to devote one's attention to the experimental consequences of Regge cuts.

A similar form was used by Freund and Oehme[9] in a comparison with the data. They took expressions of the form

$$\frac{d\sigma}{dt} = \left| g(t) \left(\frac{s}{s_0}\right)^{\alpha(t) - 1} + i\, f(t) \left(\log \frac{s}{s_0}\right)^{\beta} \right|^2$$

and obtained results very similar to those of Gatland and Moffat. A fixed cut was used because of an analogy with vector particle exchange in non-relativistic scattering. This also was a phenomenological approach. Further discussion of the experimental situation and various models has been given by Stanghellini[10].

One point of theoretical interest might be kept in mind. It is entirely possible that the so-called "Igi pole"[11] may not be a necessary part of Regge pole theory. The presence of contributions from cut terms might easily be interpreted as evidence of another Regge pole. Igi and Teplitz[12] have suggested a possible way to distinguish between a cut and a pole as the second singularity. If one could measure the polarization of the recoiling proton in πp scattering, then one could see if the maximum of $P\, d\sigma/dt$ occurs for $|t|$ smaller or larger than the width of the diffraction peak. Igi and Teplitz show that the pole + pole case gives the maximum at $|t|$ less than the width, whereas the pole + cut case puts the maximum farther out than the peak width. At present one is unable to perform the necessary

experiments to make this test.

A large portion of the motivation for the introduction of the Igi pole would be removed if one could fit the data with a less phenomenological model for the cuts. This was one of the objectives of this study. Although we did not succeed in obtaining a satisfactory detailed fit to the data, the two pole + cut model we used could fit the data as well as a similar model using three poles but no cuts. To our way of thinking, even this might be interpreted as a strong indication that the necessity for using the Igi pole is not clear.

Desiring to use a model for cuts that arise naturally from theoretical considerations, one encounters some difficulty. The cuts considered by Mandelstam and Polkinghorne are very difficult to handle. The evaluation of a series of such terms is completely beyond one's grasp at the present state of the art. It is necessary, therefore, to find some other way to consider the cuts. One such possibility is to try to make use of the fact that the cuts from Mandelstam's diagrams coincide with the AFS cuts. One would then say that the diagram

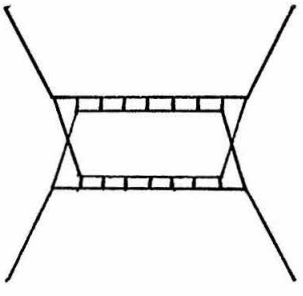

may be evaluated approximately by replacing the pairs of crossed lines by single lines of appropriate "effective mass" and using two particle unitarity cuts. Moving cuts in the angular momentum plane would then

be found, and at the correct locations. The weights of the cut terms would probably not be correctly related to the weight of the Regge pole term, but at least we would have a simple guess for them.

Since a two particle unitarity technique appears to be the only simple way to approach the subject theoretically, we undertake a study of the implications of such a model. Such a procedure is, at worst, less phenomenological than previous models have been. Our cut terms will have no free, adjustable parameters other than those of the pole itself.

The technique is essentially that originally suggested by Amati, Fubini, and Stanghellini. We have extended their considerations and attempted to fit the data. Our point of view is somewhat different, however, because Amati, Fubini, and Stanghellini considered the iterated pole diagrams to be an approximation for the elastic-intermediate-state part of the unitarity condition. We, on the other hand, consider these terms to be a crude approximation for the Mandelstam diagrams, which belong to the inelastic intermediate state part of the unitarity condition. This distinction is discussed in Section VI.

In the course of this work, we found that the bound set by S-wave inelastic unitarity was a very troublesome condition for our model. It was precisely this bound that made a satisfactory, detailed data fit impossible for us. It can be shown by an argument due to Mandelstam that this failure can be traced back to a deficiency in the Amati, Fubini, Stanghellini viewpoint. Since Mandelstam has shown that

the AFS cuts are cancelled by equal but opposite terms arising from multiparticle unitarity cuts through the rungs of the ladders, then it follows that it is conceptually necessary to have AFS type diagrams as well as poles in the multiparticle part of the unitarity condition. It follows therefore, that an iteration scheme starting with a pole approximation to the multiparticle part is not really appropriate. Such a procedure overestimates the multiparticle part and thus can lead to a divergence in the iteration. As will be clear later from our work, an iteration starting from pole term minus AFS cut terms will lead to a different series of terms, whose convergence is guaranteed, provided, not that the pole term alone satisfies the S-wave inelastic unitarity condition, but rather that the pole term minus AFS cut terms satisfies the condition. Numerically speaking, if we attempt to ignore cuts altogether and fit the existing data with pole terms alone, then parameters are required which would force the sum of these pole terms to violate the S-wave inelastic unitarity condition by 20 to 70%. This shows clearly that the AFS cut terms make a large contribution to the inelastic part in the unitarity condition. Thus, the cut model we have constructed, ignoring these contributions, is not really appropriate and forces artificial divergences in the iteration. We did find, however, that if we were to attempt to bypass this difficulty, chopping off the AFS series after one iteration and interpreting the resulting term as a "phenomenological" term without free parameters, then we could, in fact, obtain a detailed fit to the pp, $\bar{p}p$, $K^{\pm}p$, $\pi^{\pm}p$ data of Foley et al.[16] that was as good as the three-pole fit of Desai and Binford[17]. Thus, in spite of our difficulties, it is possible that the Igi pole effects are really manifestations of a cut.

Although the model we are using may not be reliable for detailed data fitting, it appears to be the only simple approach that one can make to the properties of the physical cuts in the angular momentum plane. Many of the conclusions that follow from a study of this model will very likely hold for the Mandelstam cuts also. As we discuss our model in the following sections we also attempt to gain insight into the Mandelstam diagrams and to unravel some of their complex properties.

In Section II we discuss the iteration procedure and consider the location of some of the branch points for cuts arising from the iterations. We also indicate why the resulting amplitudes imply cuts in the angular momentum plane. The evaluation of certain phase space integrals is discussed in Appendix A.

In Section III we obtain explicit expressions for the amplitudes arising from the iteration and sum these terms to obtain an approximate amplitude which includes the cut terms.

Then in Section IV we survey the implications of cut terms in the far asymptotic region. We discuss possible modifications of the Pomeranchuk theorems when one includes the effects of cut terms along with the Regge poles.

Section V is devoted to a discussion of the line reversal symmetry of Regge pole terms and of the iterated Regge pole amplitudes arising in our model. We also attempt to see if diagrams of the type discussed by Mandelstam possess a line reversal symmetry.

Finally, in Section VI we discuss our attempt to fit high-energy scattering data with a two pole + cut model. The implications of partial wave unitarity for our work and for fits using only Regge poles are also discussed.

II. ITERATION PROCEDURE AND LOCATION OF THE CUTS

It appears that there are very many cuts in the angular momentum plane. In fact, it seems that this plane is quite literally "cut to pieces". In this section we consider the location of some of these cuts. Also certain features of the iteration procedure are illustrated here and in Appendix A. The principle result of this section is that, for any shape of the Regge trajectories, it is true that for any value of $t < 0$, the tops of the cuts approach a constant value (horizontal line) over the range from t to zero as more and more Pomeranchons are exchanged. The case of linear trajectories is discussed in detail in order to furnish bounds for the positions of the cuts.

We consider the position of cuts in the angular momentum plane for negative t and large positive s. As stated above, we shall do this within the framework of the two particle unitarity relations. For the considerations of this section, we ignore the spin of the external particles.

In our notation

$$\sigma_{tot} = \frac{\sqrt{r}\, A(s,0)}{s} \quad \text{and} \quad \frac{d\sigma}{dt}(s,t) = \frac{r|T(s,t)|^2}{16\pi\, s^2}\,, \qquad \text{(II.1)}$$

where

$$T \equiv D(s,t) + iA(s,t) \qquad \text{(II.2)}$$

and

$$r \equiv \frac{s}{s_0} \approx 1\,, \qquad \textit{(II.3)}$$

where $\frac{1}{2}\sqrt{s_0} = k$ is the center of mass momentum of the incident particle. The unitarity condition is

$$\text{Im } T(s,t) = \tfrac{1}{2} \sum_{\substack{n \\ \text{intermediate} \\ \text{particles}}} \frac{2\pi\delta(E - E_n)\ T^{I}(s,t_1)\ T^{II}(s,t_2)}{\Pi\ (2\omega_i)} \qquad \text{(II.4)}$$

This gives, after a little algebra,

$$\text{Im } T(s,t) \equiv A(s,t) = \frac{1}{64\pi^2\sqrt{r}} \int d\Omega\ T^{+}_{\text{elastic}}(s,t_1)\ T_{\text{elastic}}(s,t_2) + A_{in}(s,t) \qquad \text{(II.5)}$$

where

$$A_{in}(s,t) = \sum \frac{\pi\ T^{+}_{\text{inelastic}}(s,t_1)\ T_{\text{inelastic}}(s,t_2)\ \delta(E-E_n)}{\Pi_i\ (2\omega_i)} \quad . \qquad \text{(II.6)}$$

The quantity $A_{in}(s,t)$ is just the imaginary part of the inelastic terms in the amplitude. In our approach we approximate this function by the imaginary part of the Regge pole terms. Our procedure is to iterate Eq. (II.5) using $A_{in}(s,t)$ as a first approximation for T_{el}. Such a procedure presumes that we consider s large enough that the amplitude is predominantly inelastic and almost purely imaginary. We discuss the consistency of this approach in later sections.

The real part of the scattering is to be determined from a dispersion relation such as

$$D(s,t) \approx \frac{1}{\pi} \int_{\text{threshold}}^{\infty} \frac{A(z,t)}{z - s}\ dz + \frac{I}{\pi} \int_{\text{threshold}}^{\infty} \frac{A(z,t)}{z + s}\ dz\,, \qquad \text{(II.7)}$$

where τ is a signature factor and represents the symmetry of $A(z,t)$ under reversal of the sign of z. In Section V we consider this signature factor in detail for various cases. We find, for example, that τ is always + 1 for the iteration of Pomeranchons. A subtracted dispersion relation, based on Eq. (II.7), will be used as necessary.

This iteration procedure would allow one to start with a model for the inelastic amplitude and estimate the elastic amplitude. We, however, use this procedure as a device to approximate the inelastic amplitude corresponding to diagrams with cuts in the physical angular momentum plane. This point receives consideration in Section VI.

First, consider a diagram for the exchange of only two Reggeons, P and R:

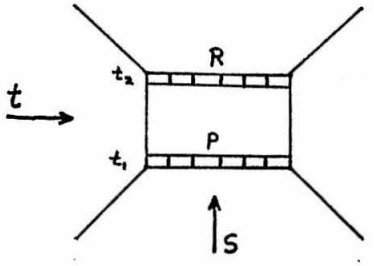

We write the amplitude for this diagram in the form

$$T^{(2)}(s,t) = D^{(2)}(s,t) + iA^{(2)}(s,t) \ . \qquad \text{(II.8)}$$

From Eq. (II.5) we write

$$A^{(2)}(s,t) = \frac{1}{64\pi^2\sqrt{r}} \left(\frac{4}{s_0}\right) \int_{-s_0}^{o}\int dt_1 dt_2 \ \tau(t,t_1,t_2) \ T_R^{(1)*}(s,t_2) \ T_P^{(1)}(s,t_1) \ , \qquad \text{(II.9)}$$

where

$$\tau(t,t_1,t_2) = \frac{\textcircled{\neq}}{\sqrt{-\ t^2 - t_1^{\ 2} - t_2^{\ 2} + 2tt_1 + 2tt_2 + 2t_1t_2 + \frac{4}{s_0}\ tt_1t_2}} \ , \qquad \text{(II.10)}$$

with $\oplus$ being 1 or 0 depending upon whether the radicand is positive or negative. $\tau(t,t_1,t_2)$ is symmetric in t, t_1, and t_2 and is often called a "triangle function" [1,26], since asymptotically it is non-zero only if a triangle exists with sides of lengths $\sqrt{|t|}$, $\sqrt{|t_1|}$, and $\sqrt{|t_2|}$. These functions and their properties are discussed in some detail in Appendix A.

Ignoring certain factors which have no bearing on the present considerations, we write for large s:

$$T_R^{(1)} = C_R(t_2)\, s^{\alpha_R(t_2)} \quad \text{and} \quad T_P^{(1)} = C_P(t_1)\, s^{\alpha_P(t_1)} . \qquad \text{(II.11)}$$

One then obtains

$$A^{(2)}(s,t) \approx \frac{(4\sqrt{r})}{64\pi^2} \int_{-\infty}^{0}\!\!\int dt_1 dt_2\; \tau(t,t_1,t_2)\; C_R(t_2)\; C_P(t_1)\; s^{\alpha_P(t_1)+\alpha_R(t_2)-1} . \qquad \text{(II.12)}$$

Performing a dispersion integral on Eq. (II.12) yields the real part, $D^{(2)}(s,t)$. Thus, one obtains the form

$$T^{(2)}(s,t) = \int_{-\infty}^{0}\!\!\int_{-\infty}^{0} dt_1 dt_2\; G(t_1,t_2)\; \tau(t,t_1,t_2)\; s^{\alpha_P(t_1)+\alpha_R(t_2)-1} . \qquad \text{(II.13)}$$

The form of this equation is indicative of a cut in the angular momentum plane.

Before discussing the position of the cut, we shall indicate briefly the connection between this equation and the angular momentum plane by considering a crude example[8]. Presume that the partial wave amplitude obeys a dispersion relation in the α-plane for fixed t.

$$T(t,\alpha) = \sum_i \frac{r_i(t)}{\alpha - \alpha_i(t)} + \frac{1}{\pi} \int_{cut} \frac{d\alpha' \, A(t,\alpha')}{\alpha' - \alpha} \quad .$$

Presume for convenience that $T(t,\alpha) \to 0$ as $|\alpha| \to \infty$ and there is a cut in the angular momentum plane lying on the real axis from $\alpha_{min}(t)$ to $\alpha_{max}(t)$. For convenience, take $-1 < \alpha_{min}(t) \leqslant 0$.

Following the Regge procedure[13], consider the function $F(t,\alpha) = T(t,\alpha)\, P_\alpha(-\cos\theta_t)/\sin\pi\alpha$. This function is analytic within the contour C and there are Regge poles at $\alpha_i(t)$ and poles from $\sin\pi\alpha$ at integral values of α and the cut mentioned above:

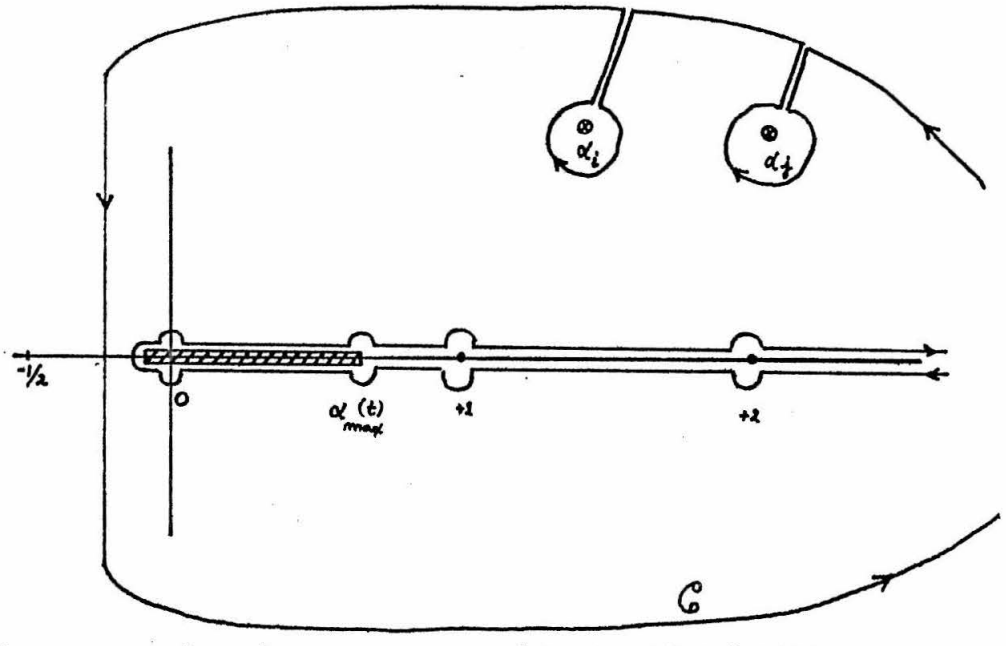

Since the contour is taken so as to enclose no singularities,

$$\oint_C F(t,\alpha)\, d\alpha = 0.$$

Then for large s, i.e., neglecting contributions from the semicircle and the vertical line, we get

$$T(s,t) \equiv \sum_{\ell} (-)^{\ell} T_{\ell}(t)\, P_{\ell}(-\cos\theta_t) = -\pi \sum_{i} \frac{r_i(t)\, P_{\alpha_i(t)}(-\cos\theta_t)}{\sin \pi\, \alpha_i(t)} +$$

$$+ \mathcal{P} \int_{\alpha_{min}(t)}^{\alpha_{max}(t)} d\alpha\, [\mathrm{Im}\, T(t,\alpha)]\, \frac{P_{\alpha}(-\cos\theta_t)}{\sin \pi\, \alpha} \qquad \text{(II.14)}$$

where, for this example, we take $T^{*}(t,\alpha) = T(t,\alpha^{*})$ and thus $A(t,\alpha) = \mathrm{Im}\, T(t,\alpha)$. Now $\cos\theta_t = 1 + 2s/(t-4)$, so as $s \to \infty$ we have $P_{\alpha}(-\cos\theta_t) \approx B(\alpha)\, s^{\alpha}$ and therefore,

$$T(s,t) \approx \sum_{i} \frac{\beta_i(t)\, s^{\alpha_i(t)}}{\sin \pi\, \alpha_i(t)} + \mathcal{P} \int_{\alpha_{min}(t)}^{\alpha_{max}(t)} \left\{ \frac{B(\alpha)\, [\mathrm{Im}\, T(t,\alpha)]}{\sin \pi\, \alpha} \right\} s^{\alpha}\, d\alpha \qquad \text{(II.15)}$$

where $\beta_i(t) \equiv -\pi\, r_i(t)\, B(\alpha_i(t))$. Now Eq. (II.15) gives $T(s,t)$ in terms of contributions from Regge poles (the discrete sum) and contributions from a Regge cut (the integral). We may now observe that $T^{(2)}(s,t)$, given by Eq. (II.13), is of the same form as the contribution of a Regge cut exhibited in Eq. (II.15). This is made more evident if Eq. (II.13) is written in the form

$$T^{(2)}(s,t) = \int_{\alpha_{min}(t)}^{\alpha_{max}(t)} \left\{ \int_{-\infty}^{0}\int_{-\infty}^{0} dt_1 dt_2\, G(t_1,t_2)\, \tau(t,t_1,t_2) \cdot \right.$$

$$\left. \cdot\, \delta\left[\alpha - (\alpha_P(t_1) + \alpha_R(t_2) - 1)\right] \right\} s^{\alpha}\, d\alpha \qquad \text{(II.16)}$$

where $\alpha_{min}(t)$ and $\alpha_{max}(t)$ are the extreme values of α for which the δ-function may be satisfied.

We shall be interested in $\alpha_{max}(t)$ because it determines the asymptotic dependence of the cut contribution. To attempt to estimate the effects of the cut one might integrate by parts repeatedly in Eq. (II.15) to obtain

$$T(s,t) = \sum_i \frac{\beta_i(t)\, s^{\alpha_i(t)}}{\sin \pi \alpha_i(t)} + \left[\frac{s^{\alpha}}{\log s} \sum_{n=0}^{\infty} (-)^n \frac{Q^{(n)}(t,\alpha)}{(\log s)^n} \right]_{\alpha_{min}(t)}^{\alpha_{max}(t)} \tag{II.17}$$

where

$$Q^{(0)}(t,\alpha) \equiv \frac{B(\alpha)[\operatorname{Im} T(t,\alpha)]}{\sin \pi \alpha}$$

and

$$Q^{(n)}(t,\alpha) = \left(\frac{\partial}{\partial \alpha}\right)^n Q^{(0)}(t,\alpha).$$

The strongest contribution from the cut then appears to be the term of the form

$$\frac{s^{\alpha_{max}(t)}}{\log s}\, Q^{(0)}(t,\, A_2(t)), \tag{II.18}$$

which is weaker than the contribution of a Regge pole (at the same α) by the factor $1/\log s$. Estimating the effect of the cut by this procedure is clearly a risky business. The effect of the cut is considered in greater detail in the next section by explicitly evaluating the integrals that occur in the iteration of Eq. (II.5). We refer to $\alpha_{max}(t)$ as the "top of the cut". This is convenient if one has the Re α vs. t plane in mind.

Now let us consider the top of the cut in the angular momentum plane implied by Eq. (II.13) or (II.16). From the discussion

above we have that

$$\alpha^{(2)}_{max}(t) = \underset{t_1,t_2}{\text{Max}} \left\{ \alpha_P(t_1) + \alpha_R(t_2) - 1 \;\middle|\; \sqrt{|t|}, \sqrt{|t_1|}, \sqrt{|t_2|} \text{ form a triangle} \right\}. \tag{II.19}$$

The superscript on $\alpha_{max}(t)$ indicates that α_{max} corresponds to a cut involving two Reggeons. $\alpha^{(2)}_{max}(t)$ certainly depends upon the shape of the trajectories $\alpha_P(t)$ and $\alpha_R(t)$.

Before discussing trajectories of very general shape, we shall consider only linear trajectories. Conclusions based upon linear trajectories may be used as bounds for the behavior under more general conditions. If we take

$$\alpha_P(t) = a_P + p_P t \text{ and } \alpha_R(t) = a_R + p_R t,$$

where $a_P \leqslant 1$, $a_R \leqslant 1$, $p_P \geqslant 0$, and $p_R \geqslant 0$ are constants, we easily obtain from Eq. (II.19)

$$\alpha^{(2)}_{max}(t) = a^{(2)} + p^{(2)} t$$

where

$$a^{(2)} = a_P + a_R - 1 \text{ and } p^{(2)} = \frac{p_P\, p_R}{p_P + p_R} = \left[\frac{1}{p_P} + \frac{1}{p_R} \right]^{-1}.$$

Thus, we find that $\alpha^{(2)}_{max}(t)$ is linear in t*. Notice that the slope of $\alpha^{(2)}_{max}(t)$ may be obtained by taking the harmonic sum of the slopes of the two pole trajectories. We use the notation

---

* This linearity holds only at large s, because we have ignored the term $(4/s_0)tt_1t_2$ in the τ-function. This point receives elaboration in Appendix A.

$$\langle p_1, p_2, \ldots, p_n \rangle_{HS} \equiv \left[\frac{1}{p_1} + \frac{1}{p_2} + \ldots + \frac{1}{p_n} \right]^{-1} .$$

Thus slopes add like resistors in parallel or like the combining of masses to obtain a reduced mass. It is clear that

$$\alpha^{(2)}_{max}(0) \leqslant 1$$

since $a_P \leqslant 1$ and $a_R \leqslant 1$.

The situation is now very simple. If this cut term is iterated in Eq. (II.5) with another Reggeon, Q, one will obtain for the new cut

$$\alpha^{(3)}_{max}(t) = a^{(3)} + p^{(3)} t$$

where

$$a^{(3)} = a^{(2)} + a_Q - 1 = a_P + a_R + a_Q - 2$$

and

$$p^{(3)} = \frac{p^{(2)} p_Q}{p^{(2)} + p_Q} = \langle p^{(2)}, p_Q \rangle_{HS} = \langle p_P, p_R, p_Q \rangle_{HS} .$$

We may now write down the position of the cut resulting from the exchange of n Reggeons for this simple case of linear trajectories. Taking

$$\alpha_i(t) = a_i + p_i t, \quad i = 1, 2, \ldots, n$$

with $a_i \leqslant 1$ and $p_i > 0$, we obtain

$$\alpha^{(n)}_{max}(t) = \left[\left(\sum_{i=1}^{n} a_i \right) - (n - 1) \right] + \langle p_1, p_2, \ldots, p_n \rangle_{HS} t. \quad \text{(II.20)}$$

The derivation of this equation is given in more detail in Appendix B. We see that $\alpha^{(n)}_{max}(0)$ is less than or equal to the largest of the a_i. The equality holds only if each $a_i = 1$, i.e., each Reggeon is a Pomeranchon. The slope of $\alpha^{(n)}_{max}(t)$ is less than the least of the p_i.

As a special case of (II.20), for the exchange of n Pomeranchons with $\alpha_P(t) = 1 + p_P t$ we find $\alpha^{(n)}_{max}(t) = 1 + (p_P/n)t \to 1$ as $n \to \infty$. Similarly, for the exchange of n Pomeranchons and another Reggeon, R, with $\alpha_R(t) = a_R + p_R t$, we find

$$\alpha^{(n+1)}_{max}(t) = a_R + \frac{p_P\, p_R}{n\, p_P + p_R}\, t \to a_R \text{ as } n \to \infty .$$

For comparison with (II.20), suppose that we allow the exchange of poles of fixed spin, σ_i, i.e., diagrams like

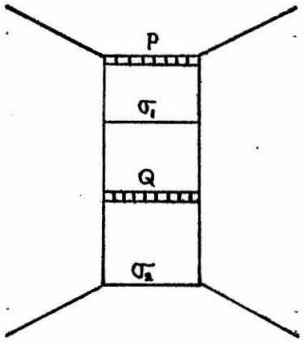

We then obtain, for (n - m) Reggeons and m fixed spin poles

$$\alpha^{(n,m)}_{max}(t) = \sum_{i=1}^{n-m} \alpha_i(0) + \sum_{i=1}^{m} \sigma_i - (n - 1) = \text{const!} \qquad \text{(II.21)}$$

This function is independent of t. It is easy to understand why this occurs in the case of linear trajectories, because the harmonic sum of zero with other numbers is zero. The expression (II.21) holds also

for non-linear Regge trajectories such that $\alpha_i(t) \leq \alpha_i(0)$ because the triangle conditions may be satisfied by Eq. (II.21) for any value of t. We see, as expected, that the exchange of fixed spin poles can lead to a violation of the Froissart limit[7].

Considering only exchanges of Reggeons, we find from (II.20) that the cuts come up higher and higher as more and more Pomeranchons are exchanged. Suppose, for example, that a certain scattering process requires the Reggeon, R, to transfer quantum numbers. For a diagram such as

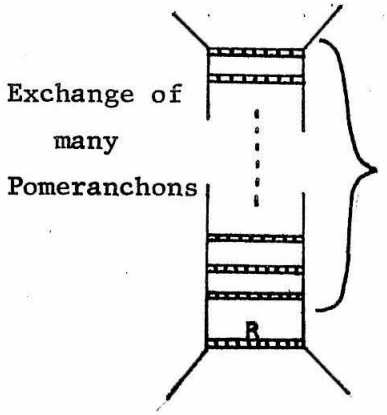

we, find say,

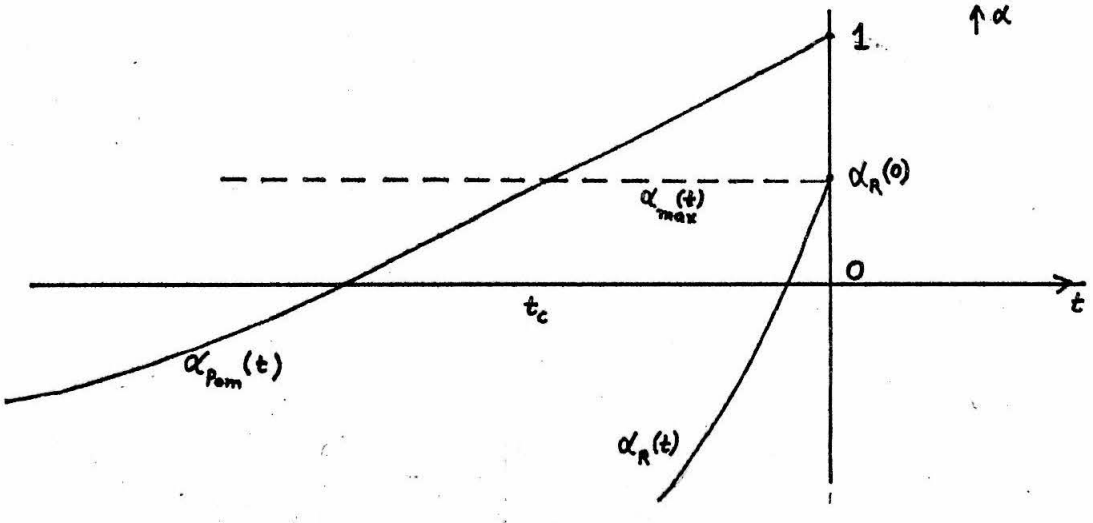

For $t < t_c$, we may expect the cut contribution to be dominant for large enough s in this simple model. We reserve extended consideration of this subject for Section III.

We now consider trajectories of a more general shape. It is commonly believed[14] that Regge trajectories are characteristically concave monotonically rising functions of t for $t < 0$, with finite slope at $t = 0$. Under these conditions we have $\alpha_i''(t) \geq 0$ for all $t < 0$ and $\alpha_i'(t)$ finite at $t = 0$. Since such trajectories lie entirely above the line

$$\alpha_i(0) + \alpha_i'(0)\, t \ ,$$

then the top of the cut,

$$\underset{t_i}{\text{Max}} \left\{ \alpha_1(t_1) + \alpha_2(t_2) + \ldots + \alpha_n(t_n) - (n-1) \,\middle|\, \text{triangle conditions} \right\}$$

must lie above the result (II.20) obtained for linear trajectories. Thus for all $t < 0$ we have the lower bound

$$\alpha_{\max}^{(n)}(t) \geq \left[\left(\sum \alpha_i(0) \right) - (n-1) \right] + \langle \alpha_1'(0), \alpha_2'(0), \ldots, \alpha_n'(0) \rangle_{HS} t \ . \tag{II.22}$$

One now can easily show, using lines of positive slope for upper bounds for the Reggeon trajectories, that, for any fixed $t < 0$,

$$\alpha_{\max}^{(n)}(t) \to 1 + [\alpha_1(0) + \alpha_2(0) + \ldots + \alpha_n(0) - n]. \tag{II.23}$$

Over the whole range from t to zero as $n \to \infty$. Thus, we see, in particular, that for concave, monotonically rising trajectories, just as for linear trajectories, the highest cut approaches a horizontal

line as more and more Pomeranchons are exchanged.

Actually, the exchange of a great many Pomeranchons leads to a horizontal line, regardless of the shape of the trajectories, provided that

1. $\alpha'_{\text{Pom}}(0)$ is finite (or at least $\alpha'_{\text{Pom}}(t)$ does not diverge too strongly as $t \to 0$);

2. for each trajectory,

$$\alpha_i(t) \leqslant \alpha_i(0) \text{ for all } t < 0.$$

This is demonstrated in Appendix B.

III. CONTRIBUTIONS OF THE CUTS TO THE SCATTERING AMPLITUDE*

In the preceding section the location of cuts in the angular momentum plane was discussed. In this section we consider the contribution of some of these cuts in the scattering amplitude. In order to obtain explicit expressions, we presume linear Regge trajectories and take an exponential form for the t-dependent "coupling coefficients". Since we are interested in the asymptotic region we may take advantage of the fact that the elastic-scattering amplitude is almost purely imaginary in this region. We, therefore, use Eq. (II.5) and iterate only the absorptive part of the amplitude. A check on the consistency of this model is presented below.

For the absorptive part resulting from a single Regge pole exchange we take

$$A^{(1)}(s,t) = \sqrt{16\pi}\ \tau\ C(t) \left(\frac{s}{\sigma_0}\right)^{\alpha(t)}, \qquad \text{(III.1)}$$

where τ is the signature of the Reggeon and σ_0 is a scaling parameter which is often thought to be of the order of magnitude, $1(\text{BeV})^2$. Actually σ_0 will depend upon the specific process considered. The function $C(t)$ might be called the "coupling coefficient" since it depends upon the particles to which the Reggeon is coupled**. In the

---

* After the completion of this work, it was brought to the author's attention that the principal results of this section had already been obtained by Amati, Cini, and Stanghellini by essentially the same techniques. For their discussion of this work, see references (10, 15).

** It is this function that contains spin and isospin information when these matters are considered.

following we take the specific form for the Reggeon R:

$$C_R(t) = \gamma_R \, \sigma_{0R} \, e^{b_R t} \quad . \tag{III.2}$$

First, let us consider the contribution of a cut resulting from the iteration of two Reggeons. The diagram under consideration is

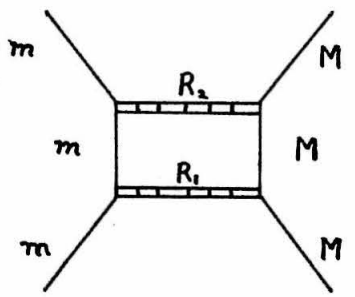

where m and M denote the masses of the corresponding particles. For this diagram we have

$$s_0 = s - 2(m^2 + M^2) + \frac{[m^2 - M^2]^2}{s} \quad , \tag{III.3}$$

and we take

$$\alpha_{R_1}(t) = a_1 + p_1 t \text{ and } \alpha_{R_2}(t) = a_2 + p_2 t. \tag{III.4}$$

Then, using Eq. (II.5) and the τ-function discussed in Appendix A, we find

$$A^{(2)}_{R_1R_2} = \frac{1}{64\pi^2\sqrt{r}} \left(\frac{4}{s_0}\right) \int\int_{-\infty}^{0} \tau(t_1,t_2,t) \; A^{(1)}_{R_1}(s,t_1) \; A^{(1)}_{R_2}(s,t_2) \; dt_1 \; dt_2$$

$$= \frac{1}{4\pi\sqrt{r}} \left(\frac{4}{s_0}\right) \tau_1\tau_2\gamma_1\gamma_2\sigma_{01}\sigma_{02} \left(\frac{s}{\sigma_{01}}\right)^{a_1} \left(\frac{s}{\sigma_{02}}\right)^{a_2} \quad . \tag{III.5}$$

$$\cdot \int\int_{-\infty}^{0} \tau(t_1,t_2,t) \; e^{z_1 t + z_2 t} \; dt_1 \; dt_2 \, ,$$

where $z_1 = b_1 + p_1(\log s/\sigma_{01})$ and $z_2 = b_2 + p_2(\log s/\sigma_{02})$. Evaluating the integral, using (A.12), we obtain

$$A^{(2)}_{R_1R_2} = \frac{2\,\tau_1\tau_2\gamma_1\gamma_2\sigma_{01}\sigma_{02}\left(\frac{s}{\sigma_{01}}\right)^{a_1}\left(\frac{s}{\sigma_{02}}\right)^{a_2} e^{-\frac{1}{2}(z_1+z_2)s_0}}{\sqrt{r}\,s_0\sqrt{(z_1+z_2)^2+\frac{4z_1z_2t}{s_0}}} \cdot$$

$$\cdot \sinh\left[\frac{s_0}{2}\sqrt{(z_1+z_2)^2+\frac{4z_1z_2t}{s_0}}\right]$$

$$= \frac{\tau_1\tau_2\gamma_1\gamma_2\sigma_{01}\sigma_{02}\left(\frac{s}{\sigma_{01}}\right)^{a_1}\left(\frac{s}{\sigma_{02}}\right)^{a_2}}{\sqrt{r}\,s_0\,(z_1+z_2)}\left[e^{\frac{z_1z_2}{z_1+z_2}t}\right]\left[1+O\left(\frac{1}{s_0}\right)\right] . \qquad \text{(III.6)}$$

Now, for comparison with (III.6) we replace (III.5) by the asymptotic unitarity condition discussed in Section II. Using (A.11) we obtain

$$A^{(2)}_{R_1R_2} \approx \frac{\tau_1\tau_2\gamma_1\gamma_2\sigma_{01}\sigma_{02}\left(\frac{s}{\sigma_{01}}\right)^{a_1}\left(\frac{s}{\sigma_{02}}\right)^{a_2}}{\sqrt{r}\,s_0\,(z_1+z_2)}\, e^{\frac{z_1z_2}{z_1+z_2}t} . \qquad \text{(III.7)}$$

Comparing Eq. (III.7) with the asymptotic form of (III.6) we see that it is appropriate to use the asymptotic unitarity condition for our estimates, so long as we are interested in very large s. We are making an expansion in powers of $1/s_0$ and will, therefore, consider terms like $(1/\log s)$ to be of order 1 in our expansions, and so forth.

Now, using the asymptotic unitarity condition, the contribution from the exchange of any number of Reggeons is easily obtained by comparing (III.7) with the expression for a Regge pole. We find

$$A^{(n)}_{R_1 R_2 \ldots R_n} = \sqrt{16\pi}\, C_n \left(\frac{r}{16\pi}\right)^{\frac{m-1}{2}} \left[s^{a_1+a_2+\ldots+a_n-(m-1)}\right] \cdot \qquad \text{(III.8)}$$

$$\cdot \frac{\langle z_1 z_2 \ldots z_n \rangle_{HS}}{z_1 z_2 \ldots z_n} \; e^{\langle z_1 z_2 \ldots z_n \rangle_{HS}\, t},$$

where

$$C_n = (\tau_1 \tau_2 \ldots \tau_n)(\gamma_1 \gamma_2 \ldots \gamma_n) \left[\left(\frac{1}{\sigma_{01}}\right)^{1-a_1} \left(\frac{1}{\sigma_{02}}\right)^{1-a_2} \ldots \left(\frac{1}{\sigma_{0n}}\right)^{1-a_n}\right]$$

and, as above, we use

$$\langle z_1 z_2 \ldots z_n \rangle_{HS} \equiv \left[\frac{1}{z_1} + \frac{1}{z_2} + \ldots + \frac{1}{z_n}\right]^{-1}.$$

We recover (III.7) from (III.8) by setting n = 2 and, furthermore, we find that we obtain (III.1), the pole term itself, by setting n = 1.

The iteration of Eq. (II.5) will, of course, require that we add together the contributions from all possible unitarity cut diagrams corresponding to a given Feynman diagram, e.g.,

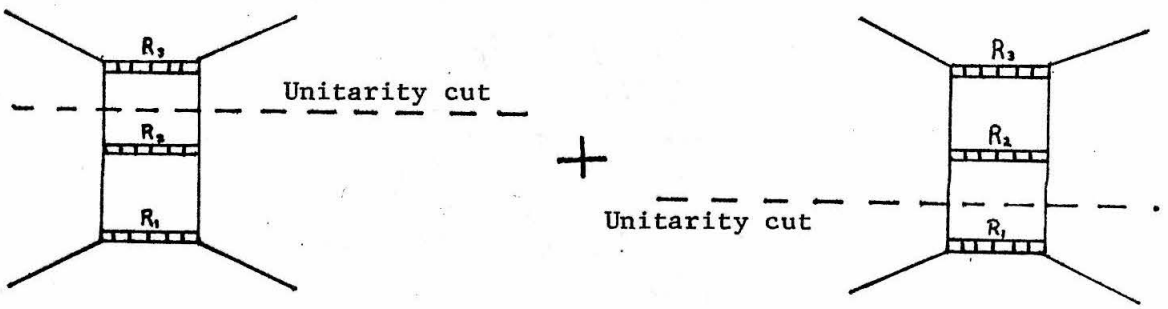

It is shown in Appendix A that all the various ways to make two particle unitarity cuts yield the same value. Thus, since we keep only the two particle unitarity cuts, we need only multiply Eq. (III.8) by Q_n, the number of ways to cut through two particle intermediate states. This is a combinatorial question and Q_n is determined in Appendix C.

We may now give the sum of the contributions of the following set of iterated ladder diagrams

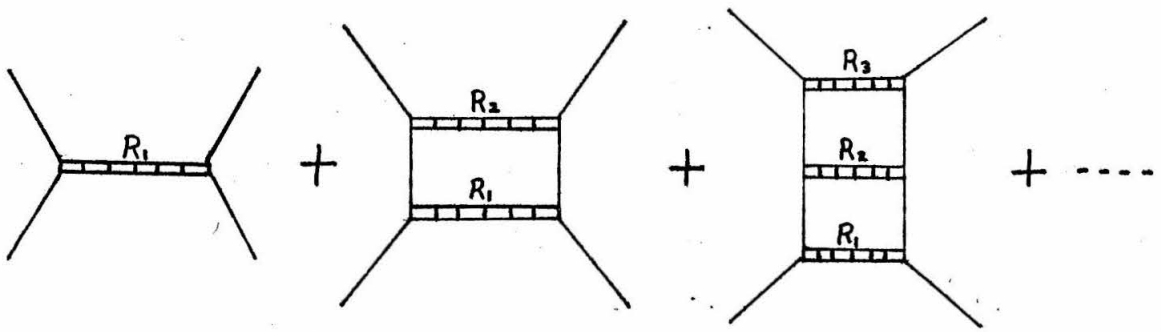

by the expression

$$A(s,t) = \sum_{n=1}^{\infty} Q_n A^{(n)} , \qquad \text{(III.9)}$$

where $A^{(n)}$ is given by (III.8) and $Q_{n+1} = (2n)!/[n!(n+1)!]$. One should realize that Eq. (III.9) is not the sum over all of the diagrams that occur in the iteration of (II.5), but rather the sum over the subset indicated by the above diagrams. For example, we would use (III.9) if we were only interested in the iteration of Pomeranchons, in which case, each $R_i \equiv$ Pomeranchon. If, on the other hand, we wanted the set of all diagrams exchanging the Reggeon, R, once along with any number of Pomeranchons,

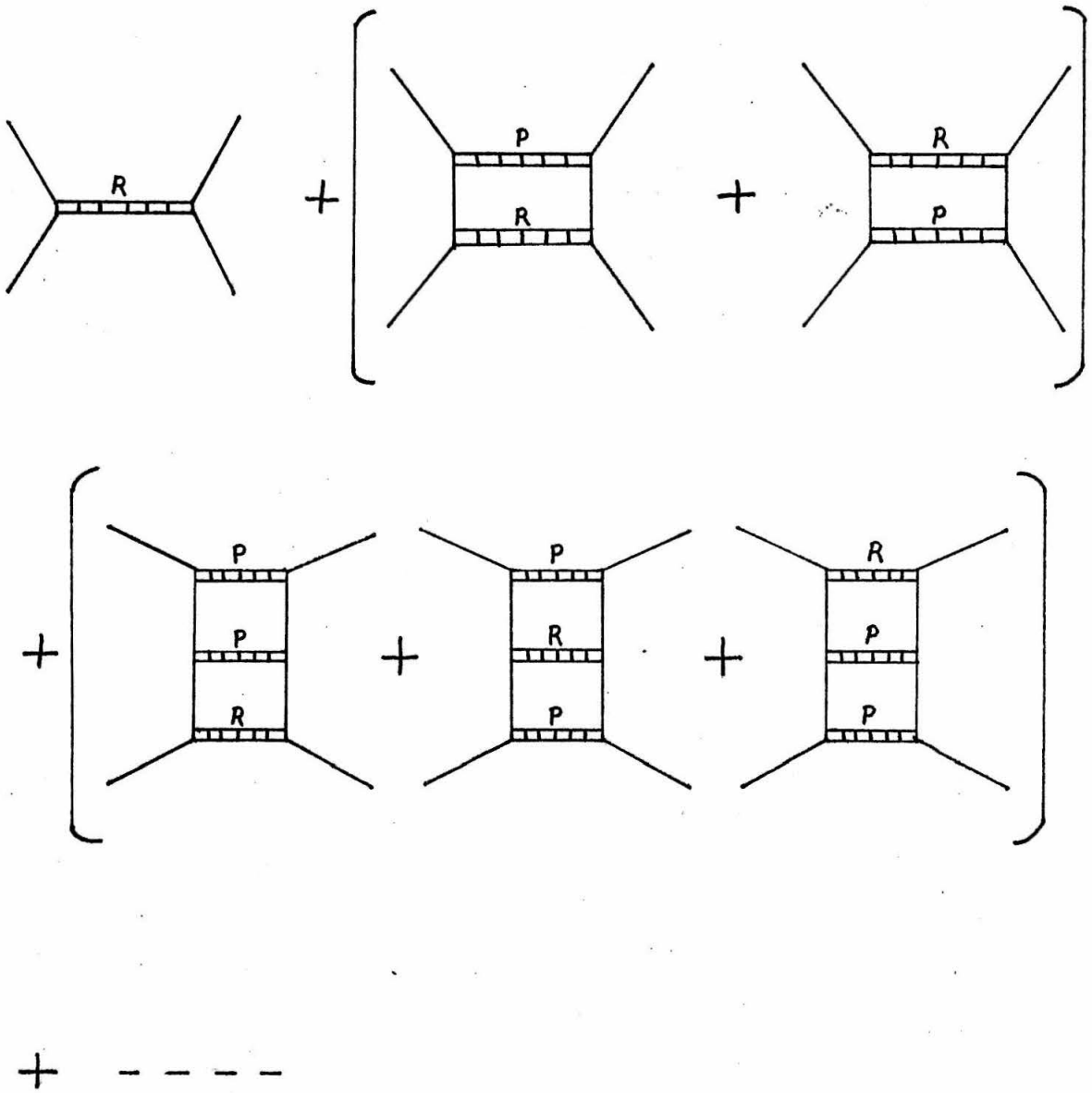

... then we would have to multiply the

summand of (III.9) by another combinatorial function, in this case n. Thus, for this set of diagrams we would want

$$A_P(s,t) = \sum_{n=1}^{\infty} n\, Q_n\, A^{(n)} \quad . \tag{III.10}$$

We now consider the sum of Eq. (III.9) for the case for which we expect the strongest asymptotic contribution. It was remarked in Section II that the cuts are highest, hence have the strongest effect, when only Pomeranchons are exchanged. In this event Eq. (III.8) reduces to

$$A_P^{(n)} = \sqrt{16\pi}\,\gamma\, s\, \frac{1}{n} \left(\frac{\gamma \sqrt{r}}{\sqrt{16\pi}\, z} \right)^{n-1} e^{\frac{zt}{n}} \tag{III.11}$$

so that (III.9) becomes

$$A_P(s,t) = \sqrt{16\pi}\,\gamma\, s \sum_{n=0}^{\infty} \frac{(2n)!}{[(n+1)!]^2} \left(\frac{\gamma \sqrt{r}}{\sqrt{16\pi}\, z} \right)^{n} e^{\frac{zt}{n+1}} \tag{III.12}$$

where $z \equiv b + p \log s/\sigma_0$.

In our model, using exponentially damped coupling coefficients, there is a certain redundancy in the parameters b and σ_0. For convenience we combine these two parameters for each Reggeon so that

$$z_R = p_R \log \frac{s}{\sigma_R} \quad \text{where } \sigma_R = \sigma_{0R} e^{-b_R/p_R} \tag{III.13}$$

The parameter σ_R depends upon the Reggeon and upon the particles exchanging that Reggeon. It will also prove convenient later to use

$$\Gamma_R \equiv \gamma_R(0)\, e^{\frac{b_R}{p_R}(1 - a_R)} \quad . \tag{III.14}$$

Asymptotically the terms in (III.12) are proportional to

$$\frac{\left(\frac{s}{\sigma}\right)^{1+\frac{pt}{n+1}}}{\left[\log\left(\frac{s}{\sigma}\right)\right]^n},$$

so they behave like Regge poles of smaller and smaller slope, divided by increasing powers of log s. This behavior differs from that obtained in Section II from integration by parts in that the contribution from the cut is divided by $(\log s)^n$ instead of simply log s.

To examine the sum in (III.12) we note that for large n,

$$\frac{(2n)!}{[(n+1)!]^2} \approx \frac{4^n e^{-\frac{1}{8n}}}{\sqrt{\pi}\sqrt{n}\,(n+1)^2} \approx \frac{4^n}{\sqrt{\pi}\sqrt{n}\,(n+1)^2}. \qquad \text{(III.15)}$$

It is apparent from the ratio test that the sum does not converge unless

$$\frac{1}{R} \equiv \frac{\Gamma\sqrt{r}}{\sqrt{16\pi}\,z} \leqslant \frac{1}{4}. \qquad \text{(III.16)}$$

The physical reason for this divergence is that at this point the S-wave inelastic scattering begins to violate unitarity. This matter is considered in detail in Section VI. It is clear, however, that for large enough s it will occur that $z = p \log(s/\sigma)$ will bring $R \geqslant 4$, so that (III.12) will converge.

At t = 0, the terms in (III.12) decrease monotonically with n and the sum may be expressed in closed form. We find

$$A_p(s,0) = \sqrt{16\pi}\,\Gamma\, s \sum_{n=0}^{\infty} \frac{(2n)!}{[(n+1)!]^2}\,\frac{1}{R^n} = \sqrt{16\pi}\,\Gamma\, s\, R\left[1 - \sqrt{1-\frac{4}{R}} + \right.$$

$$\left. + \log \frac{1+\sqrt{1-\frac{4}{R}}}{2}\right] . \qquad \text{(III.17)}$$

This is a decreasing function of R. Writing

$$\sigma_{tot} = \frac{\sqrt{r}\, A_p(s,0)}{s} = \sigma_{pole} + \sigma_{cuts} = \frac{\sqrt{r}\, A_{pole}(s,0)}{s} + \frac{\sqrt{r}\, A_{cuts}(s,0)}{s}$$

we have

$$\sigma_{pole} = \text{(contribution from Pomeranchon pole)} = \sqrt{r}\sqrt{16\pi}\,\Gamma$$

and

$$\frac{\sigma_{cuts}}{\sigma_{pole}} = R\left[1 - \sqrt{1-\frac{4}{R}} + \log \frac{1+\sqrt{1-\frac{4}{R}}}{2}\right] - 1 .$$

Thus, if we use a model in which only Pomeranchons are exchanged we find that on the verge of the asymptotic region, i.e., R = 4,

$$\frac{\sigma_{cuts}}{\sigma_{pole}} = 4[1 - \log 2] - 1 = 0.23 .$$

This ratio decreases monotonically to zero as s gets larger.

Now when $t \neq 0$, the terms in (III.12) either decrease monotonically with n, or the terms increase at first and then decrease monotonically for $n > N$. The largest term occurs for $n = N$ and N is determined by the relative magnitudes of s and t. It is easy to see that for fixed t, N increases as s increases. Using (III.15), one may easily verify that the largest term occurs for

$$N \approx \frac{5}{4} \cdot \frac{\sqrt{1 + \frac{16}{25} z\,|t| \log \frac{R}{4}} - 1}{\log \frac{R}{4}} \quad . \tag{III.18}$$

We can obtain an approximation to (III.12) appropriate for very large s, i.e., N very large. From (III.18) we find that

$$N \gg 1 \Rightarrow z|t| \gg (\log \tfrac{R}{4}) + \tfrac{5}{2} \quad . \tag{III.19}$$

Since $z \sim \log s$ and $\log R \sim \text{loglog } s$ we see clearly that N gets very large as $s \to \infty$. The terms in (III.12) drop to 1/e of the largest term at

$$n = N \pm \sqrt{\frac{N^2}{\frac{5}{4} + N \log \frac{R}{4}}} \quad ,$$

so the width of the peak goes like $\sqrt{N}$ for very large N. Thus when condition (III.19) is satisfied we may replace the sum in (III.12) by an integral. Then we have

$$A_p(s,t) \approx 4\Gamma s \int_0^\infty dn \quad e^{- n \log \frac{R}{4} - \frac{2|t|}{n} - (5/2) \log n} =$$

$$= \sqrt{16\pi}\, \Gamma\, s \frac{\sqrt{\log \frac{R}{4}}}{z\,|t|} \left(1 + \frac{1}{2\sqrt{z|t| \log \frac{R}{4}}}\right) e^{-2\sqrt{z|t| \log \frac{5}{4}}} \quad . \tag{III.20}$$

We have obtained expressions (III.12), (III.17), and (III.20) by iterating only the imaginary part of the Pomeranchon pole in (II.5). Justification of this procedure requires that we examine the real parts occuring in the iterations and the real part corresponding to the entire series. These checks are presented in Appendix D. It is

found that our method is consistent in this regard.

The criterion for the validity of (III.20) is given by (III.19). We must, of course,be working in the asymptotic range, i.e. $R > 4$. We have found that it is appropriate to use (III.17) for total cross-sections and for the differential cross-section at $t = 0$. At larger values of $|t|$, we may use (III.20), if condition (III.19) is satisfied. For intermediate values of $|t|$, if (III.19) is not fulfilled, then we must use (III.12) directly and compute the first several terms.

In conclusion, the behavior at $t = 0$ and for $|t|$ very small has been shown above to be dominated by the processes represented by the Regge pole. However, (III.19) indicates that, for any fixed $t \neq 0$, for large enough s it is appropriate to use (III.20). The amplitude under these conditions is drastically different from the behavior of the Regge pole alone. The cut terms modify the amplitude to the extent that it does not behave like a power of s. Other characteristics of (III.20) are considered in the next section.

IV. EXPERIMENTAL CONSEQUENCES OF REGGE CUTS AT VERY HIGH ENERGY

The description of high-energy scattering processes in terms of a dominant Regge pole leads to some simple and rather distinctive predictions. Two such predictions are:

i) for a given scattering process

$$\frac{\frac{d\sigma}{dt}(s_1,t)}{\frac{d\sigma}{dt}(s_2,t)} \longrightarrow \left(\frac{s_1}{s_2}\right)^{2\alpha(t)\,-\,2} < 1$$

for $s_1 > s_2$ because $\alpha(t) \leqslant 1$ and $d\alpha(t)/dt > 0$.

ii) for two different scattering processes

$$\frac{\frac{d\sigma_1}{dt}(s,t)}{\frac{d\sigma_2}{dt}(s,t)} \longrightarrow \text{a function of t only .}$$

These predictions would be easily recognized if the pp and πp scattering data had this behavior. The fact of the matter is that at present machine energies the data do not agree with these predictions[21].

In order to use a Regge approach at present energies, one is forced to add in more and more poles. The Pomeranchon trajectory was invented in order to account for nearly constant total cross-sections and to make the scattering amplitude predominantly imaginary. Since the predictions of this "single dominant pole" did not agree in detail with the data, one was forced to conclude that the data was collected in an "intermediate energy range". The natural thing to try next was to include the ω and ρ trajectories in order to attempt to fit NN - $\bar{N}N$

scattering. The ω and ρ are the known particles having higher spin. Even this did not work because the model could not explain why the total cross-section, σ_{pp}, is nearly constant up to very high energies, but $\sigma_{\bar{p}p}$ is not. It was to erase this failure and to explain discrepancies in scattering lengths that the Igi pole was invented. Thus the explanation of presently accessible data by means of Regge pole terms must involve a great number of parameters and be, at best, a complicated matter.

We return now to the uncluttered Regge pole model: the single dominant trajectory. It is certainly possible that at the "asymptotic region" of the energy rainbow we will find the Pomeranchuk theorems[22] describing the data. Anticipating this event, we discuss now the Pomeranchuk theorems in light of our model for the Regge cuts. We presume for this discussion that s is very, very large.

First, we compare the shrinking of the differential cross-section as given by the Pomeranchuk pole alone, with that obtained from our model for the Pomeranchon and associated cuts. A useful quantity for measuring the shrinkage is

$$S = -\tfrac{1}{2}\,\frac{d \log\left(\frac{d\sigma}{dt}\right)}{d \log s} \quad . \tag{IV.1}$$

Approximating $d\sigma/dt$ by $\frac{1}{16\pi}\left[\frac{A(s,t)}{s}\right]^2$, we obtain for the Pomeranchuk pole

$$S_{pole} = 1 - \alpha(t) = p|t| \text{ and } \frac{d\, S_{pole}}{d \log s} = 0 \quad . \tag{IV.2}$$

Thus, the shrinkage from the pole term is independent of s and is larger for larger values of $|t|$ since $d\alpha/dt > 0$.

Now for our model discussed in Section III, at very large s the behavior depends upon the relative size of $|t|$. For $|t| \approx 0$ the pole dominates and shrinking appears much as in (IV.2). For larger $|t|$, such that condition (III.19) is fulfilled,

$$z|t| \gg (\log \tfrac{R}{4}) + \tfrac{5}{2} ,$$

we then must consider the amplitude as given by (III.20). For intermediate values of t we would have to consider the series (III.12) directly and would find intermediate behavior for the shrinking. From (III.20) we calculate the shrinkage for pole + cut terms to be

$$S' = \frac{3p}{2z} + \frac{2p|t|(1 + \log \frac{R}{4})}{1 + 2\sqrt{z|t|\log \frac{R}{4}}} \xrightarrow[\text{as } z \to \infty]{} p(1 + \log \tfrac{R}{4}) \sqrt{\frac{|t|}{z \log \frac{R}{4}}} \qquad \text{(IV.3)}$$

and

$$\frac{d\,S'}{d \log s} \xrightarrow[\text{as } z \to \infty]{} \frac{-p^2\sqrt{|t|}}{2(z\ell)^{3/2}} (1 + \ell^2) \text{ with } \ell = \log \tfrac{R}{4} .$$

Equations (IV.2) and (IV.3) show somewhat different behavior, since the cuts decrease the rate of shrinking as a function of t. They make the diffraction peak broader than it would otherwise be. In fact as $z \to \infty$, the shrinkage disappears roughly as $\sqrt{p|t|}\ \sqrt{\text{loglog } s/\log s}$. The pole itself leads to a constant shrinkage, independent of s, but the rate of change of S' with s goes to zero only like $-(\sqrt{p\,t}/2)\sqrt{\text{loglog } s/(\log s)^3}$.

We also observe that the size of the effect depends upon the process itself, since R depends upon the coupling, Γ. These effects of the cuts will appear at smaller and smaller values of $|t|$ as the energy increases according to condition (III.19). We might, therefore, expect that the shrinkage phenomenon will not be an aspect of the asymptotic region and that the simple predictions i) and ii) above will never be appropriate except at very tiny $|t|$.

Another prediction of Regge pole theory is that

iii) $$\frac{\frac{d\sigma}{dt}\text{ (charge exchange)}}{\frac{d\sigma}{dt}\text{ (no charge exchange)}} \xrightarrow{s \to \infty} 0 \text{ like a power of } s.$$

For example, in the case of $\pi^- p$ scattering

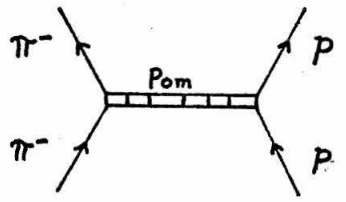

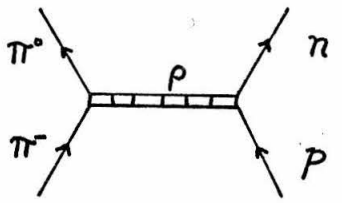

,

the dominant trajectory for the direct process is the Pomeranchon, but is the ρ in the charge exchange process. Now $\alpha_\rho(t) < \alpha_{Pom}(t)$ so that the dominant pole idea indicates that charge exchange loses out like $s^{2(\alpha_{Pom}(t) - \alpha_\rho(t))}$. If one includes the effect of cuts, then one considers something like

$$\left[\frac{A_{\rho P}(s,t)}{A_P(s,t)}\right]^2$$

with $A_{\rho P}(s,t)$ similar to (E.10) and $A_P(s,t)$ as given by (III.12). At very small t the pole terms dominate the expressions so that charge exchange loses out as before. For larger values of t we expect the factor $(s/\bar{\sigma})^{\alpha_\rho(0)-1}$ occuring in $A_{\rho P}$ to continue to reduce the ratio. It is clear, however, that the approach to asymptotic behavior will be slower and the predictions less distinctive.

The dominant trajectory picture also gives a line reversal prediction:

iv) $\frac{d\sigma}{dt}(AB \to CD) - \frac{d\sigma}{dt}(\bar{C}B \to \bar{A}D) \xrightarrow{s \to \infty} 0$ like a power of s.

These conclusions follow directly for eigenstates of C or G. Otherwise there is a parity argument[23]. This matter is discussed in detail in Section V. Consider first the nucleon-nucleon case.

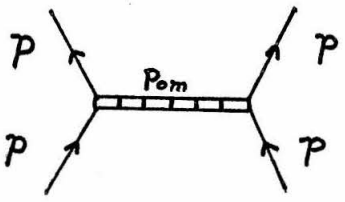

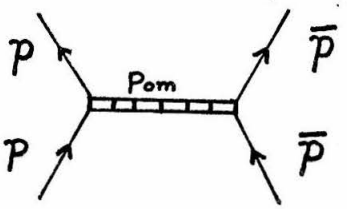

Since these processes involve states of definite C, we have $T^{Pom}_{pp}(s,t) = T^{Pom}_{\bar{p}p}(s,t)$ so that asymptotically

$$\frac{d\sigma}{dt}(pp \to pp) - \frac{d\sigma}{dt}(\bar{p}p \to \bar{p}p) \to 0 \text{ like } s^{2\alpha_{Pom}(t) - 2}.$$

The same situation obtains in the presence of cuts, except the approach to zero is weaker than a power of s. In other cases, like

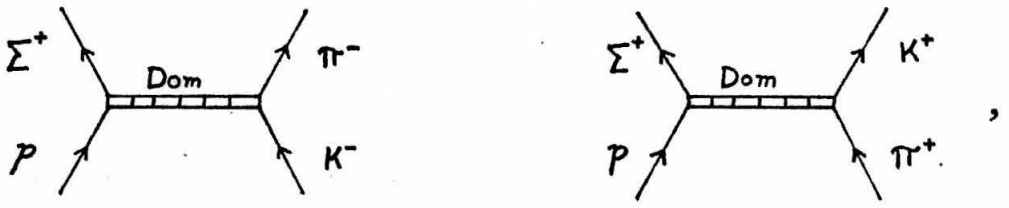

the dominant trajectory must be something with strangeness, i.e., no definite C or G. Under such conditions the cut terms arising in our model can seriously alter the simple prediction of iv). It is possible, however, that the line reversal symmetry is not spoiled by the physical cuts in the angular momentum plane. The diagrams discussed by Mandelstam appear to have a greater line reversal symmetry than do the diagrams arising in our scheme. This matter is considered in greater detail in Section V.

The factoring theorem for total cross-sections[24] is also given by the dominant Regge pole model. For example,

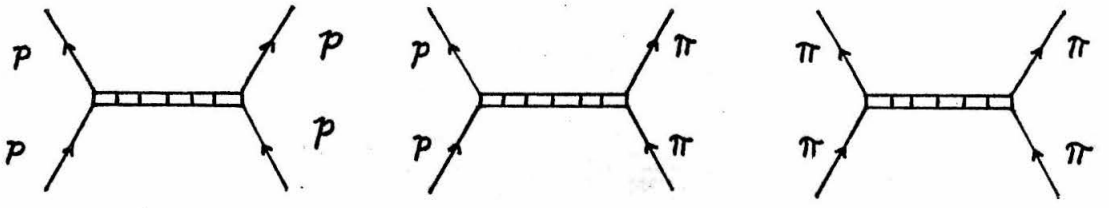

$\sigma_{NN} \sim \frac{A}{s} \sim g_N^2$ $\qquad$ $\sigma_{\pi N} \sim g_N g_\pi$ $\qquad$ $\sigma_{\pi\pi} \sim g_\pi^2$.

Since the other factors are the same in each case, we obtain

$$\sigma_{\pi\pi}\sigma_{NN} \xrightarrow{s \to \infty} (\sigma_{\pi N})^2 \quad .$$

When the effect of the cuts is included, this relationship will still be obtained because as $R \to \infty$, the pole term completely dominates expression (III.17).

The over-all effect of the cut terms upon the asymptotic predictions of the dominant Regge pole model is to allow essentially the same predictions, except that the approach to the simple behavior is expected to be much slower.

We emphasize that one is faced with a whole hierarchy of "asymptotic regions". We first have the region where a Regge model begins to be useful. Next, one expects a region where the effects of a dominant trajectory are a good approximation to the data. Finally, we might expect to find a region where the theorems discussed above agree with the data and are simply explained.

Some of the theorems discussed in this section can be deduced from more general arguments than the Regge pole model[25]. If however, we may use the failures of the Regge models at present machine energies as a guide, we must estimate that the "asymptotic region" corresponding to these theorems must be considerably higher than the energy region presently accessible to us.

V. PROPERTIES OF CUT TERMS UNDER LINE REVERSAL

It is of interest to attempt to understand the connection between particle - antiparticle scattering and particle-particle scattering. Since such a connection is closely related to symmetry between the s and u channels, we are interested in the "signature" of the amplitudes associated with the cuts in the angular momentum plane. We argue in this section that in many cases the iterated Regge pole diagram of the AFS type, or of the Mandelstam type, do possess a definite signature. The signature turns out to be equal to the product of the signatures of the exchanged Reggeons, as one might guess.

First, let us review some of the line reversal properties of Regge pole terms. Wagner[28] has examined the couplings of fermions and spinless bosons to Reggeons and determined the resulting line reversal symmetry or signature. Since the same approach may be used for diagrams producing cuts in the angular momentum plane, we now consider his analysis of the signature of poles.

Diagramatically, we are interested in the relation between

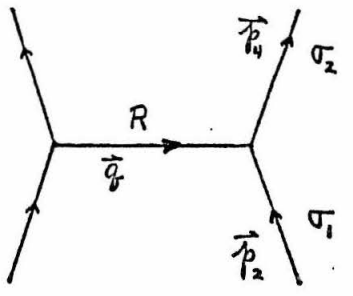

I

and

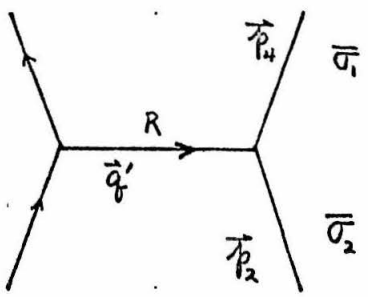

II

where σ_1 and σ_2 are two spinless bosons. In this case the considerations are very simple. We take the spin, J, of the exchanged Reggeon to be integral for the purposes of formulating the rule. It is consistent to assign a signature to the Regge poles if for all odd J the line reversal symmetry is odd and for all even J the line reversal symmetry is even. The approach is, therefore, to find the rule by considering the spin of the Reggeon to be integral and then to appeal to Carlson's theorem to continue the symmetry to non-integral spin.

For integral J the intermediate boson, R, may be represented by a tensor field of rank J, symmetric and divergenceless in all indices and traceless in any pair of indices, e.g.,

$$R_{\mu\nu\sigma} = R_{\mu\sigma\nu} = R_{\sigma\mu\nu}$$

$$R_{\mu\nu\sigma}q_\nu = R_{\mu\nu\sigma}q_\mu = 0$$

$$R_{\mu\mu\sigma} = \delta_{\mu\nu}R_{\mu\nu\sigma} = 0$$

where repeated indices imply summation.

The vertex must also be a symmetric, divergenceless, traceless tensor of rank J, constructed from the momenta p_2 and p_4. It is more convenient, however, to construct the vertex tensor from the momenta Σ and q, where $\Sigma = p_4 + p_2$ and $q = p_4 - p_2$. When energies are high enough that we can neglect any mass differences, q will appear with the same sign in process I and in process II, but Σ will occur with opposite signs in the two processes. This is, of course, due to the fact that in

a Lagrangian model, the operator ∂_μ onto a quantized field brings in the momentum of a created particle with one sign and the momentum of a destroyed particle with the opposite sign. Thus in going from process I to process II we have

$$q_\mu \rightarrow q_\mu$$

$$\Sigma_\mu \rightarrow - \Sigma_\mu \ .$$

Now, the vertex tensor, constructed from Σ_μ and q_μ will be dotted into the propagator of rank 2J conveying the Reggeon R across the diagram. In the J indices available to the right hand vertex, this propagator has the same symmetry properties as the tensor field, R, mentioned above. It is therefore clear that the antisymmetric tensor $\epsilon_{\alpha\beta\gamma\delta}$ can give no contribution because the propagator is symmetric in its indices and because there are only two available momentum vectors, Σ and q. Similarly, free indices in the vertex tensor coming from $\delta_{\alpha\beta}$ or from q_μ are ineffective because the propagator is traceless and divergenceless when on the mass shell. In the present point of view the Reggeon, R, is always "on the mass shell", but the mass is variable and equal to $-q^2 = t$.

Thus, we see that the only terms in the vertex tensor which can contribute are constructed entirely from the vector Σ. The vertex which couples to the Reggeon of spin J is the direct product of $J(\Sigma_\mu$'s). Therefore, we obtain the factor $(-)^J$ under line reversal. Thus, it is consistent to assign a definite signature or line reversal symmetry to the Reggeon, i.e., if a Regge trajectory only has a physical

manifestation for even (odd) spin, then the line reversal symmetry, τ, is a property of the trajectory and is $\tau = +$ ($\tau = -$). In the following discussion, we will refer to $(-)^J$ as the signature of the Reggeon, thus allowing simultaneous consideration of both cases.

For the reversal of baryon lines we are interested in comparing the processes

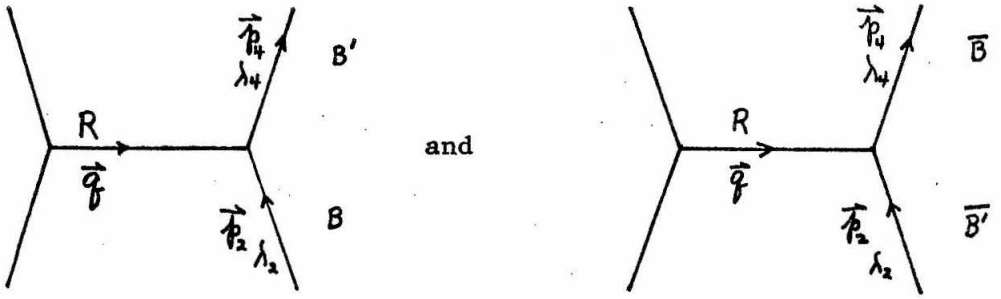

I II

where the λ's indicate the helicities. This time we must also consider the difference in the Dirac matrices for these two processes as we write both amplitudes in terms of particle (not antiparticle) spinors. This difference is the same as the transformation under particle - antiparticle conjugation:

$$1 \to 1,\ \gamma_5 \to \gamma_5,\ \gamma_5\gamma_\mu \to \gamma_5\gamma_\mu,\ \gamma_\mu \to -\gamma_\mu,\ \sigma_{\mu\nu} \to -\sigma_{\mu\nu}\ . \quad (V.1)$$

This transformation includes the relative minus sign resulting from " anticommutation of fermion fields". Again, of course, the propagator for R is always on the mass shell, so that we have it symmetric, divergenceless, and traceless. Now $\sigma_{\mu\nu}\ \Sigma_\nu \sim q_\mu$ by virtue of the Dirac

equation. Hence, such a term can give no contribution when dotted into the traceless propagator. The term $\sigma_{\mu\nu} q_\nu$, however, is a vector and is odd under line reversal, just as γ_μ and Σ_μ. As before, we may ignore $\delta_{\alpha\beta}$ terms when dotted into the traceless propagator. An $\epsilon_{\alpha\beta\gamma\delta}$ term with two or more free indices gives zero when dotted into the symmetric propagator. The term $\epsilon_{\alpha\beta\gamma\delta}\, q_\alpha\, \Sigma_\beta\, \sigma_{\gamma\delta}$ is pseudoscalar and is even under line reversal, just as γ_5. We observe that the two pseudovectors $\epsilon_{\alpha\beta\gamma\delta}\, q_\beta\, \sigma_{\gamma\delta}$ and $\epsilon_{\alpha\beta\gamma\delta}\, \Sigma_\beta\, \sigma_{\gamma\delta}$ behave oppositely under line reversal, just as do $\Sigma_\mu\gamma_5$ and $\gamma_5\gamma_\mu$, but since $\epsilon_{\alpha\beta\gamma\delta}$ may be written in terms of γ matrices, such terms may be expressed in terms of the 16 usual Dirac matrices.

We see that there is difficulty with the behavior under line reversal when R has negative intrinsic parity because the two pseudovector vertex terms transform oppositely. Similarly, there is, in general, no symmetry between these amplitudes if R is not an eigenstate of parity or if parity is not conserved at the vertex.

However, we obtain a line reversal symmetry $(-)^J$, as in the scalar boson case above, if R has positive intrinsic parity and parity is conserved at the vertex. We may summarize these conclusions with the relation

$$\text{line reversal phase} = \epsilon(-)^J$$

where $\epsilon = +1$ unless $\gamma_5\gamma_\mu$ is involved, in which case $\epsilon = -1$. The factor ϵ is always $+1$ whenever, for the Reggeon,
(signature) (parity) $= +1$, which is the case for the exchange of the K^*, the ρ, and the ω, for example.

For the case that (signature) (parity) = - 1, we will find a line reversal symmetry if there is a symmetry among the baryons that prohibits the mixing of $\Sigma_\mu\gamma_5$ and $\gamma_5\gamma_\mu$. Such a selection rule is provided if the Reggeon has definite C and/or G. For a neutral Reggeon, with charge conjugation parity C = + 1, only $\gamma_5\gamma_\mu$ can contribute to proton scattering whereas if C = - 1, only $\gamma_5\partial_\mu$ can contribute. In general, reversal of baryon lines in the same isotopic spin multiplet introduces the factor $(-)^I G$ which is C for the neutral Reggeon. Under such conditions we have:

$$\text{line reversal phase} = (-)^I G.$$

The crucial point to be noticed in this analysis is that the result of line reversal is fundamentally determined by the Lorentz transformation properties of the couplings. One need appeal to eigenstates of C or G only when the Reggeon has negative intrinsic parity.

One consideration, not discussed by Wagner, might be mentioned at this point. We refer to the curious lack of symmetry in the above conclusions between Reggeons of positive and negative intrinsic parity. The line reversed diagram, II, is simply related to I only if the Reggeon has positive intrinsic parity. It turns out that in many cases there also exists a line reversed diagram, II', that is simply related to I only if the Reggeon has negative intrinsic parity. For example, the diagrams

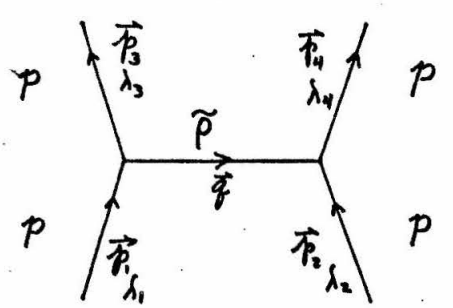

I

and

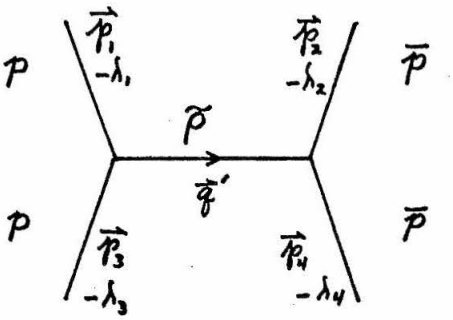

II'

,

where $\tilde{\rho}$ is an axial vector meson coupling through both $\Sigma_\mu \gamma_5$ and $\gamma_5 \gamma_\mu$, are simply related. In this case, we find that there is just a phase between processes I and II' for axial vector couplings, but that one must appeal to eigenstates of C to find a symmetry in the case of the vector couplings. This time it is Σ_μ and γ_μ which transform oppositely. This is another aspect of symmetry between s and u channels. We note that process II' is p-$\bar{p}$ scattering at the same energy and momentum transfer as in the corresponding process II. The labeling of the momenta and helicities indicates the difference in the physical processes related by "line reversal" in the two cases.

We now consider the line reversal symmetry of the iterated Regge pole type diagrams. First, we examine the Amati, Fubini, Stanghellini (AFS) type diagrams. Following the discussion of the AFS diagrams, we will consider the much more complicated diagrams suggested by Mandelstam. Consider A + B $\rightarrow$ A + B, via the diagrams

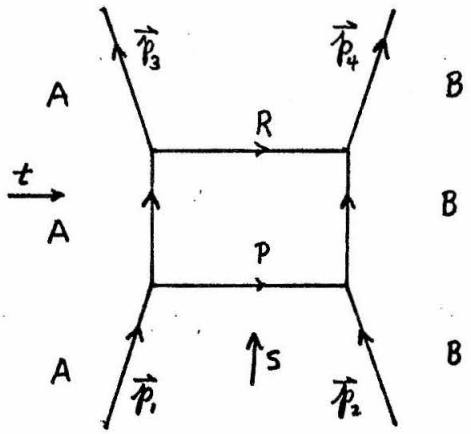

I

and

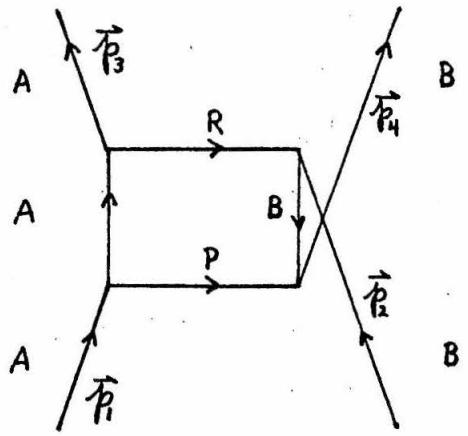

II

The diagram I has a cut in s and a cut in t, whereas the related diagram II has a cut in u and a cut in t. For these diagrams we have $p_1 + p_2 = p_3 + p_4$ and

$$s = -(p_1 + p_2)^2 = -(p_3 + p_4)^2 > 0$$

$$t = -(p_3 - p_1)^2 = -(p_4 - p_2)^2 \leqslant 0$$

$$u = -(p_4 - p_1)^2 = -(p_3 - p_2)^2 < 0$$

The amplitude for process I is written $T_I(s,t)$ and that for process II is written $T_{II}(s,t)$. Consider the Feynman integrals for these two diagrams. If one can show that the Feynman integral for II is the same (except possibly for an over-all sign) as that for I, provided that the four vector $\vec{p}_2$ is replaced by $-\vec{p}_4$ and $\vec{p}_4$ is replaced by $-\vec{p}_2$, then it would be clear that

$$T_{II}(s,t) = \pm T_I(s',t') \qquad (V.2)$$

where s' and t' and u' are determined by

$$s = -(p_1 + p_2)^2 \rightarrow s' = -(p_1 - p_4)^2 = u < 0$$

$$t = -(p_3 - p_1)^2 \rightarrow t' = -(p_3 - p_1)^2 = t \leqslant 0$$

$$u = -(p_4 - p_1)^2 \rightarrow u' = -(-p_2 - p_1)^2 = s > 0.$$

Thus Eq. (V.2) would tell us that the amplitude, $T_{II}(s,t)$, for process II is equal, except for a phase, to the functional form $T_I(s,t)$ where the variable $s > 0$ must be replaced by the variable $u < 0$ in this functional form. This is an example of symmetry between the s- and u-channels. The phase factor that enters is the signature of the part of the amplitude corresponding to I.

Our discussion is somewhat simpler if we employ the $\vec{p}_2 \leftrightarrow -\vec{p}_4$ transformation indirectly and, instead of comparing I and II, we compare the diagrams

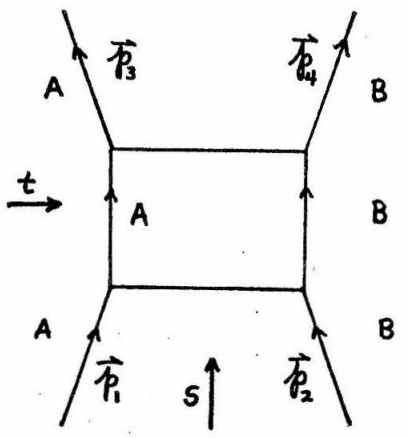

I

and

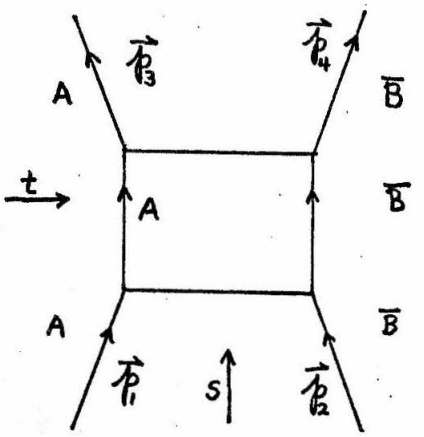

II'

This amounts to a redrawing and relabeling of II. Now we have the amplitudes $T_I(s,t)$ and $T_{II'}(s,t)$. Now, if it is true that

$$T_{II'}(s,t) = \pm T(s,t)$$

then the sign is the signature of the part of the amplitude corresponding to I.

It is easy to see that in general the AFS diagrams will contribute both a positive signature piece and a negative signature piece to the amplitude, i.e., the iterated Regge pole diagrams do not have definite signature. Consider, for example, the exchange of a Pomeranchon and a K^*-Reggeon:

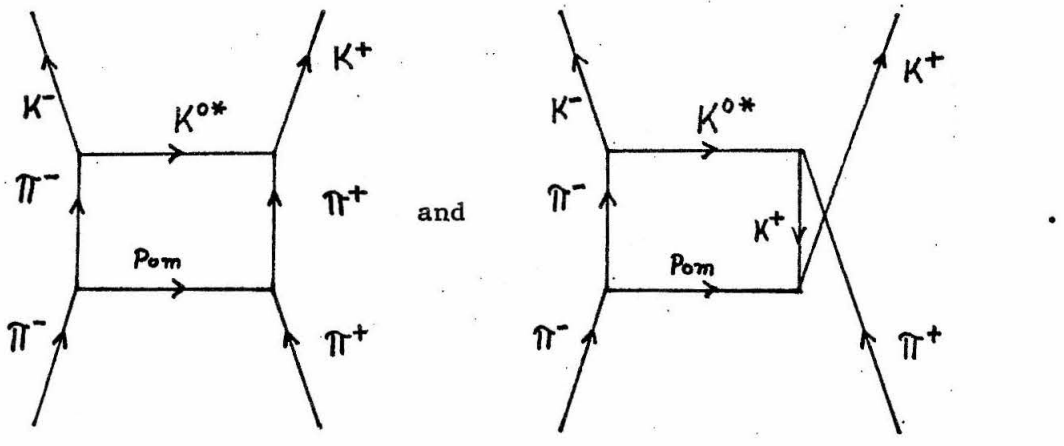

I II

This "strangeness exchange" process leads to difficulty because the intermediate state must be different in the process with a cut in the

u-channel. There cannot be a definite signature unless one is prepared, at least, to say that the coupling constant for the Pomeranchon to kaons is the same as for the coupling to pions. It is clear that, in general, we cannot expect the AFS diagrams to produce a definite signature contribution to the amplitude, because exchange of strangeness forces the intermediate states to have different strangeness in the two processes.

We now investigate several cases where there is a definite signature for the AFS terms. Consider a diagram involving spinless bosons on the right side and with exchange of two non-strange Reggeons like Pomeranchon, Igi pole, ρ or ω. We call these Reggeons P and R:

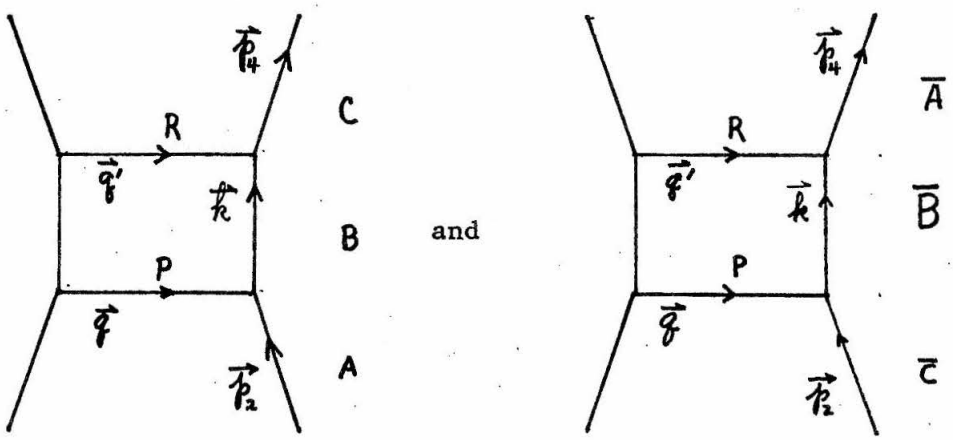

I II

where the labeling of the momenta implicitly assumes that we may ignore mass differences at high enough energy. We are interested in the relation between these two processes. The left-hand side is the same in I and II.

As before, we will examine couplings of Reggeons of spin J_P and J_R which we take to be integral for purposes of formulating the rule. We can see if it is consistent to assign a definite line reversal symmetry i.e., signature, to these amplitudes, based on the signatures of the exchanged Regge poles. To accomplish this objective we must consider all possible couplings at each of the double infinity of integral spin assignments for J_P and J_R. Having obtained the rule, we again continue the symmetry to non-integral spins.

The analysis would be much simpler now if we could argue, as we did in the case of single pole exchange, that for each J_P and J_R the Reggeon propagators are symmetric, divergenceless, and traceless. This would allow us to ignore, for example, terms like $\delta_{\mu\nu}$ and $q'_\nu = (p_4 - k)_\nu$ in the vertex tensors. These properties of the propagators obtain, however, only when the Reggeons are "on the mass shell". For the diagrams under consideration there is no reason to believe that it is correct to consider the Reggeons to be on the mass shell.

It appears that it is possible to eliminate the unwanted couplings from our considerations, however. For each pair of integral spins J_P and J_R there are corresponding propagators of rank $2J_P$ and $2J_R$. Given these propagators we can write the Feynman integrals corresponding to I and II. Now both I and II have the same "two particle" cut in the variable t. These two Feynman integrals may be performed by dispersion integrals if we know the respective discontinuities across the cut in t. We know from unitarity that the

discontinuities may be computed by placing the two relevant particle lines on the mass shell. This means that we may think of the two Reggeon propagators as being on the mass shell. Adopting this point of view, we have symmetric, divergenceless, traceless Reggeon propagators for each J_P and J_R and our objective is to show a symmetry between the discontinuities*.

Let us now specialize our considerations to the case $A \equiv B \equiv C =$, say, π^+:

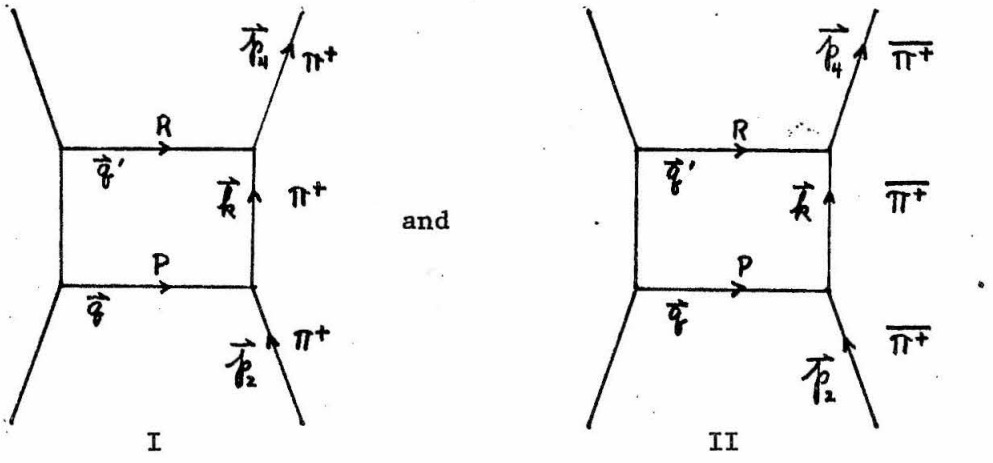

I and II

We may anticipate one more difficulty. If the internal line with momentum $\vec{k}$ is not on the mass shell then certain couplings can give rise to differences in the integrands for I and II which do not

---

* In practice, it looks as if this crude argument might breakdown if subtractions were necessary. However, it is reasonable to expect that subtractions are not necessary, regardless of the spin, when the particle lines are correctly treated as Reggeons. Thus, we do not expect to be led astray if we ignore the possibility of subtractions.

manifestly indicate a line reversal symmetry. For example, the interaction $P(\partial_\mu \partial_\mu \bar{\pi}^+)\pi^+$ would introduce a k^2 into the integrand of I, but would give a $p_2^2 = -m^2$ in II. This complication in our analysis may be avoided by considering the double spectral function for the Feynman integrals. The integrals for the t-discontinuity still possess a cut in s, at the same place for both diagrams. Thus, the t-discontinuity can be computed by a dispersion integral if we know its discontinuity across the cut in s. As before, this discontinuity may be computed by putting the remaining two internal legs on the mass shell, i.e., $k^2 = -m^2$. Our approach will be to compare the double spectral functions, ρ_{st}, for I and II.

The analysis now is very much like that for the pole terms. We define the four momenta $\Sigma = k + p_2$, $q = k - p_2$, $\Sigma' = p_4 + k$, and $q' = p_4 - k$. Since the Regge propagators may be taken to be symmetric, divergenceless, and traceless, it is again true that q_ν, q'_ν, $\delta_{\mu\nu}$, and $\epsilon_{\mu\nu\sigma\tau}$ will not give contributions. Thus, the vertex tensor coupling to P must be constructed from the direct product of J_P Σ_μ's and the vertex tensor coupling to R must be constructed from J_R Σ'_μ's. Now, both Σ_μ and Σ'_μ enter with opposite sign into I and II. We have already removed any k^2 terms from the analysis, so that there are no scalar variables in the integrand. Thus, we can conclude that

$$T_{II}(s,t) = (-)^{J_P} (-)^{J_R} T_I(s,t) .$$

For this case we have found that there is a definite signature for the ASF terms and that this signature is equal to the product of the

signatures of the two Regge poles involved.

We can now extend our considerations somewhat by making use of isotopic spin. We now presume that the three spinless bosons A, B, and C all belong to the same isotopic spin multiplet. We will neglect any differences in mass among the members of the multiplet. For example, we consider the diagrams

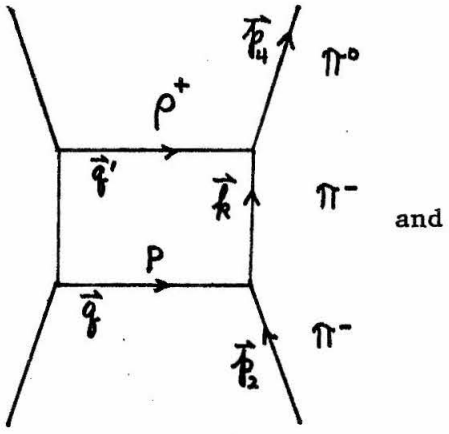

and

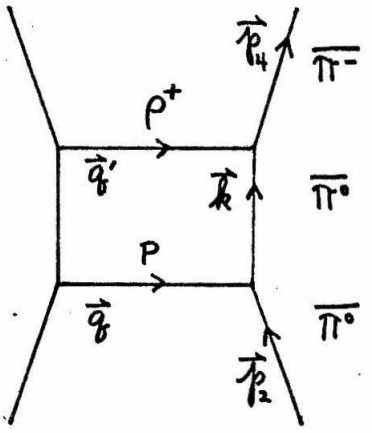

I II

where P is a Pomeranchon. The vertex tensor coupling to ρ^+ must be the direct product of J_P Σ'_μ's and the vertex tensor coupling to P is the product of J_P Σ_μ's. The same interaction that destroys the π^- and creates the π^0 will destroy $\overline{\pi^0}$ and create the $\overline{\pi^-}$. The only phases entering are those that give $\Sigma'_\mu \to -\Sigma'_\mu$. Similarly, the isoscalar Pomeranchon couples to π^-'s and to $\overline{\pi^0}$'s with the same strength and sign, so that the only phases entering are those that give $\Sigma_\mu \to -\Sigma_\mu$.

Thus, under line reversal we find the phase $(-)^{J_P}\ (-)^{J_\rho}$. Again the signature is the product of the signatures of the two exchanged Reggeons. This result holds whenever one of the Reggeons is a Pomeranchon and A,B, and C all belong to the same isotopic spin multiplet.

This analysis also indicates a definite signature for all other cases for which A, B, C all belong to the same integral isotopic spin multiplet, provided that it is applied to diagrams that possess a companion diagram under line reversal. For example, the pair

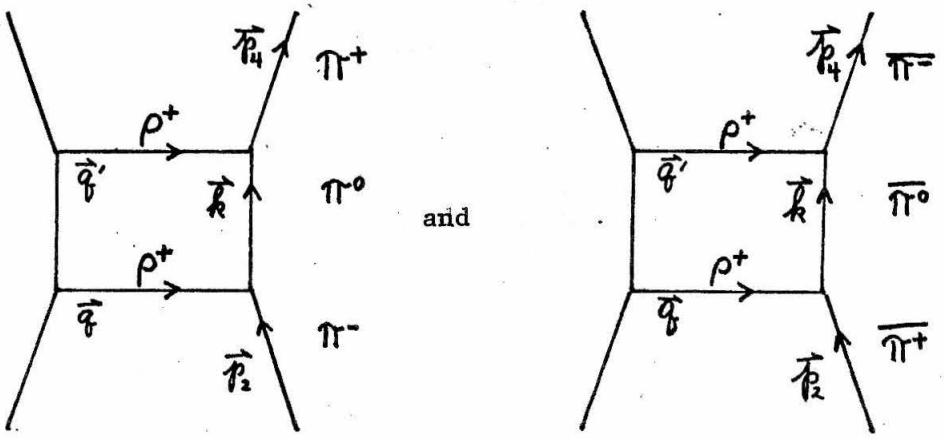

and

I II

are found to have a line reversal symmetry of $(-)^{J_{\rho^+}}\ (-)^{J'_{\rho^+}}$. The signature is the product of the signatures of the two Reggeons. We note that, in this example, the s-channel and u-channel processes are the same physical process. The same conclusions follow for exchange of two neutral ρ's. On the other hand, for the diagrams

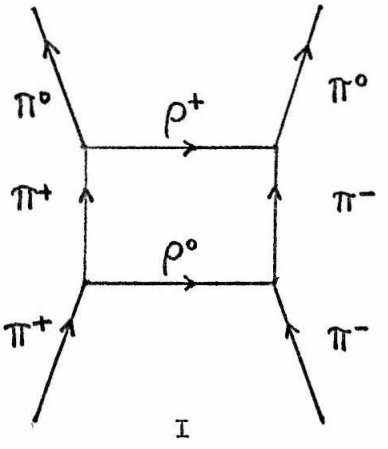

I

and

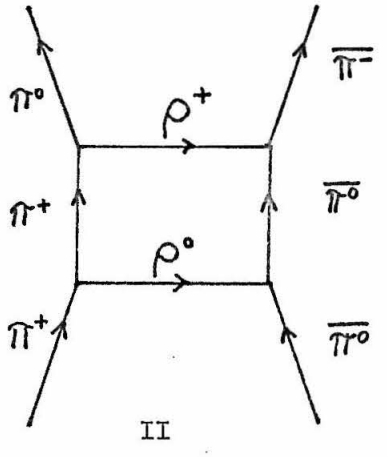

II

,

there is no line reversal symmetry because the second diagram is identically zero. The coupling of ρ^0 to two π^0's cannot occur without violating isotopic spin restrictions. In this example, process I does not possess a companion diagram under line reversal. This piece of the amplitude, consequently, does not possess a definite signature.

When the three particles A,B, and C belong to the same isotopic spin multiplet, but have half-integral isotopic spin, the conclusions are the same. For example, suppose the particles are kaons and the exchanged Reggeons are ρ's. For the diagrams

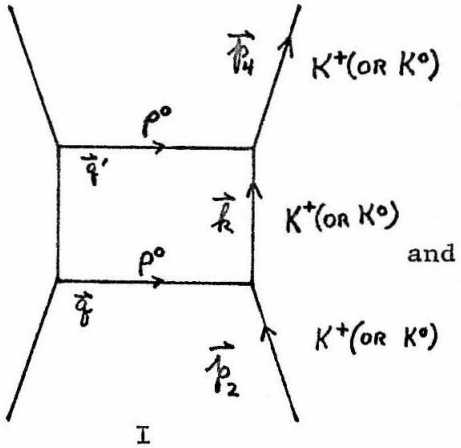

I

and

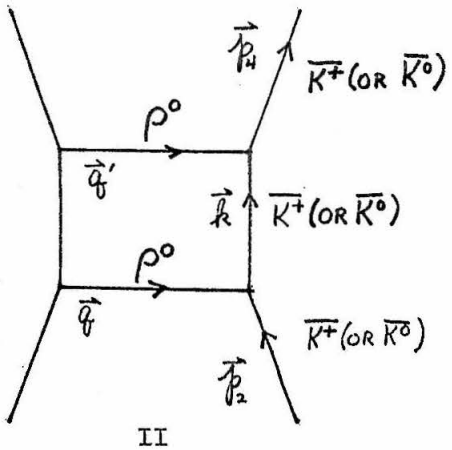

II

the above analysis applies and we find the line reversal symmetry $(-)^J\ (-)^{J'}$. There are no extra phases entering because the same operator that destroys (creates) a K^+ will create (destroy) a $\overline{K^+}$ without introducing phases.

Neither of the diagrams

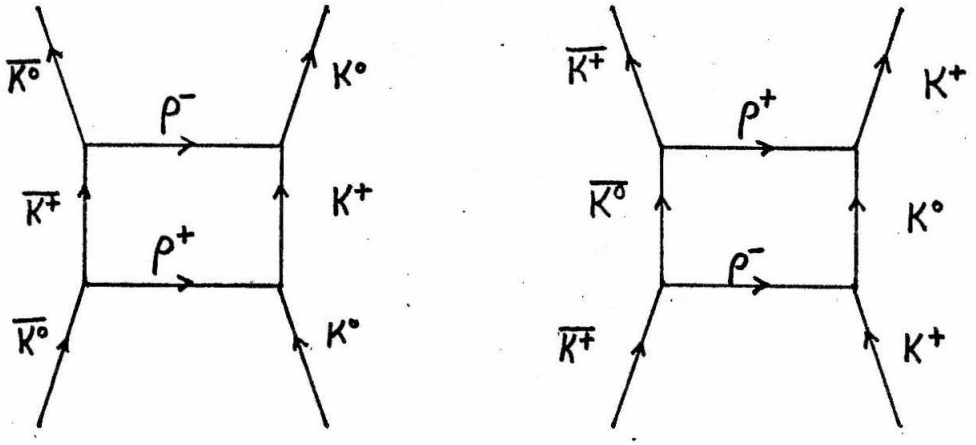

has a definite line reversal symmetry because neither possesses a companion diagram under line reversal. So, except for special cases to be mentioned later, there is no line reversal symmetry when A,B, and C are kaons and the two exchanged Reggeons are ρ^+ and ρ^-.

In the above analysis we have encountered certain diagrams which possessed no companion diagram under line reversal. Under certain conditions a companion diagram of a slightly different sort exists, i.e., we can mean something different by "line reversal". For example, we were unable to find a line reversal symmetry in the example above in which A,B, and C were pions and the exchanged Reggeons were ρ^0 and ρ^+. If, however, the left-hand side of the process had been different, say

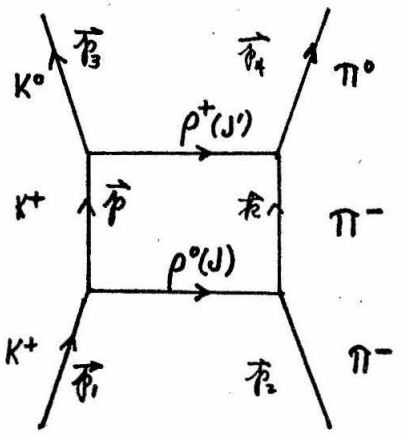

then it is possible to pair the above diagram with the "line reversed" diagram

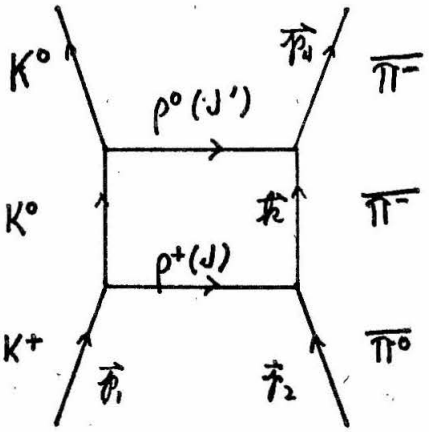

Then, using the isoscalar, charge conjugation invariant Lagrangian, we find that the couplings are zero unless both J and J' are odd, in which case we obtain the phase, + 1, between the two processes.

Now, we consider line reversal symmetry of the AFS diagrams when the particles on the right are baryons. For example, in the case of protons on the right side and the exchange of the Reggeons P and R we have the diagrams

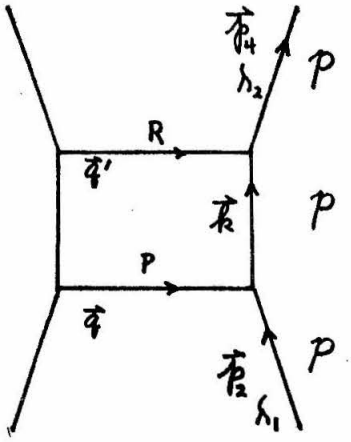

I

and

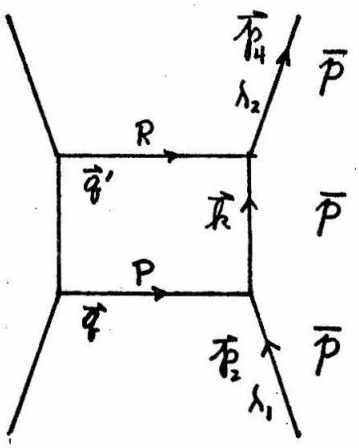

II

and, as above, we take $\Sigma = k + p_2$, $\Sigma' = p_4 + k$, $q = k - p_2$, and $q' = p_4 - k$. We again consider the double spectral functions so that we may have the internal legs on the mass shell. We must now consider all possible couplings at the vertices in all possible combinations for all integral J_P and J_R, where J_P is the integral spin of P and J_R is the integral spin of R. The general coupling to spin J has the form

$$(\delta_{\alpha\beta})^r(\delta_{\beta\gamma})^u \left[(\Box^2)^q (\partial_\mu)^s \partial_{\alpha_1}\partial_{\alpha_2} \cdots \partial_{\alpha_\ell} \bar{p}\right] \hat{o}_{\beta_1\beta_2\cdots\beta_m} \cdot$$

$$\left[(\Box^2)^{q'} (\partial_\mu)^s \partial_{\gamma_1}\partial_{\gamma_2} \cdots \partial_{\gamma_n} p\right]$$

where the nucleon fields are represented by the symbol for the particle which they destroy. The numbers q, q', s, r, and u are integers and the notation $(\partial_\mu)^s$ indicates that s gradients of $\bar{p}$

are contracted with s gradients of p. The quantity $\hat{O}_{\beta_1\beta_2 \cdots \beta_m}$ is a Dirac operator. The notation $(\delta_{\alpha\beta})^r (\delta_{\beta\gamma})^u$ indicates that r of the indices, α, are contracted into the Dirac operator and that u of the indices, β, are contracted into the Dirac operator. Since this coupling is to have J free indices, we must have $(\ell - r) + (n - u) + + (m - r - u) = J$. A $\delta_{\mu\nu}$ term cannot occur because the propagator is traceless. Any $\epsilon_{\alpha\beta\gamma\delta}$ terms may be expressed in terms of the sixteen Dirac operators and are therefore included in a sum of couplings of the form given above.

The Laplacians may be dismissed from our analysis, because they only give squares of the nucleon mass and, consequently, contribute in the same way to the two diagrams. Similarly, the $(\partial_\mu)^s$ terms may be disregarded because they produce the same factors in I and II, e.g., if they introduce $(-)^s (p_4 \cdot k)$ or $(-)^s (k \cdot p_2)$ into I then they introduce the same factor into II. Another way to see this is to realize that these terms produce scalars like $(\Sigma \cdot \Sigma)$, $(q \cdot q)$, and $(\Sigma \cdot q)$. Now, $(\Sigma \cdot \Sigma)$ and $(q \cdot q)$ are even under line reversal and $\Sigma \cdot q$ is zero on the mass shell, so that the contribution is the same for the two processes.

The ∂_α and ∂_γ parts introduce Σ_μ and q_μ. The q_μ part gives no contribution because the propagator is traceless on the mass shell. Consequently, the gradients introduce the direct product of $[(\ell - r) + (n - u)]\Sigma_\mu$'s. We already know that Σ_μ is odd under line reversal, so that a phase $(-)^{(\ell - r) + (n - u)}$ results from this part.

This reduction leaves only a few terms to be considered. When Reggeons of positive intrinsic parity are exchanged, the couplings which are still to be analyzed are $(-)^{(\ell - r) + (n - u)}$ times the following terms

1) $\bar{p}\, p$: $(m - r - u) = 0$

2) $(\partial_\alpha \bar{p})\, \gamma_\alpha p$ and $\bar{p}\, \gamma_\alpha (\partial_\alpha p)$: $(m - r - u) = 0$

3) $\bar{p}\, \gamma_\alpha\, p$: $(m - r - u) = 1$

4) $(\partial_\beta \bar{p})\, \sigma_{\alpha\beta}\, p$ and $\bar{p}\, \sigma_{\alpha\beta} (\partial_\beta p)$: $(m - r - u) = 1$

5) $(\partial_\alpha \bar{p})\, \sigma_{\alpha\beta}\, (\partial_\beta p)$: $(m - r - u) = 0$

All other couplings either give no contribution or can be expressed in terms of these. When these interactions couple to R, they involve the momenta k and p_4, or, equivalently, Σ' and q'. When they couple to P, they involve the momenta p_2 and k, i.e., Σ and q. Now, concentrating on the Dirac operators and the spinors, let us suppose that P couples to the Dirac operator $\hat{O}_P$ and that R couples to the operator $\hat{O}_R$. Appealing again to the behavior of spinors and Dirac operators under charge conjugation, we find in the intergrands for processes I and II:

$$\text{I} : \int \text{---}\ \bar{u}_{p_4 \lambda_2}\ \hat{O}_R\ (\not{k} + iM)\ \hat{O}_P\ u_{p_2 \lambda_1}$$

$$\text{II} : \int \text{---}\ \bar{u}_{p_4 \lambda_2}\ \tilde{O}_R\ (\not{k} + iM)\ \tilde{O}_P\ u_{p_2 \lambda_1}$$

where $\hat{O} \to \tilde{O}$ in the following way

$$1 \to 1,\ \gamma_5 \to \gamma_5,\ \gamma_5\gamma_\mu \to \gamma_5\gamma_\mu,\ \gamma_\mu \to -\gamma_\mu,\ \sigma_{\mu\nu} \to -\sigma_{\mu\nu}\ .$$

Now we can consider the remaining couplings in light of these mappings. We see that the coupling (1), $\bar{p}\ p$, is even under line reversal, contributing a factor $+1 = (-)^0 = (-)^{m-r-u}$. The couplings (2) can introduce the terms $\Sigma_\mu\gamma_\mu$ and $q_\mu\gamma_\mu$ (or $\Sigma'_\mu\gamma_\mu$ and $q'_\mu\gamma_\mu$ for coupling to R). Now we observe that

$$\bar{u}_{p_4\lambda_2}\not{q}'(\not{k} + iM) = \bar{u}_{p_4\lambda_2}(\not{p}_4 - \not{k})(\not{k} + iM) = \bar{u}_{p_4\lambda_2}(iM - iM)(\not{k} + iM) = 0,$$

since, by the Dirac equation,

$$\bar{u}_{p_4\lambda_2}\not{p}_4 = iM\,\bar{u}_{p_4\lambda_2}$$

and, on the mass shell

$$\not{k}\not{k} = k^2 = -M^2, \text{ so that } \not{k}(\not{k} + iM) = iM(\not{k} + iM).$$

Therefore, the $\not{q}'$ coupling gives no contribution. Similar considerations also rule out $\not{q}$. The remaining terms, $\not{\Sigma}$ and $\not{\Sigma}'$ are even under line reversal, so that the net effect is the phase $+1 = (-)^0 = (-)^{m-r-u}$.

The coupling (3), $\bar{p}\ \gamma_\alpha\ p$, is odd under line reversal. Therefore, it contributes the phase $(-)^1 = (-)^{m-r-u}$. The couplings, (4), can introduce $\sigma_{\alpha\beta}\ \Sigma_\beta$ and $\sigma_{\alpha\beta}\ q_\beta$ for coupling to P or $\sigma_{\alpha\beta}\ \Sigma'_\beta$ and $\sigma_{\alpha\beta}\ q'_\beta$ for coupling to R. From the Dirac equation and the fact that $\not{k}\not{k} = -M^2$ it follows that $\sigma_{\alpha\beta}\ \Sigma_\beta \sim q_\alpha$ and $\sigma_{\alpha\beta}\ \Sigma'_\beta \sim q'_\beta$, so that these terms are ineffective. The remaining terms, $\sigma_{\alpha\beta}\ q_\beta$ and $\sigma_{\alpha\beta}\ q'_\beta$, are odd under line reversal and consequently, introduce the phase $(-)^1 = (-)^{m-r-u}$.

Finally, the coupling, (5), can introduce $\sigma_{\alpha\beta}\ \Sigma_\alpha\ q_\beta$ for coupling to P or $\sigma_{\alpha\beta}\ \Sigma'_\alpha\ q'_\beta$ for coupling to R. In either case, the term is even under line reversal, so that the phase introduced is $+1 = (-)^0 = (-)^{m-r-u}$.

Summarizing the results of this analysis we find, for all possibilities, that the phase under line reversal for coupling to the Reggeon of spin J is $(-)^{(\ell-r)+(n-u)+(m-r-u)} = (-)^J$. Thus, we have shown that when both of the Reggeons have positive intrinsic parity and have integral spins J_P and J_R, then there is a definite line reversal symmetry of $(-)^{J_P}\ (-)^{J_R}$. This result holds at every integral J_P and J_R, regardless of what linear combination of the possible couplings either Reggeon might use at that integral spin. This symmetry will continue to be present, even for non-integral J_P and J_R and we conclude that the signature of this iterated Regge pole diagram is equal to the product of the signatures of the two Regge poles.

When one or both of the Reggeons has negative intrinsic parity, i.e., (signature) (parity) = - 1 we must use a selection rule to avoid the mixing of the two pseudovector couplings: $\Sigma_\mu\gamma_5$ and $\gamma_5\gamma_\mu$. Just as in the case of single Reggeon exchange, the selection rule is provided by considering a negative parity Reggeon with definite C and/or G. For the proton scattering example, there are three cases:

1. parity of P = - , parity of R = +, line reversal phase = $C_P(-)^{J_R}$
2. parity of P = +, parity of R = -, line reversal phase = $C_R(-)^{J_P}$
3. parity of P = -,,parity of R = -, line reversal phase = $C_P C_R$.

for all integral J_P and J_R.

It is clear that the same conclusions follow for the other baryons under exchange of neutral, non-strange Reggeons, i.e., $A \equiv B \equiv C = n, \Lambda, \Sigma$, or Ξ. Generalization to charge exchange processes by considering isotopic spin is similar to the boson cases discussed above. We must again be sure that a companion diagram exists.

For diagrams exchanging more than two Reggeons, the analysis is essentially the same. One again considers the double spectral functions in order to simplify the analysis. The resulting conclusions are are apparent, e.g.,

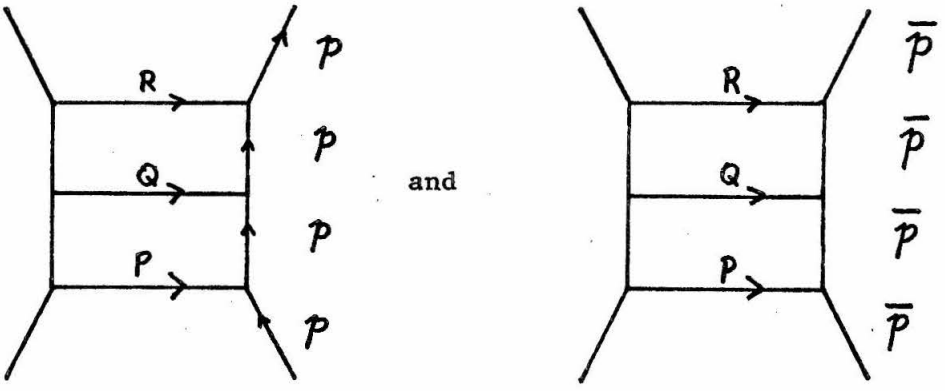

for scattering of protons by Reggeons P, Q, and R of positive intrinsic parity, the line reversal phase is $(-)^{J_P}(-)^{J_Q}(-)^{J_R}$.

We emphasize that we have found that, in many cases, there is a definite line reversal symmetry for the AFS diagrams. Furthermore, we find that the diagrams pertaining to important scattering processes, from the standpoint of present day interest, do possess such a symmetry.

For example, direct scatterings proceeding by exchange of Pomeranchons (or any neutral, non-strange Reggeons) possess this symmetry. The symmetry factor τ appearing in Eq. (II.7) is chosen on the basis of the conclusion reached in this section, e.g., for p p scattering via exchange of N Pomeranchons, M Igi poles, L ω-poles, we get $\tau = (+)^N (+)^M (-)^L = (-)^L$. These assignments allowed us to obtain the real part of the scattering amplitude for our attempted data fitting.

We now consider diagrams of the type considered by Mandelstam. The properties of these diagrams is of great interest because these diagrams actually produce Regge cuts on the physical sheet of the angular momentum plane. Unfortunately, they are far more difficult to analyze, so that we will only be able to treat a portion of the amplitude resulting from these diagrams.

One interesting feature of these diagrams is that the companion diagram under line reversal always exists, even if the Reggeons carry strangeness. Consider the diagrams:

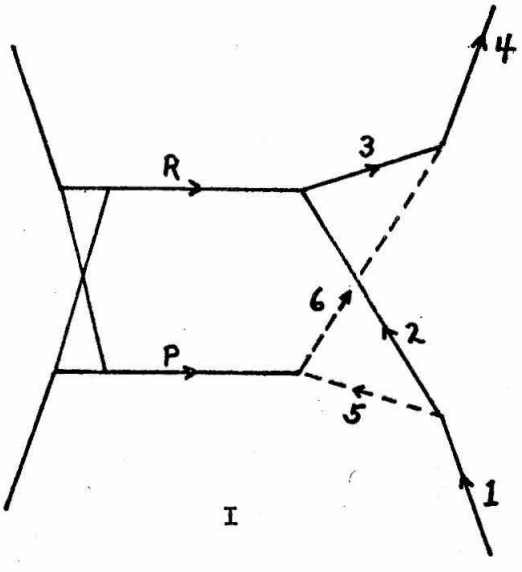

I

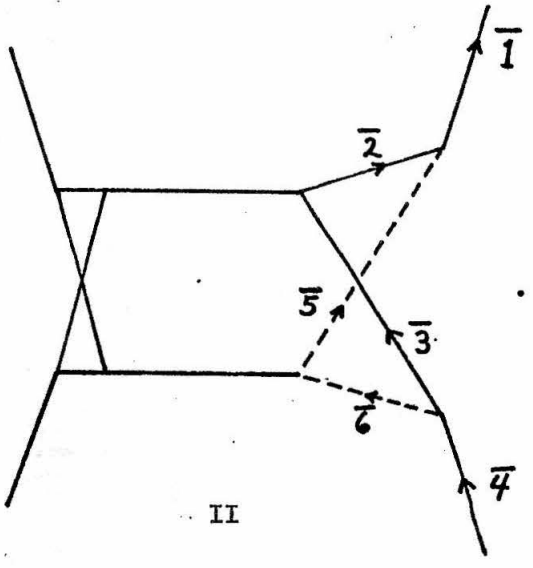

II

We observe that the existence of process I guarantees the existence of II, because the existence of all couplings found in II follows from the couplings occuring in I. It appears on the basis of our crude analysis, that this property will enlarge the list of cases with definite signature.

In order to apply the understanding of the couplings that we obtained from the analysis of the AFS diagrams, we restrict our considerations to those cases in which each of the particles 2, 3, 5, and 6 is either a spinless boson or a spin one-half baryon. For purposes of discussion we shall label the momenta in the following way

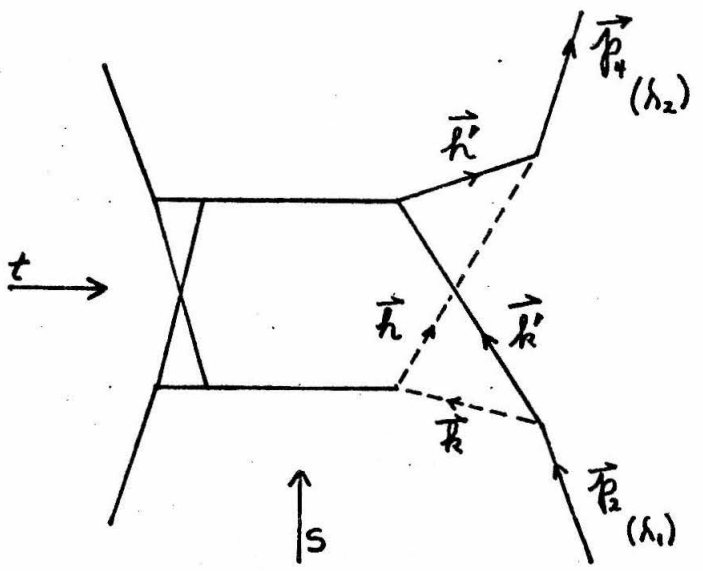

We will need to simplify the analysis, as before, by putting all internal legs on the mass shell. This diagram, however, is far

more complicated than the AFS diagrams. The Feynman integral for this graph has a very complex structure and we will be able to consider only part of the amplitude corresponding to this graph. There are three particle cuts in the t-channel that we are not able to take into account. We will attempt to understand the line reversal properties of the piece of the amplitude resulting from the discontinuity across the "two particle" unitarity cut through the two Reggeons in the t-channel. We then can estimate the discontinuity by putting the remaining internal legs on the mass shell and dispersing the resulting double spectral functions over their corresponding cuts. This is, of course, a drastic oversimplification of a very complex situation. It turns out, though, that we can find a manifest line reversal symmetry by putting all internal legs on the mass shell. Thus, at least, the part of the diagram that we can study in detail does possess a line reversal symmetry.*

---

* With some reflection, one might guess that it might be possible to see a manifest symmetry without putting the internal legs 2, 3, 5, and 6 on the mass shell. The idea might be that there is some freedom allowed in the assignment of the internal momenta that was not found in the AFS diagrams. We refer to the fact that under the exchange of the labels h and k', all other momentum labels remain the same, except $h' \to h' + h - k'$ and $k \to k + k' - h$. There is also another transformation possible that leaves all momentum labels unchanged except for $k' \to -h'$, $h' \to -k'$, $k \to k + h' + k'$, $h \to h + h' + k'$. We find it impossible to obtain a manifest symmetry by expressing the amplitude various ways in terms of these possibilities.

For example, consider the processes

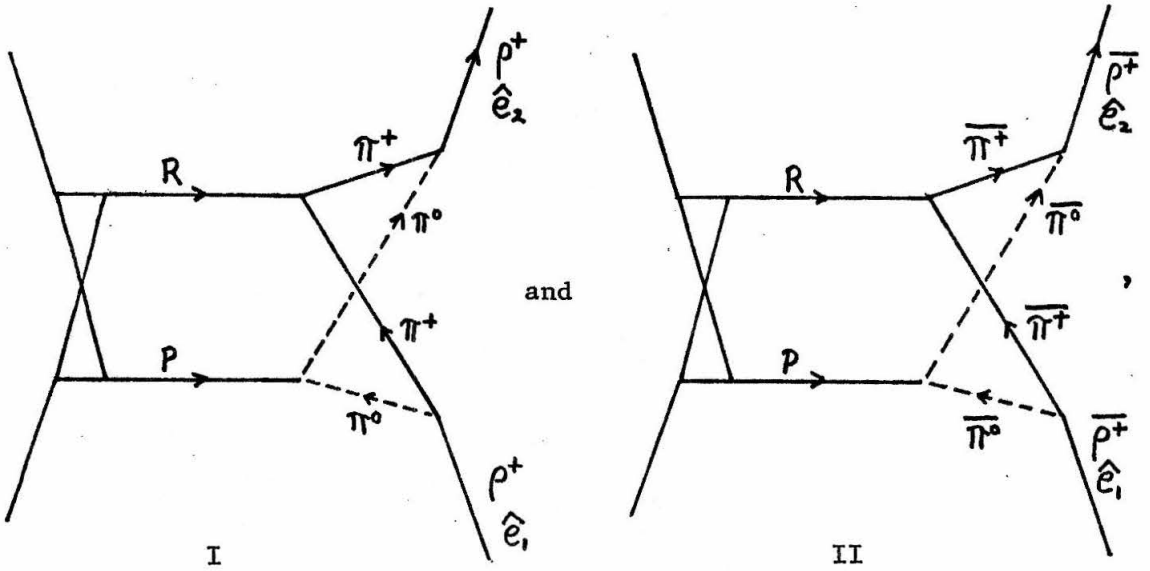

where $\hat{e}_1$ and $\hat{e}_2$ are polarization vectors for the ρ. For the interaction of the ρ with two pions we take $\mathcal{L} \sim \rho_\alpha \, \pi \times \partial_\alpha \, \pi$. The $\rho\pi\pi$ vertices are both odd under line reversal so that the net effect is + 1 from this part. The analysis above for the AFS diagrams applies to the coupling of the pions to the nucleons, so that we may conclude that there is a line reversal symmetry of $(-)^{J_P}(-)^{J_R}$. The same conclusion holds for the other diagrams one might draw, even for the charge exchange processes, i.e., even when the Reggeons carry charge. One may easily see that the factor $(-)^{J_P}(-)^{J_R}$ occurs whenever particles 2, 3, 5, and 6 are scalar bosons.

For processes involving spin one-half baryons, we again exclude Reggeons with (signature)(parity) = - 1. As an example, consider

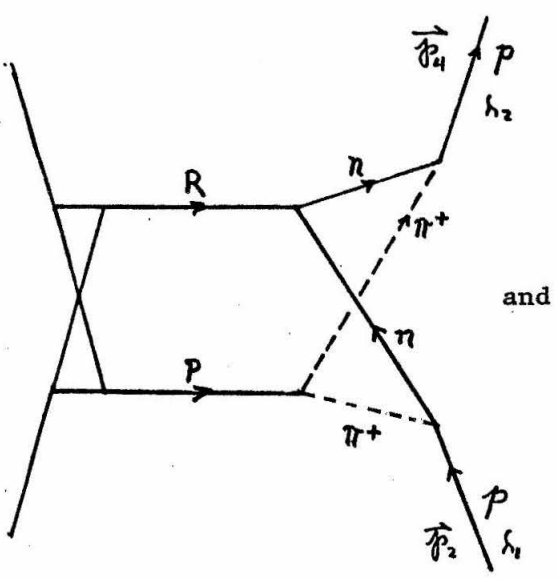

and

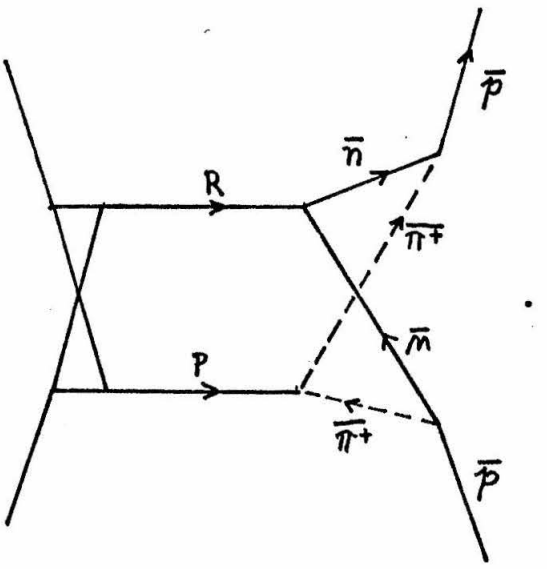

We take the πNN interactions to be $\mathcal{L} \sim \pi \cdot \bar{N}\, \tau\gamma_5\, N$. The relevant part of the integrand of the Feynman integrals may be written

$$T_I \sim \int \cdots V^{(k,h)}_{P\pi^+\pi^+}\, \bar{u}_{p_4\lambda_2}\, \sqrt{2}\, \gamma_5\, (\not{k}' + iM)\, V^{(k',h')}_{Rnn} \cdot$$

$$\cdot\, (\not{k}' + iM)\, \sqrt{2}\, \gamma_5\, u_{p_2\lambda_1}$$

$$T_{II} \sim \int \cdots V^{(k,h)}_{P\pi^-\pi^-}\, \bar{u}_{p_4\lambda_2}\, \sqrt{2}\, \gamma_5\, (\not{k} + iM)\, \tilde{V}^{(k',h')}_{R\bar{n}\bar{n}} \cdot$$

$$\cdot\, (\not{k}' + iM)\, \sqrt{2}\, \gamma_5\, u_{p_2\lambda_1}$$

where the V's denote the contributions from the Reggeon vertices. We already understand the vertex parts from our previous analysis of the AFS diagrams and can say that the line reversal symmetry is $(-)^{J_P}(-)^{J_R}$

provided R has positive intrinsic parity. These conclusions plainly hold for other baryon processes. We remark that when the Reggeons carry strangeness the same analysis pertains and leads to the same conclusions, provided that the energy is high enough that mass differences may be ignored.*

---

* We mention that even for the Mandelstam diagrams, however, there are some cases where there appears to be no line reversal symmetry. For example, suppose that there exists a particle, ξ, with the same mass as the ρ meson, but with T = S = Q = J = 0, P = +, G = +, i.e., a heavy (ABC) particle. We take identical masses for convenience in discussion. We consider the diagrams

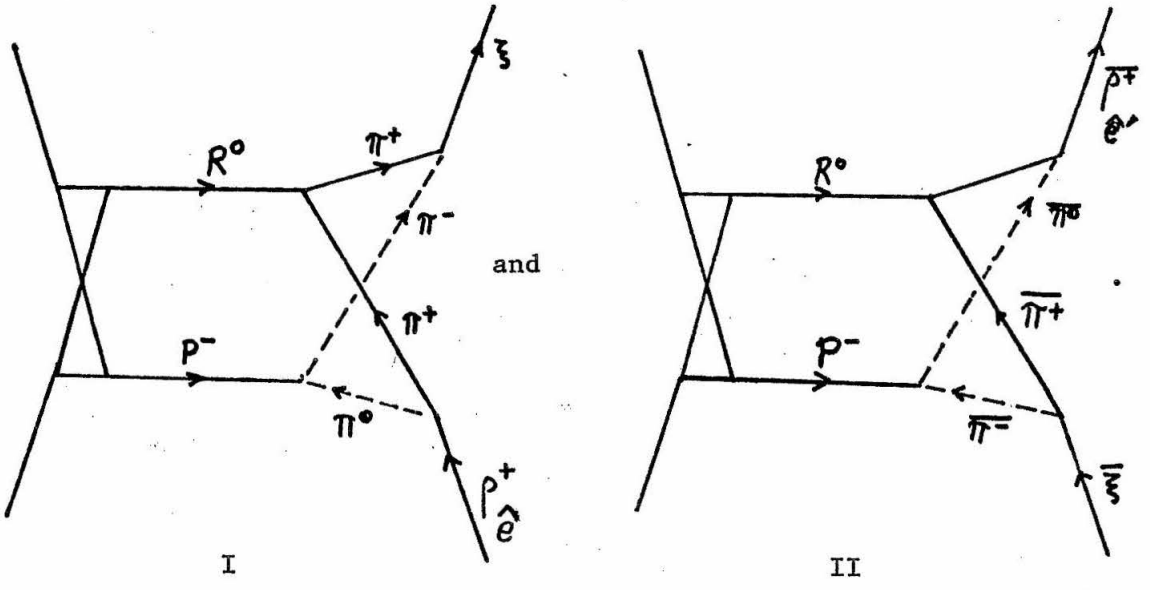

I II

Suppose we have the interactions $\mathcal{L} \sim \xi\, \vec{\pi} \cdot \vec{\pi}$ and $\mathcal{L} \sim \vec{\rho}_\alpha \cdot \vec{\pi} \times \partial_\alpha \vec{\pi}$. The difficulty comes from the fact that in I we find the momenta $\hat{e} \cdot (k - k')$ in the integrand, but in II we get $\hat{e} \cdot (h - h')$. This effect forces us to be cautious, but with the usual Yukawa couplings the mechanism operates in very few special cases.

To summarize, we have used an analysis similar to Wagner's analysis of Regge pole terms. By considering all possible couplings to intermediate bosons with arbitrary integral spin, we obtain the line reversal symmetry. We find results, in most important cases, consistent with the supposition that the iterated Regge pole diagrams make a definite signature contribution to the scattering amplitude. We were only able to study a portion of the Mandelstam diagrams in detail. However, we found that this piece does possess a line reversal symmetry in most cases.

VI. EXPERIMENTAL TEST OF THE MODEL AT MACHINE ENERGIES

Having discussed the nature of our model for the cuts in detail, we now consider its relation to the existing experimental data. In this section we discuss our attempts to fit the high-energy elastic scattering data of Foley et al.[16]. Our objective was to find out if the cuts could replace the Igi pole[17] and still allow a detailed fit to the data. Consequently we employed only the Pomeranchuk and ω Reggeons together with the associated cuts generated by our procedure. We found that such a model is unable to fit the existing data if all of the iteration terms are kept. This failure may be traced to the convergence condition of Eq. (III.16). We studied the physical nature of this condition and found it to be equivalent to the partial wave unitarity bound on the inelastic part of the amplitude. Thus, any appropriate scattering model must satisfy this condition. Examination of various Regge pole fits[17,19,27,28,29] reveals that the parameters are such that a partial wave projection of the pole terms is 20 to 70% larger than the low partial wave inelastic unitarity limit. This limit applies, of course, to the projection of the entire inelastic part, not just the pole term. We therefore, find that the AFS cut terms, present in the inelastic part and, according to Mandelstam, cancelling part of the pole terms, must be a significant fraction of the size of the pole terms. One may anticipate this result by looking at the data directly.

We enter into the discussion of these matters by first considering the physical nature of the convergence criterion (III.16).

In our notation, the unitarity condition is given by (II.5)

$$A(s,t) = \frac{1}{64\pi^2\sqrt{r}} \int d\Omega \; T^{+}_{el} \; T_{el} + A_{in}(s,t) \; .$$

The partial wave expansion of the amplitude is

$$T(s,t) = D(s,t) + iA(s,t) = 16\pi\sqrt{r} \sum_{\ell=0}^{\infty} (2\ell + 1) \left[\frac{a_\ell - 1}{2i}\right] P_\ell \; (\cos \theta)$$

(VI.1)

where $a_\ell = e^{2i\delta_\ell}$ and δ_ℓ is a complex phase shift. The expressions for cross-sections then become

$$\frac{d\sigma}{d\Omega} = \frac{1}{64\pi^2 s} \left| T(s,t) \right|^2$$

(VI.2)

$$\frac{d\sigma}{dt} = \frac{r|T(s,t)|^2}{16\pi s^2}$$

$$\sigma_{elastic} = \frac{4\pi r}{s} \sum_{\ell=0}^{\infty} (2\ell + 1) \left| 1 - a_\ell \right|^2$$

$$\sigma_{inelastic} = \frac{4\pi r}{s} \sum_{\ell=0}^{\infty} (2\ell + 1) \left[1 - \left| a_\ell \right|^2 \right] = \frac{\sqrt{r}\, A_{in}(s,0)}{s}$$

$$\sigma_{TOTAL} = \sigma_{el} + \sigma_{in} = \frac{8\pi r}{s} \sum_{\ell=0}^{\infty} (2\ell + 1) \left[1 - \text{Re } a_\ell \right] = \frac{\sqrt{r}\, A(s,0)}{s} \qquad \text{(VI.2)}$$

where $s_0 = 4k^2$ and $r = \frac{s}{s_0}$.

We define

$$T_\ell \equiv \frac{a_\ell - 1}{2i} \quad , \text{ so} \quad \text{Im } T_\ell = \frac{1 - \text{Re } a_\ell}{2} \leqslant 1 \ . \qquad \text{(VI.3)}$$

Equation (VI.1) then gives

$$A(s,t) = 16\pi \sqrt{r} \sum_{\ell=0}^{\infty} (2\ell + 1) \left[\text{Im } T_\ell \right] P_\ell(\cos \theta) \ . \qquad \text{(VI.4)}$$

Putting (VI.1) and (VI.4) into the unitarity condition and making use of the orthogonality properties of Legendre polynomials, we have

$$\text{Im } T_\ell = \left| T_\ell \right|^2 + B_\ell \qquad \text{(VI.5)}$$

where B_ℓ is real and is given by

$$B_\ell \equiv \frac{1}{32\pi \sqrt{r}} \int_{-1}^{1} d(\cos \theta)\, P_\ell(\cos \theta)\, A_{in}(s,t) \ . \qquad \text{(VI.6)}$$

If we now take

$$T_\ell \equiv u_\ell + i\, v_\ell = \frac{1}{2} \text{Im } a_\ell + \frac{i}{2} (1 - \text{Re } a_\ell) \qquad \text{(VI.7)}$$

equation (VI.5) becomes

$$v_\ell = u_\ell^2 + v_\ell^2 + B_\ell$$

or

$$v_\ell = \frac{1}{2} \pm \sqrt{\frac{1}{4} - u_\ell^2 - B_\ell} \ . \qquad \text{(VI.8)}$$

Since v_ℓ is a real quantity, Eq. (VI.8) gives the restriction

$$B_\ell \leqslant \frac{1}{4} (1 - \mathrm{Im}^2\, a_\ell) \leqslant \frac{1}{4} \ . \qquad \text{(VI.9)}$$

The condition given in (VI.9) can be directly related to the bound for inelastic scattering cross-sections. It must be true that

$$1 - \left| a_\ell \right|^2 \leqslant 1,$$

but

$$a_\ell = 1 + 2i\, T_\ell \ .$$

so that

$$1 - \left| a_\ell \right|^2 = 4\, \mathrm{Im}\, T_\ell - 4 \left| T_\ell \right|^2 \ .$$

Then, using (VI.5) we conclude

$$1 \geqslant 1 - \left| a_\ell \right|^2 = 4\, B_\ell \Longrightarrow B_\ell \leqslant \frac{1}{4} \ . \qquad \text{(VI.10)}$$

This condition is in agreement with (VI.9).

Any scattering model must be consistent with (VI.10). In order to see that this condition is related to our convergence criterion (III.16), let us recall that our iteration procedure is started by a Regge pole term. This effectively assumes that it is appropriate to approximate the inelastic-intermediate-state part of the unitarity

relation by a Regge pole term. For example, if all of the inelastic effects could be represented by a Pomeranchuk pole alone, then

$$A_{in}(s,t) = \sqrt{16\pi}\ \Gamma\ s \left(\frac{s}{\sigma}\right)^{pt} . \qquad \text{(VI.11)}$$

We consider the S-wave projection:

$$B_0 = \frac{1}{32\pi\sqrt{r}} \left[\sqrt{16\pi}\ \Gamma\ s\right] \int_{-1}^{1} d(\cos\theta)\ P_0(\cos\theta)\ e^{zt} \qquad \text{(VI.12)}$$

where $t = -1/2\ s_0(1 - \cos\theta)$. Performing the integral, we obtain

$$B_0 = \frac{\Gamma\sqrt{r}}{\sqrt{16\pi}\ z} = \frac{1}{R} , \text{ so that } B_0 \leqslant \frac{1}{4} \Rightarrow R \geqslant 4 . \qquad \text{(VI.13)}$$

We have therefore furnished a physical explanation for the convergence criterion (III.16).

To obtain some feeling for the implications of our criterion, let us consider the pp data of Foley et al.[16]. The data at incident momentum 8.8 BeV/c, i.e., $s = 18.37\ \text{BeV}^2$, is

$$\frac{d\sigma}{dt} \gtrsim \frac{1}{0.390} \left(\frac{\text{BeV}^{-2}}{\text{mb}}\right) \cdot e^{4.66 + 9.47t} \left(\frac{\text{mb}}{\text{BeV}^2}\right) = \frac{r}{16\pi s^2} \left|T(s,t)\right|^2 .$$

So we must have

$$\left|T(s,t)\right| = \frac{\sqrt{16\pi}\ s}{\sqrt{0.390}\ \sqrt{r}}\ e^{2.33 + 4.73t} .$$

Now as a measure of how close this data may be to pure inelastic absorption scattering, let us suppose T(s,t) is purely imaginary, at least, for very small t, since our integral will be almost entirely determined by the small t region. This allows us to write

$$A_{in}(s,t) \approx \frac{\sqrt{16\pi}\, s}{\sqrt{0.390}\sqrt{r}}\; e^{2.33 + 4.73t} .$$

We then find

$$B_0 \approx \frac{1}{32\pi\sqrt{r}} \left[\frac{\sqrt{16\pi}\, s}{\sqrt{0.390}\sqrt{r}}\right] \int_{-1}^{1} d(\cos\theta)\; e^{2.33 + 4.73t} = \frac{1.97}{4}$$

which would violate the bound $B_0 \leqslant \frac{1}{4}$. At the higher energy 16.7 BeV/c, $s = 33.15$ BeV^2,

$$\frac{d\sigma}{dt} \approx \frac{1}{0.390}\; e^{4.52 + 9.44t}$$

and the bound would be violated in the same way. For $\bar{p}p$ scattering at 12.0 BeV/c, $s = 24.36$

$$\frac{d\sigma}{dt} \approx \frac{1}{0.390}\; e^{4.99 + 12.46t}$$

which gives $B_0 \approx 1.76/4$.

These results make it abundantly clear that the data in this region is not to be fit with a pure inelastic absorption scattering model, i.e., a successful model must contain a large real part or a considerable elastic part.

As an example of a pole model we consider the analysis made by Desai and Binford[17] which employs three Regge poles. The Pomeranchon, Igi pole, and ω pole are used to fit the pp, $\bar{p}p$, K^+p, and K^-p data of Foley et al.[16]. The π^+p and π^-p data are fit without the ω. Linear trajectories of equal slopes were presupposed, with the Igi and ω trajectories passing through $\alpha = 1/2$ for $t = 0$. The

slope for best fit was $\alpha'(0) \approx 0.4$ BeV^{-2}. The coupling coefficients at t = 0 were presumed equal for the Igi and ω poles. Instead of taking a pure exponential form like (III.2), they chose the form

$$\bar{\gamma}_i(t) = \bar{\gamma}_i(0)(1 - b_i t)^{-\epsilon_i} \quad , \quad i = P, \text{ Igi}$$

with ϵ_i and b_i chosen to give appropriate exponential fall off for small t and to be consistent with the Serber result[18] that for pp scattering, $d\sigma/dt$ goes like $|t|^{-5}$ for large -t. Their form falls off less rapidly than the pure exponential form. For the ω pole the form

$$\bar{\gamma}_\omega(t) = \bar{\gamma}_\omega(0)(1 - b_\omega t)^{-\epsilon_\omega}\left[1 + \frac{t}{t_0}\right]$$

was used. The extra factor of $(1 + t/t_0)$ was included so that the model would allow the pp and $\bar{p}p$ cross-section curves to cross. The fact that the $\bar{p}p$ differential cross-section is greater than the pp at t = 0 and less at t = - 0.5 BeV^2 can only be represented in this model by allowing $\bar{\gamma}(t)$ to have a zero[19] *. The parameter t_0 was found to be 0.074 for $\bar{p}p$ - pp scattering. This model is unable to account for any differences in π^+p and π^-p scattering.

Desai and Binford obtain rather nice fits to the data for t between 0 and - 0.4 or -0.5. Supposing that the Regge poles contribute only to the part of the unitarity condition corresponding to inelastic intermediate states, we might identify the imaginary part of the three

---

* Desai has shown[20], on the basis of potential theory, that if there is a strong short range repulsion in addition to long range attraction, then $\bar{\gamma}(t)$ can change sign.

pole amplitude of Desai and Binford with the term $A_{in}(s,t)$ in the unitarity condition (II.5). Then, for example, in the case of pp scattering at s = 18.37 BeV^2 we would find, using their parameters,

$$B_0 > \frac{1.2}{4} \quad .$$

Similarly, the other Regge pole fits to various scattering processes[19,27,28,29] are always found to yield an S-wave projection which is 20 to 70% larger than 1/4. This excess in the projection occurs for the first four or five partial waves*. It is clear that this excess is not due to the existence of a real part in the amplitude, because the fitting to the data was performed with the real part represented and the parameters occuring in the projection reflect this fact. Thus, providing that these fits are, in fact, consistent with unitarity, we have a measure of the relative magnitudes of the AFS cut terms and the pole terms. Since Mandelstam has shown that the AFS cut terms occur in the inelastic amplitude with sign opposite to that of the pole term, we infer that they must be large enough to account for the 20 to 70% effect. It is clear

---

* For the scattering of particles with spin, one can easily show, using the simplifications of Jacob and Wick[30], that the only modification necessary is that, for helicity non-flip amplitudes, the inversion formula (IV.6) will involve $d^j_{11}(\theta)$ for πN scattering or $d^j_{11}(\theta)$ and $d^j_{00}(\theta)$ for NN scattering. However, since the amplitudes drop off so rapidly in t, and since all of the lowest partial wave d-functions are unity to a very good approximation over the important values of θ, the presence of spin does not modify our analysis significantly. The $P_\ell(\theta)$ are also unity over the important range, so that excesses would occur for the first four or five or more partial waves.

from this discussion that there must be large terms other than the Regge poles in the inelastic part of the amplitude*.

Having considered the Regge pole models, we turn now to our own attempt at data fitting. We have made a serious effort to fit the same data[16] using the Pomeranchuk and ω poles and some of the cut terms that arise in our iteration technique. Our objective was to see if we could obtain fits as good as those of Desai without using the Igi pole. We wanted to see if the "Igi pole" might, in fact, be a contribution arising from cut terms.

The cut terms that contribute most strongly are those from iteration of Pomeranchons

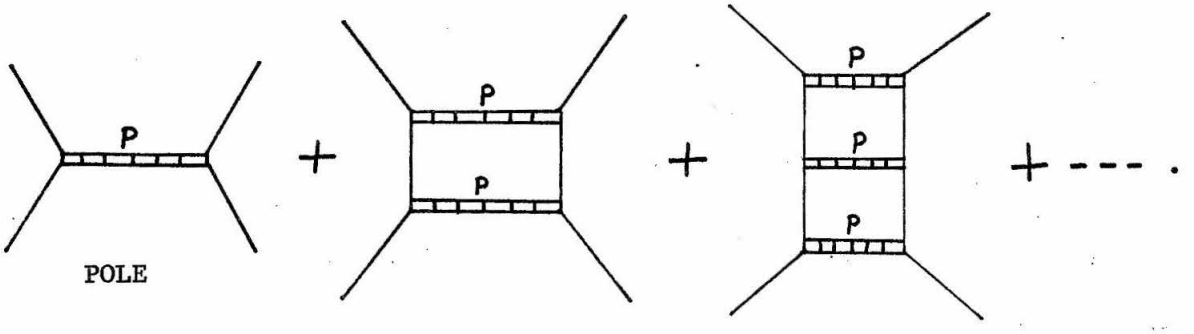

These terms are collected as indicated in (III.9) and lead to expression (III.12). Another series of cut terms, contributing more weakly, is that from the iteration of one ω pole with any number of Pomeranchons:

---

* I am indebted to Dr. Stanley Mandelstam and Dr. Geoffrey Chew for a very helpful discussion of this point.

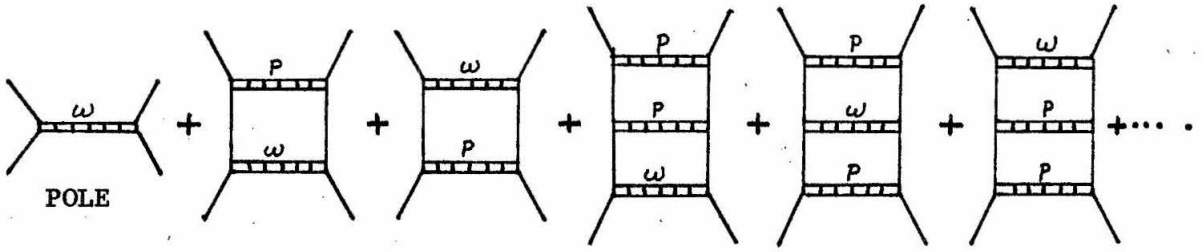

These terms are collected as indicated in (III.10) and the corresponding series is discussed in Appendix E. This series is somewhat more complicated because, for the imaginary part of the ω pole term, we have taken

$$A^{\omega}_{in}(s,t) = -\sqrt{16\pi}\,\bar{\Gamma}s\left(\frac{s}{\bar{\sigma}}\right)^{a-1}\, e^{\bar{z}t}\,\left(1 + \frac{t}{t_0}\right) \qquad \text{(VI.14)}$$

where a is the intercept of the ω trajectory at t = 0. This expression for ω pole term is derived from (III.1) and is analogous to (VI.12) above. The over-all minus sign occurs because the ω trajectory has negative signature. The quantities $\bar{\Gamma}$, $\bar{\sigma}$, $\bar{z}$ are the analogs of Γ, σ, z for the Pomeranchon and result from the notation defined in (III.13) and (III.14). The factor $(1 + t/t_0)$ is added to $C_{\omega}(t)$ to allow the $\bar{p}p$ differential cross-section to cross that for pp. From plotting the cross-section data of Foley et al., we found this crossing point to be in the neighborhood of $t \approx -0.15$ BeV^2, so we took $t_0 \equiv 0.15$. We observe that Desai and Binford treated t_0 as a parameter and determined upon 0.074. In our fitting we noted no significant

improvement from a variation of t_0 away from 0.15.

As shown in Appendix E, the factor $(1 + t/t_0)$ reproduces itself in the unitarity integrals to the extent that the first several terms in the series behave like the ω pole term as a function of t. For higher order iterations the resulting terms do not change sign as a function of t. This behavior caused no difficulty, because, when the series converged, these higher order iterations were small compared to the first several terms.

The real parts of the scattering amplitude are determined as in (D.1) - (D.5). For example, for the pole terms we obtain

$$D_{in}^{Pom}(s,t) = \sqrt{16\pi}\,\Gamma\, s \left(\frac{s}{\sigma}\right)^{pt} \quad \mathrm{Re}\left[\xi_p(t)\right]$$

$$D_{in}^{\omega}(s,t) = \sqrt{16\pi}\,\bar{\Gamma}\, s \left(\frac{s}{\bar{\sigma}}\right)^{a-1}\left(\frac{s}{\bar{\sigma}}\right)^{\bar{p}t}\left(1 + \frac{t}{t_0}\right) \mathrm{Re}\left[\xi_\omega(t)\right] \quad \text{(VI.15)}$$

where

$$\xi_i(t) = -\frac{1 + \tau_i\, e^{-i\pi\alpha_i(t)}}{\sin \pi\alpha_i(t)} \,.$$

and $\tau_p = +1$, $\tau_\omega = -1$, $\alpha_p(t) = 1 + pt$, $\alpha_\omega(t) = a + \bar{p}t$. We might remark that we are not in a region for which expression (III.20) can be used.

The actual fitting was attempted with the aid of a computer. First, it is interesting to note that we can reproduce the fits of Desai and Binford with our model, replacing the "Igi pole" with cut terms. In order to fit the data as well as they did, we too employed

parameters such that the pole terms, by themselves, exceeded the S-wave unitarity limit. This, however, means that the convergence criterion (III.16) was violated. We of course, had to do something about the divergence of the two infinite series. For the parameters giving a fit, we observed that the contribution from the iteration of Pomeranchons was stronger than that from the iterations involving the ω. Furthermore, the successive terms decreased for a while, then began to diverge. Interpreting this as the behavior of an "asymptotic series" we elected to keep only the cut term arising from the exchange of two Pomeranchons. This "interpretation" just means that we took a new model for the cut terms, namely the single diagram:

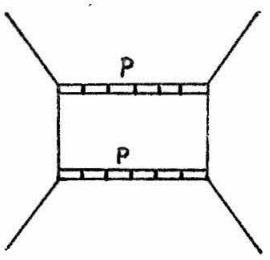

Then, ignoring the criterion (VI.10) above, we found we could obtain a good fit to the data of Foley et al. at all the energies of their experiments for pp, $\bar{p}p$, $K^{\pm}p$, and $\pi^{\pm}p$. For purposes of this fit we took

$$\alpha_{Pom}(t) = 1 + 0.4t$$

$$\alpha_{\omega}(t) = \frac{1}{2} + 0.8t \ .$$

The ω intercept was arbitrarily set at 1/2 and the slope then chosen so that a linear trajectory would pass through $\alpha_{\omega} = 1$ at the physical ω mass. Fitting the data in this way, we found that the fits exceeded the S-wave unitarity bound by the amounts indicated in the table below.

Scattering Process	S	$4B_0$
$\pi^+ p$	13.66	1.42
$\pi^+ p$	32.24	1.10
$\pi^- p$	14.04	1.28
$\pi^- p$	32.80	1.10
p p	14.64	1.78
p p	38.58	1.39
$\bar{p}$ p	15.38	1.73
$\bar{p}$ p	24.35	1.54
$K^+ p$	13.92	1.31
$K^+ p$	28.91	1.11
$K^- p$	14.67	1.30
$K^- p$	18.04	1.22

We see in each case that we are closer to the bound at the higher energy. The pp - $\bar{p}$p fit is farthest from the bound.

Thus, we see how much AFS correction we would need to satisfy S-wave unitarity. The numbers are about the same as for the pole fits, so our demands appear to be reasonable. This fit is not entirely satisfactory, because we have no way to be sure that, if the AFS cut terms were put into the unitarity condition in some self-consistent way, it would be true that their effect would be strong enough to give consistency with the partial wave inelastic unitarity condition. This doubt is present because we have, in fact, used an AFS cut term to approximate the Mandelstam cuts. We do not know how serious this

approximation might be. On the basis of this fit, however, it does appear that it is possible to replace the Igi pole by the Regge cut.

We next made a serious effort to fit the data without exceeding the S-wave unitarity bound, i.e., in the region where the series actually converge.

For pp and $\bar{p}p$ scattering at low and high energies we have varied Γ, $\bar{\Gamma}$, σ, and $\bar{\sigma}$ to obtain "best fits" for various choices for p, $\bar{p}$, a, and t_0. In no case can we obtain a useful fit to the data. In order to determine parameters we must use data at two different energies. If we arrange things so that (VI.10) is satisfied for the S-wave at the low energy, then (VI.10) is, of course, satisfied for the higher energies, but the curves tend to fall well beneath the data at $|t| \approx 0.5$ BeV^2. The basic reason for this difficulty is that (VI.10) requires that the contribution from the Pomeranchuk pole and, consequently, for the series of Pomeranchon cuts, fall off too fast as $|t|$ increases. It is possible to arrange things so that the data is simultaneously fit fairly well for both processes and for all energies at $t = 0$ and $t = -0.5$ BeV^2. The choice of parameters for this situation is unpleasant because once away from $t = 0$, the ω terms are much larger than the Pomeranchon terms. Even this ruse, however, does not yield a fit to the data, because the curves then have very large curvature and fall well below the data before rising to cross it at $t = -0.5$. We find that adding curvature to the trajectories and similar devices still will not allow us to fit the data with parameters chosen so that the series actually converge. Thus, we conclude that

in order to fit the data we are forced to use pole parameters which make our series diverge. This divergence is forced upon us, because we do not know how to put all the AFS cuts in the unitarity condition in a self-consistent way.

Our approach to the topic of cuts in the angular momentum plane has been to do what we can do and learn what we can learn. We chose what appears to be the only simple approach to a very complex subject. Our approximation for the series of Mandelstam cuts has inherent in it the unfortunate property that the estimate diverges when the pole parameters approach their expected values. It appears that in order to pursue this topic farther, a much more sophisticated approach would be required.

APPENDIX A τ-FUNCTIONS

A. How the τ-functions arise

One becomes involved with the τ-functions in doing unitarity integrals. One may easily obtain expressions involving these functions by considering an integral over the solid angle variables of the intermediate state. We may write the amplitude for the process

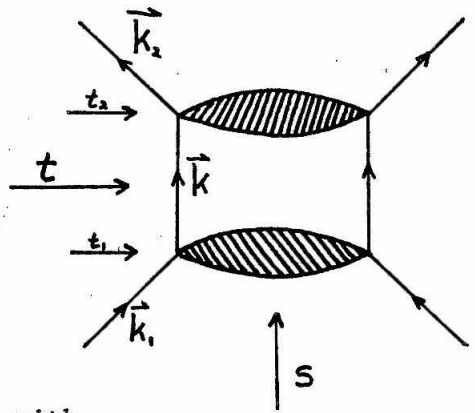

as $T(s,t) = D(s,t) + i\,A(s,t)$

with

$$A(s,t) = \left(\frac{1}{64\pi^2\sqrt{r}}\right)\int d\Omega_{\vec{k}}\; T_2(s,t_2)\; T_1(s,t_1)\;, \qquad \text{(A.1)}$$

where r is defined in (II.3). $T_1(s,t_1)$ and $T_2(s,t_2)$ are the amplitudes for the processes

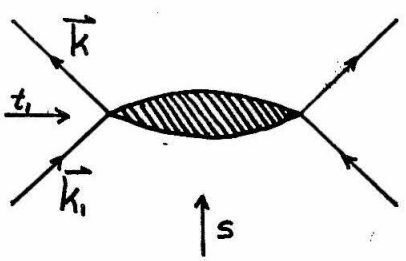

and

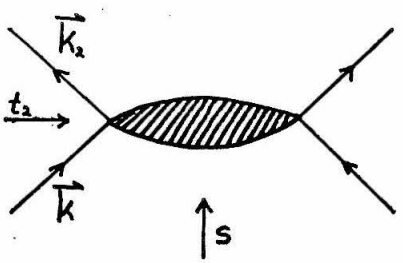

respectively.

We are using $T_1(s,t_1) = \langle \vec{k} | T_1 | \vec{k}_1 \rangle$ and $T_2(s,t_2) = \langle \vec{k}_2 | T_2 | \vec{k} \rangle$. We shall speak of the momentum transfer t as the "sum" of the momentum transfers t_1 and t_2.

Working in the center of mass system

$$t_1 = -\frac{s_0}{2}(1 - x_1),\ t_2 = -\frac{s_0}{2}(1 - x_2),\ t = -\frac{s_0}{2}(1 - x) \qquad (A.2)$$

where

$$x_1 = (\hat{k}_1 \cdot \hat{k}),\ x_2 = (\hat{k}_2 \cdot \hat{k}),\ x = (\hat{k}_1 \cdot \hat{k}_2).$$

We choose co-ordinates so that

$$k_1 = (0,\ 0,\ 1)$$

$$k_2 = (0,\ \sin\theta_2,\ \cos\theta_2)$$

$$k = (\sin\theta\cos\varphi,\ \sin\theta\sin\varphi,\ \cos\theta).$$

Then $x_1 = \cos\theta$, $x_2 = \sin\theta\sin\varphi\sin\theta_2 + \cos\theta\cos\theta_2$, $x = \cos\theta_2$, and

$$\int d\Omega_{\vec{k}} = \int_0^{2\pi}\int_0^{\pi} \sin\theta\ d\theta\ d\varphi\ .$$

This integration may be converted to an integral over x_1 and x_2 by a change of variables:

$$\int d\Omega_{\vec{k}} = \int_0^{2\pi}\int_0^{\pi} \sin\theta\ d\theta\ d\varphi = 2\int_{-1}^{1}\int_{-1}^{1} \frac{dx_1\ dx_2\ \theta(x_1,x_2,x)}{\sqrt{1 - x_1^2 - x_2^2 - x^2 + 2xx_1x_2}} = 4\pi\ . \qquad (A.3)$$

This equation is obtained, of course, for any values of the particle masses. Now using Eq. (A.2) to change variables again:

$$\int d\Omega_k = \frac{4}{s_0} \int_{-s_0}^{0} \int_{-s_0}^{0} \frac{dt_1\, dt_2\, \theta(t_1,t_2,t,s_0)}{\sqrt{-t_1^2 - t_2^2 - t^2 + 2t_1t + 2t_2t + 2t_1t_2 + \frac{4}{s_0} t_1t_2t}} \tag{A.4}$$

The θ functions are 0 or 1 depending on whether the corresponding radicand is negative or positive. The lower limit of integration in (A.4) may be taken to be $-\infty$ since the θ function does not allow the region of integration to extend past $-s_0$ anyhow. The τ-function has appeared

$$\tau(t_1t_2t) \equiv \frac{\theta(t_1,t_2,t,s_0)}{\sqrt{-t_1^2 - t_2^2 - t^2 + 2t_1t + 2t_2t + 2t_1t_2 + \frac{4}{s_0} t_1t_2t}} \tag{A.5}$$

and we obtain the unitarity integral (II.9) of the text.

B. The asymptotic unitarity condition

Since we are interested in the behavior of amplitudes at large values of the "energy variable", s, it will be convenient to consider a certain approximation to (II.9)*. This asymptotic unitarity condition[1] replaces $\tau(t_1,t_2,t)$ by

$$\tau_a(t_1,t_2,t) \equiv \frac{\theta_a(t_1,t_2,t)}{\sqrt{-t_1^2 - t_2^2 - t^2 + 2t_1t + 2t_2t + 2t_1t_2}} . \tag{A.6}$$

Thus one would have

---

* The results obtained in this paper do not depend on this approximation. The asymptotic unitarity condition is employed here *only to* simplify the expressions which determine the top of the cut.

$$A(s,t) \approx \left(\frac{1}{64\pi^2\sqrt{r}}\right)\left(\frac{4}{s_0}\right)\int_{-\infty}^{0}\int_{-\infty}^{0}\tau_a(t_1,t_2,t)\ T_2(s,t_2)^*T_1(s,t_1)dt_1\ dt_2 . \quad (A.7)$$

However, it may be noticed from (A.4) above that since $\int d\Omega_{\vec{k}} = 4\pi$, it must be that

$$\int_{-\infty}^{0}\int_{-\infty}^{0}\tau(t_1,t_2,t)\ dt_1\ dt_2 = \pi s_0 , \quad (A.8)$$

which goes to ∞ as $s_0 \to \infty$. Therefore,

$$\int_{-\infty}^{0}\int_{-\infty}^{0}\tau_a(t_1,t_2,t)\ dt_1\ dt_2 \quad (A.9)$$

is a divergent integral.

Let us compare the regions of integration allowed by the functions $\theta(t_1,t_2,t,s_0)$ and $\theta_a(t_1,t_2,t)$ for $s_0 > |t|$. The region of integration allowed by $\theta(t_1,t_2,t,s_0)$ is the interior of an ellipse in the (t_1,t_2)-plane, whereas $\theta_a(t_1,t_2,t)$ allows integration over the interior of a parabola. Both the ellipse and the parabola lie entirely within the third quadrant, of course. Both regions are tangent to the co-ordinate axes at the points $(-t,0)$ and $(0,-t)$ and are symmetric about the line $t_1 = t_2$. The vertices of the ellipse are at the points

$$\left(\frac{s_0}{2}\left[1 - \sqrt{1 - \frac{|t|}{s_0}}\right],\ \frac{s_0}{2}\left[1 - \sqrt{1 - \frac{|t|}{s_0}}\right]\right) \approx \left(\frac{|t|}{4} + \frac{|t|^2}{16 s_0},\ \frac{|t|}{4} + \frac{|t|^2}{16 s_0}\right)$$

and

$$\left(\frac{s_0}{2}\left[1 + \sqrt{1 - \frac{|t|}{s_0}}\right],\ \frac{s_0}{2}\left[1 + \sqrt{1 - \frac{|t|}{s_0}}\right]\right) \approx \left(s_0 - \frac{|t|}{4},\ s_0 - \frac{|t|}{4}\right) .$$

The parabola has vertex at $(|t|/4, |t|/4)$. Thus the ellipse lies entirely within the parabola, except for a small region near the vertex of the parabola. As $s_0 \to \infty$, the ellipse approaches the parabolic limit allowed by $\theta_a(t_1,t_2,t)$. Clearly the integral (A.9) fails to converge because of contributions from large values of $|t_1|$ and $|t_2|$. This is clear because, if we stop the integrals at $-s_0$, we find the value:

$$\int_{-s_0}^{0}\int_{-s_0}^{0} \tau_a(t_1,t_2,t)\,dt_1\,dt_2 = 2s_0\,\mathrm{Cos}^{-1}\frac{\sqrt{-t}}{2\sqrt{s_0}} - \sqrt{-t}\sqrt{s_0+\frac{t}{4}} \approx$$

$$\approx \pi s_0 - 2\sqrt{-t}\sqrt{s_0} + 0\left(\frac{1}{\sqrt{s_0}}\right)$$

which should be compared to Eq. (A.8). Thus, we see that there is no chance to use τ_a in (A.8) unless $T_2(s,t_2)^*$ and $T_1(s,t_1)$ die off sufficiently fast for large values of $|t_1|$ and $|t_2|$. Let us find how fast these functions must die off in order for the integral in (A.7) to converge.

One may easily verify that[26]

$$\tau_a \equiv \frac{\theta(t_1,t_2,t)}{\sqrt{-t_1^2-t_2^2-t^2+2t_1t+2t_2t+2t_1t_2}} = \int_{-\infty}^{\infty}\int_{-\infty}^{\infty} d^2q\;\delta(q^2+t_1)\;\cdot$$

$$\cdot\;\delta[(\vec{q}-\vec{p})^2+t_2] \qquad \text{(A.10)}$$

where $\vec{q}$ and $\vec{p}$ are vectors in a two-dimensional space and $p^2 = |t|$.

Then

$$\iint_{-\infty}^{0} \tau_a(t_1,t_2,t)\, f(t_1)\, g(t_2)\, dt_1\, dt_2 = \iint d^2\vec{q} \iint_{-\infty}^{0} f(t_1)\, g(t_2)\, \delta[q^2 + t_1] \cdot$$

$$\cdot\, \delta[(q - p)^2 + t_2]\, dt = \iint d^2\vec{q}\, f(-q^2)\, g(-(q - p)^2).$$

We see from this expression that convergence requires that $f(-\upsilon)g(-\upsilon)$ falls off faster than const/$|\upsilon|$ as $\upsilon \to \infty$. Thus we find that the integral in (A.8) cannot converge unless $T_2(s,t)^*\, T_1(s,t)$ falls off faster than const/$|t|$ as $t \to -\infty$. One certainly expects the amplitudes to fall off fast enough to satisfy this condition. For example, Serber[11] finds that pp scattering cross-sections fall off like $|t|^{-5}$ for large -t.

We may compare the behavior of these two kernels with an example. One can show that for α and $\beta > 0$:

$$\iint_{-\infty}^{0} \frac{dt_1\, dt_2\, \theta_a}{\sqrt{-t_1^2 - t_2^2 - t^2 + 2t_1t_2 + 2t_1t + 2t_2t}}\, e^{\alpha t_1}\, e^{\beta t_2} = \frac{\pi}{\alpha + \beta}\, e^{\frac{\alpha\beta}{\alpha + \beta} t} \tag{A.11}$$

and

$$\iint_{-\infty}^{0} \frac{dt_1\, dt_2\, \theta}{\sqrt{-t_1^2 - t_2^2 - t^2 + 2t_1t_2 + 2t_1t + 2t_2t + \frac{4}{s_0} tt_1t_2}}\, e^{\alpha t_1}\, e^{\beta t_2} =$$

$$= \frac{\pi}{\sqrt{(\alpha + \beta)^2 + \frac{4\alpha\beta t}{s_0}}} \left\{ 2e^{-\frac{1}{2}(\alpha + \beta)s_0} \sinh\left[\frac{s_0}{2} \sqrt{(\alpha + \beta)^2 + \frac{4\alpha\beta t}{s_0}} \right] \right\}$$

$$= \frac{\pi}{\alpha + \beta}\, e^{\frac{\alpha\beta}{\alpha + \beta} t} + O\left(\frac{1}{s_0}\right). \tag{A.12}$$

If $\beta = 0$ these agree to $O(e^{-\alpha s_0})$ that the integral should be π/α, independent of t.

This same asymptotic unitarity condition will be used here for the unequal mass case. For the diagram

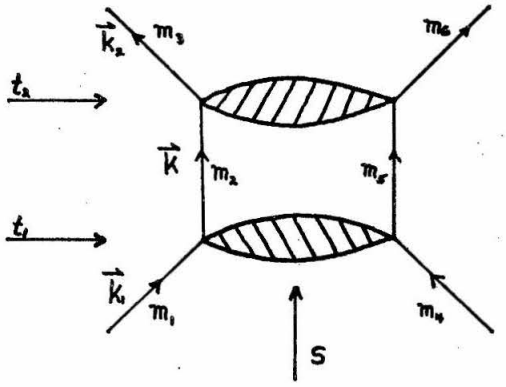

one finds for the squares of the 3-momenta:

$$\vec{k}_1^{\,2} = \frac{s}{4} - \frac{(m_1^2 + m_4^2)}{2} + \frac{(m_1^2 - m_4^2)^2}{4s} \approx \frac{s}{4} - \frac{(m_1^2 + m_4^2)}{2}$$

$$\vec{k}^2 = \frac{s}{4} - \frac{(m_2^2 + m_5^2)}{2} + \frac{(m_2^2 - m_5^2)^2}{4s} \approx \frac{s}{4} - \frac{(m_2^2 + m_5^2)}{2}$$

$$\vec{k}_2^{\,2} = \frac{s}{4} - \frac{(m_3^2 + m_6^2)}{2} + \frac{(m_3^2 - m_6^2)^2}{4s} \approx \frac{s}{4} - \frac{(m_3^2 + m_6^2)}{2}$$

Then, with these approximations, one obtains

$$\int_{-1}^{1}\int_{-1}^{1} \frac{\theta\, dx_1\, dx_2}{\sqrt{1 - x_1^2 - x_2^2 - x^2 + 2x_1x_2x}} \approx \frac{2}{\sqrt{Q_1Q_2}} \int_{-Q_1}^{0} dt_1 \int_{-Q_2}^{0} dt_2$$

$$\frac{\theta}{\sqrt{-\frac{Q_2}{Q_1}t_1^2 - \frac{Q_1}{Q_2}t_2^2 - \frac{Q_1Q_2}{QQ}t^2 + 2\frac{Q_2}{Q}t_1t + 2\frac{Q_1}{Q}t_2t + 2t_1t_2 + \frac{4}{Q}t_1t_2t}}.$$

where

$$Q_1 = s - (m_1^2 + m_4^2 + m_2^2 + m_5^2)$$

$$Q = s - (m_1^2 + m_4^2 + m_3^2 + m_6^2)$$

$$Q_2 = s - (m_2^2 + m_5^2 + m_3^2 + m_6^2)$$

Since the ratios of the Q's approach 1 as $s \to \infty$ we shall use (A.7) even for the unequal mass case. Again, the conclusions of this paper do not depend on this approximation. The reason for the approximation shall become clear in the section below concerning polygon conditions.

C. Some integrals of the τ-functions

The addition theorem for Legendre polynomials states that

$$P_n(\cos\theta\cos\theta_2 + \sin\theta\sin\theta_2\cos\varphi_0) = P_n(\cos\theta)\,P_n(\cos\theta_2) + 2\sum_{m=1}^{\infty}(-)^m P_n^{-m}(\cos\theta)\,P_n^{m}(\cos\theta_2)\cos m\varphi_0.$$

From this theorem and the orthogonality properties of the Legendre polynomials we obtain, after taking $\varphi_0 = \pi/2 - \varphi$:

$$\int_0^{2\pi}\int_0^{\pi} P_n(\cos\theta\cos\theta_2 + \sin\theta\sin\theta_2\sin\varphi)\,P_m(\cos\theta)\sin\theta\,d\theta\,d\varphi = \frac{4\pi}{2n+1}\delta_{mn}P_n(\cos\theta_2).$$

In terms of x_1, x_2, and x, defined above, this gives

$$\int_{-1}^{1}\int_{-1}^{1} \frac{dx_1\, dx_2\, \theta(x_1,x_2,x)}{\sqrt{1 - x_1^2 - x_2^2 - x^2 + 2x_1x_2x}}\, P_m(x_1)\, P_n(x_2) = \frac{2\pi}{2n+1}\, \delta_{mn}\, P_n(x). \tag{A.13}$$

From this result we easily deduce the following facts

$$\frac{\theta(x_1,x_2,x_3)}{\sqrt{1 - x_1^2 - x_2^2 - x_3^2 + 2x_1x_2x_3}} = \frac{\pi}{2} \sum_{n=0}^{\infty} (2n+1)\, P_n(x_1)\, P_n(x_2)\, P_n(x_3) \tag{A.14}$$

$$\int_{-1}^{1} \frac{dx_1\, \theta(x_1,x_2,x_3)\, P_n(x_1)}{\sqrt{1 - x_1^2 - x_2^2 - x_3^2 + 2x_1x_2x_3}} = \pi\, P_n(x_2)\, P_n(x_3) \tag{A.15}$$

$$\int_{-1}^{1}\int_{-1}^{1}\int_{-1}^{1} \frac{dx_1 dx_2 dx_3\, \theta(x_1,x_2,x_3)\, P_m(x_1)\, P_n(x_2)\, P_r(x_3)}{\sqrt{1 - x_1^2 - x_2^2 - x_3^2 + 2x_1x_2x_3}} = \frac{4\pi}{(2n+1)^2}\, \delta_{mn}\, \delta_{nr} \tag{A.16}$$

$$\int_{-1}^{1} \frac{\theta(x_1,x_2,x_3)}{\sqrt{1 - x_1^2 - x_2^2 - x_3^2 + 2x_1x_2x_3}}\, \frac{\theta(x_3,x_4,x_5)\, dx_3}{\sqrt{1 - x_3^2 - x_4^2 - x_5^2 + 2x_3x_4x_5}} =$$

$$= \frac{\pi^2}{2} \sum_{n=0}^{\infty} (2n+1)\, P_n(x_1)\, P_n(x_2)\, P_n(x_4)\, P_n(x_5) \tag{A.17}$$

Stated in terms of the τ-functions, these results become

$$\frac{s_0}{2}\, \tau(t_1,t_2,t_3) = \frac{\pi}{2} \sum_{n=0}^{\infty} (2n+1)\, P_n\left(1 + \frac{2t_1}{s_0}\right)\, P_n\left(1 + \frac{2t_2}{s_0}\right)\, P_n\left(1 + \frac{2t_3}{s_0}\right) \tag{A.18}$$

$$\int_{-\infty}^{0} \tau(t_1,t_2,t_3)\, P_n\left(1 + \frac{2t_3}{s_0}\right)\, dt_3 = \pi\, P_n\left(1 + \frac{2t_1}{s_0}\right)\, P_n\left(1 + \frac{2t_2}{s_0}\right) \tag{A.19}$$

$$\frac{2}{s_0}\int_{-\infty}^{0}\!\!\int \tau(t_1,t_2,t_3)\, P_m\left(1+\frac{2t_1}{s_0}\right) P_n\left(1+\frac{2t_2}{s_0}\right) dt_1 dt_2 = \frac{2\pi}{2n+1} \cdot$$

$$\cdot\, \delta_{mn}\, P_n\left(1+\frac{2t_3}{s_0}\right) \qquad (A.20)$$

$$\left(\frac{2}{s_0}\right)^2 \int_{-\infty}^{0}\!\!\int\!\!\int \tau(t_1,t_2,t_3)\, P_m\left(1+\frac{2t_1}{s_0}\right) P_n\left(1+\frac{2t_2}{s_0}\right) P_r\left(1+\frac{2t_3}{s_0}\right) \cdot =$$

$$= \frac{4\pi}{(2n+1)^2}\, \delta_{mn}\delta_{nr}\, dt_1 dt_2 dt_3 \qquad (A.21)$$

$$\frac{s_0}{2}\int_{-\infty}^{0} \tau(t_1,t_2,t_3)\, \tau(t_3,t_4,t_5)\, dt_3 = \frac{\pi^2}{2}\sum_{n=0}^{\infty} (2n+1)\, P_n\left(1+\frac{2t_1}{s_0}\right) \cdot$$

$$P_n\left(1+\frac{2t_2}{s_0}\right) P_n\left(1+\frac{2t_4}{s_0}\right) P_n\left(1+\frac{2t_5}{s_0}\right) . \qquad (A.22)$$

We note here that

$$\int_{-s_0}^{0} P_n\left(1+\frac{2t_1}{s_0}\right) P_n\left(1+\frac{2t_1}{s_0}\right) dt_1 = \frac{s_0}{2} \cdot \frac{2}{2n+1}\, \delta_{nm} . \qquad (A.23)$$

Although the above integrals appear to go from $-\infty$ to 0, recall that the θ-function is represented in the sum over Legendre polynomials, so that all of our integrals are automatically stopped at $-s_0$. Thus (A.22) may, of course, be deduced directly from (A.18), using (A.23).

D. Contractions of τ-functions

When we evaluate a diagram for the exchange of, say, eight Reggeons

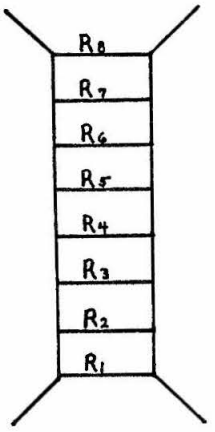

we must include contributions from all the various ways of making two particle unitarity cuts. For example, three of the unitarity diagrams corresponding to this Feynman diagram are

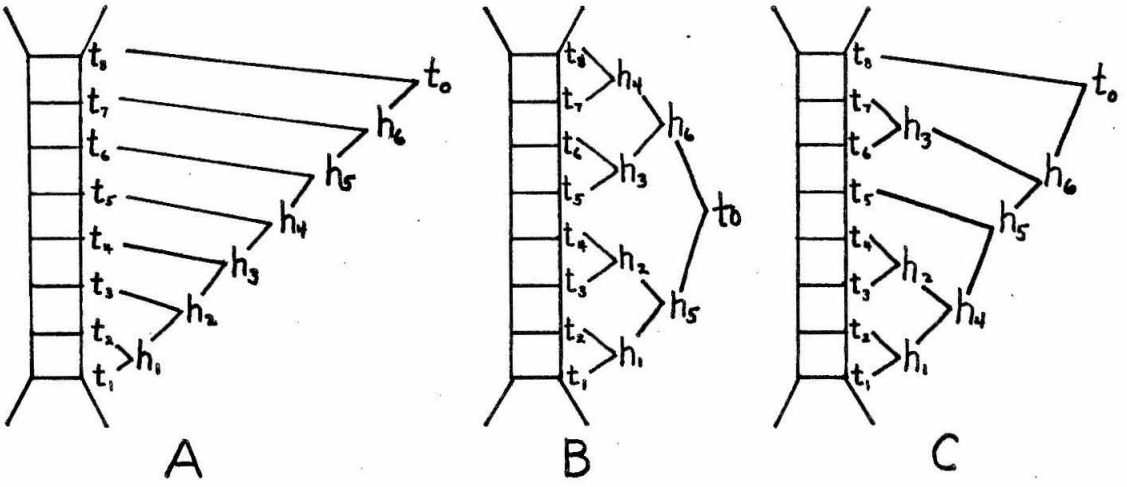

where $t_0 \equiv t$ is the total momentum transfer and the other variables t_i represent the momentum transfer carried across the ladder by the corresponding rung. Each h_i represents the "sum" of the two momentum transfers enclosed by the corresponding bracket. The two particle unitarity evaluations of these diagrams will have the form

$$T_x^{(8)} \sim \int dh_1 \,..\, dh_6 dt_1 \cdots dt_8 \; G_x(t_1, \ldots, t_8)\; W_x(t_1, \ldots, t_8, h_1 \cdots h_6) \cdot S\left(\sum_{i=1}^{8} \alpha_{R_i}(t_i) - 7\right)$$

with the subscript, x, being A, B, or C to indicate which of the three diagrams is being evaluated. The variables, h_i, appear only in the weight function, W_x, so that these integrations may be carried out immediately to leave the contracted weight function W_x^o. For the cases under consideration we have

$$W_A = \tau(t_1 t_2 h_1)\; \tau(h_1 t_3 h_2)\; \tau(h_2 t_4 h_3)\; \tau(h_3 t_5 h_4)\; \tau(h_4 t_6 h_5)\; \tau(h_5 t_7 h_6)\; \tau(h_6 t_8 t_0)$$

$$W_B = \tau(t_1 t_2 h_1)\; \tau(t_3 t_4 h_2)\; \tau(h_1 h_2 h_5)\; \tau(t_5 t_6 h_3)\; \tau(t_7 t_8 h_4)\; \tau(h_3 h_4 h_6)\; \tau(h_5 h_6 t_0)$$

$$W_C = \tau(t_1 t_2 h_1)\; \tau(t_3 t_4 h_2)\; \tau(h_1 h_2 h_4)\; \tau(h_4 t_5 h_5)\; \tau(t_6 t_7 h_3)\; \tau(h_3 h_5 h_6)\; \tau(h_6 t_8 t_0)$$

We may represent these three situations by the figures:

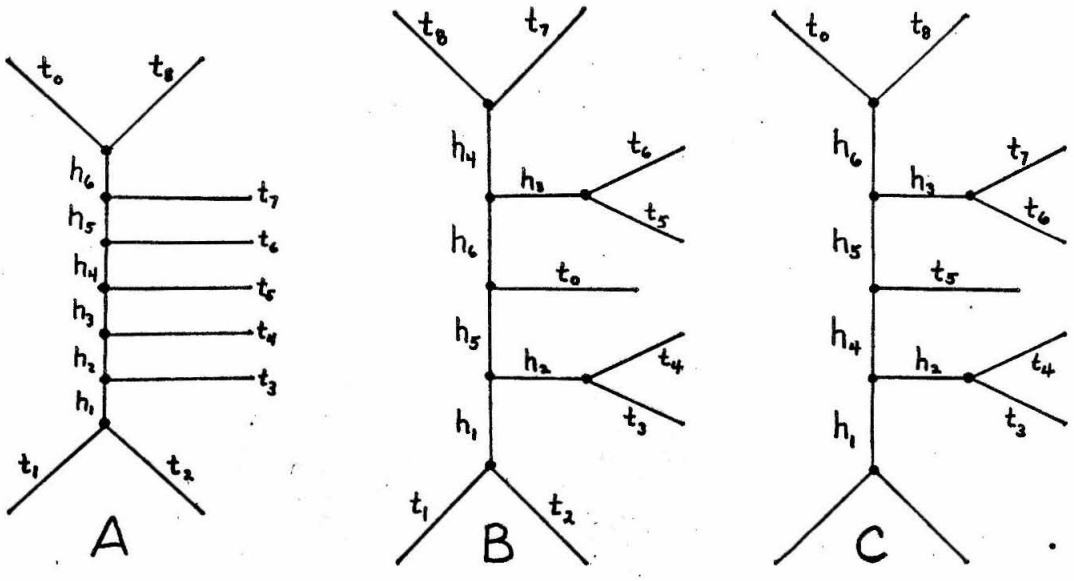

In these figures each vertex represents a τ-function and the three lines leading into each vertex name the three arguments of the τ-function. The contractable variables will always name the internal lines.

Now, Figs. B and C give topologically equivalent ways for the τ-functions to link the non-contractable variables. The topologically distinct patterns that can result from the exchange of eight Reggeons are

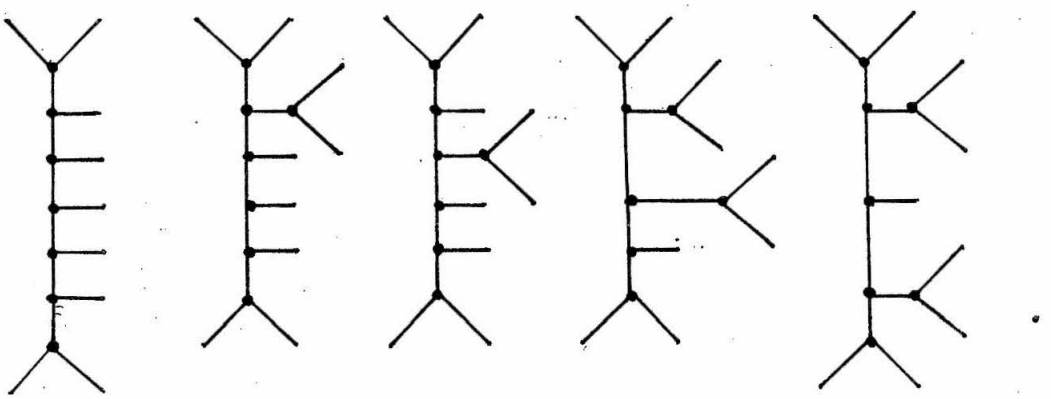

Of course, to each pattern we can assign the t_i to the external legs and the h_i to the internal legs in a great many ways*. We want to show that for each of these patterns we obtain a symmetric function of the t_i after contracting out the h_i. This would demonstrate that any permutation of the names of the external legs leads to the same function upon contraction of all internal legs, e.g., $W_B^o = W_C^o$. We also want to argue that the contracted weight functions are identical for all the above patterns, e.g., $W_A^o = W_B^o$.

---

* The number of ways to make the assignments is determined in Appendix C.

Since the argument is straightforward, we may as well have the exchange of n Reggeons in mind. This would involve patterns with (n - 1) vertices, (n + 1) external legs, and (n - 2) internal legs. The stated objectives are quickly established by induction. We have from (A.22) that the contraction of two τ-functions gives

$$W^0(t_1,t_2,t_3,t_4) = \int_{-\infty}^{0} \tau(t_1,t_2,h)\,\tau(h,t_3,t_4)\,dh = \frac{(\pi)^2}{s_0}\sum_{n=0}^{\infty}(2n+1)\cdot$$

$$\cdot P_n(1+\frac{2t_1}{s_0})\,P_n(1+\frac{2t_2}{s_0})\,P_n(1+\frac{2t_3}{s_0})\,P_n(1+\frac{2t_4}{s_0})$$

Furthermore, if we have a function such as

$$\frac{\text{const}}{s_0}\sum_{n=0}^{\infty}(2n+1)\,P_n(1+\frac{2t_1}{s_0})\,P_n(1+\frac{2t_2}{s_0})\,\ldots\,P_n(1+\frac{2t_n}{s_0})\,P_n(1+\frac{2h}{s_0}),$$

and we contract one of the variables, say h, against a τ-function, say, $\tau(h,t_{n+1},h')$, we obtain, using (A.19)

$$\frac{\pi\,(\text{const})}{s_0}\sum_{n=0}^{\infty}(2n+1)\,P_n(1+\frac{2t_1}{s_0})\,\ldots\,P_n(1+\frac{2t_n}{s_0})\,P_n(1+\frac{2t_{n+1}}{s_0})\cdot$$

$$\cdot P_n(1+\frac{2h'}{s_0}),$$

which is certainly of the same form. One may now contract out the next internal leg and so forth. Thus we may contract out one internal leg at a time to obtain for the completely contracted weight function for the exchange of n Reggeons:

$$W^0(t_1,t_2,t_3,\ldots,t_n,t) = \frac{(\pi)^{n-1}}{s_0} \sum_{\alpha=0}^{\infty} (2\alpha+1)\, P_\alpha\left(1+\frac{2t_1}{s_0}\right) P_\alpha\left(1+\frac{2t_2}{s_0}\right) \cdot \ldots P_\alpha\left(1+\frac{2t_n}{s_0}\right) P_\alpha\left(1+\frac{2t}{s_0}\right). \quad (A.24)$$

This form explicitly demonstrates the desired symmetry. This symmetry allows us to always use the standard form

$$W(t_1,t_2 \ldots t_n,t,h_1,h_2, \ldots h_{n-2}) = \tau(t\, t_1 h_1)\, \tau(h_1 t_2 h_2)\, \tau(h_2 t_3 h_3) \cdot \tau(h_3 t_4 h_4) \ldots \tau(h_{n-4} t_{n-3} h_{n-3})\, \tau(h_{n-3} t_{n-2} h_{n-2})\, \tau(h_{n-2} t_{n-1} t_n) \quad (A.25)$$

for the weight function for exchange of n Reggeons.

E. Polygon conditions

In this section we consider the region of integration allowed by the contracted weight functions, $W^0(t_1 t_2 \ldots t_n t)$. First consider the region allowed by $W^0(t_1 t_2 t)$. For the equal mass case,

$$W^0(t_1 t_2 t) = \tau(t_1,t_2,t) = \frac{\theta}{\sqrt{-t_1^2 - t_2^2 - t^2 + 2t_1t_2 + 2t_1t + 2t_2t + \frac{4}{s_0} t_1 t_2 t}}.$$

The region of integration allowed by the θ-function is that for which we have

$$4t_2t_1\left[1+\frac{t}{s_0}\right] \geq \left[t - t_1 - t_2\right]^2 \qquad \text{(A.26)}$$

This is, of course, the interior of the ellipse discussed above. For our discussion of the properties of the top of the cuts, we only need to consider values of $|t_1|$ and $|t_2|$ which are less than $|t|$, so that for large enough s_0 we may rewrite (A.26) as

$$4t_2t_1 \geq \left[t - t_1 - t_2\right]^2 \qquad \text{(A.27)}$$

This region is the interior of the parabola discussed above. Thus, in order to take advantage of the fact that we will be interested in $|t_i| < |t|$ we have introduced the "asymptotic unitarity condition" discussed above. It is also this fact that allows us to conveniently incorporate the unequal mass case, mentioned above, into the same discussion.

Now, therefore, we study the regions of integration allowed by the asymptotic unitarity condition. The region specified by (A.27) is the region such that

$$\sqrt{|t|} \leq \sqrt{|t_1|} + \sqrt{|t_2|}$$

$$\sqrt{|t_1|} \leq \sqrt{|t|} + \sqrt{|t_2|}$$

$$\sqrt{|t_2|} \leq \sqrt{|t_1|} + \sqrt{|t|}$$

i.e., it is the region such that a triangle exists with sides $\sqrt{|t|}$, $\sqrt{|t_1|}$, and $\sqrt{|t_2|}$. One may also notice that the denominator of the

weight function $\tau_a(t_1 t_2 t)$ may be written

$$\sqrt{- t_1^2 - t_2^2 - t^2 + 2t_1 t_2 + 2t_1 t + 2t_2 t} = 4A \ .$$

A is the area of the triangle with sides $\sqrt{|t|}$, $\sqrt{|t_1|}$, $\sqrt{|t_2|}$, as reference to Hero's area formula will easily reveal. The weight function τ_a, therefore, gives greatest emphasis to values of t_1 and t_2 allowing triangles of very small area*.

Now, let $W_a^0 (t_1 t_2 \ldots t_n t)$ denote the completely contracted weight function obtained when the asymptotic unitarity condition is employed. We want to argue that $W_a^0 (t_1 t_2 \ldots t_n t)$ is non-zero only in the region for which a polygon exists with sides $\sqrt{|t|}$, $\sqrt{|t_1|}$, $\sqrt{|t_2|}$, ..., $\sqrt{|t_n|}$.

First, take the case of one contraction

$$W_a^0 (t_1 t_2 t_3 t) = \int_{-\infty}^{0} \tau_a(t_1 t_2 h)\, \tau_a(h\, t_3 t)\, dh \ .$$

For every h allowed by the two θ-functions, there exists the figure

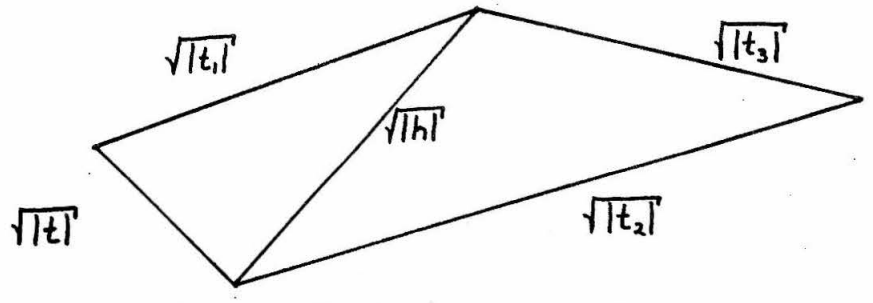

Thus, for any h, contributions are possible only if a quadrilateral

---

* This fact was also noticed by Bertocchi et al.[26].

exists. Conversely, if a quadrileteral exists then one exists with sides ordered as in the figure. The existence of a diagonal of length $\sqrt{|h|}$ then implies that a contribution is allowed. Thus $W_a^0\ (t_1 t_2 t_3 t)$ is non-zero if and only if a quadrilateral exists with sides $\sqrt{|t|}$, $\sqrt{|t_1|}$, $\sqrt{|t_2|}$, $\sqrt{|t_3|}$.

Now, the argument for the general case is exactly the same and may be accomplished by taking the standard form indicated in (A.25) and merely drawing pictures:

$$W_a^0\ (t_1 t_2 \ \dots\ t_n t) = \iiint \tau(t\ t_1 h_1)\ \tau(h_1 t_2 h_2)\ \tau(h_2 t_3 h_3)\ \dots$$

$$\dots\ \tau(h_{n-3} t_{n-2} h_{n-2})\ \tau(h_{n-2} t_{n-1} t_n)\, dh_1 dh_2 \dots dh_{n-2}.$$

n odd

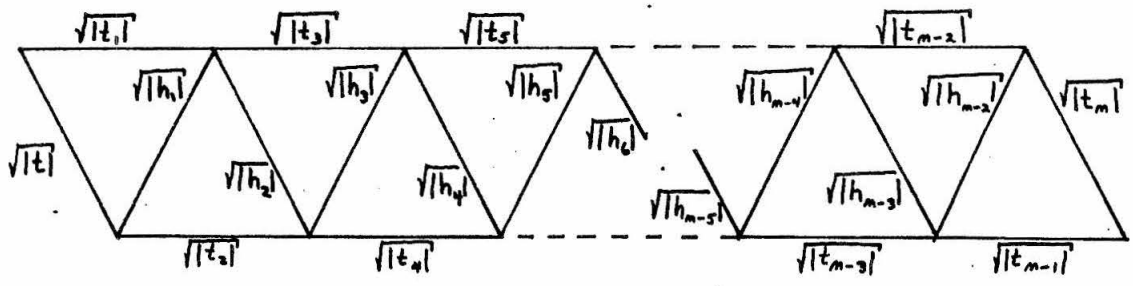

n even

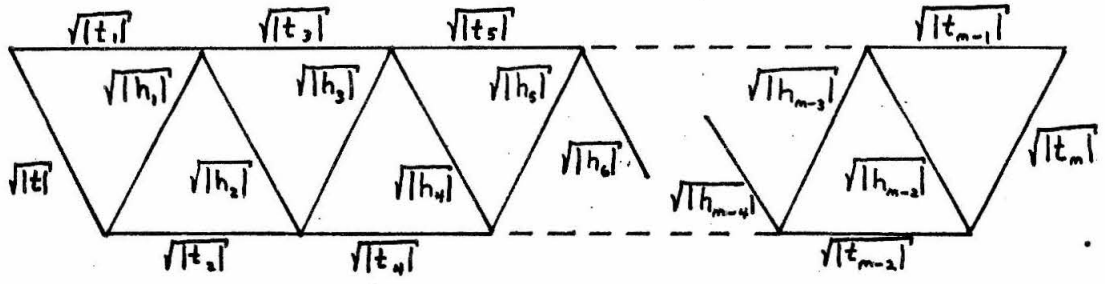

We notice in each case that the weight function gives the most emphasis to polygons of very small area.

APPENDIX B. LIMITS FOR THE HIGHEST CUTS

A. Top of the Cut for Linear Trajectories

For the exchange of n Reggeons, the top of the cut is the maximum of

$$\alpha_1(t_1) + \alpha_2(t_2) + \ldots + \alpha_n(t_n) - (n - 1) \tag{B.1}$$

subject to the polygon condition on the variables t, t_1, t_2, ..., t_n. For linear trajectories we take

$$\alpha_i(t_i) = a_i + p_i t_i \tag{B.2}$$

where the constant, $p_i \geqslant 0$, is the slope of the i-th trajectory. From Eq.(B.2) we see that in order to maximize (B.1) we must minimize

$$p_1\mu_1^2 + p_2\mu_2^2 + p_3\mu_3^2 + \ldots + p_n\mu_n^2 , \tag{B.3}$$

subject to the condition that a polygon exists with legs of length $\mu, \mu_1, \mu_2, \ldots, \mu_n$, where

$$\mu \equiv \sqrt{|t|} \text{ and } \mu_i \equiv \sqrt{|t_1|} \equiv \frac{r_i}{\sqrt{p_i}} . \tag{B.4}$$

Now one of the polygon conditions is

$$\mu_1 + \mu_2 + \ldots + \mu_n \geqslant \mu . \tag{B.5}$$

The problem may now be stated in terms of the r_i. Minimize

$$r_1^2 + r_2^2 + r_3^2 + \ldots + r_n^2 \tag{B.6}$$

with

$$\frac{r_1}{\sqrt{p_1}} + \frac{r_2}{\sqrt{p_2}} + \ldots + \frac{r_n}{\sqrt{p_n}} \geq \mu \ . \tag{B.7}$$

The equation $r_1/\sqrt{p_1} + r_2/\sqrt{p_2} + \ldots + r_n/\sqrt{p_n} = \mu$ determines a plane in an n-dimensional space with intercept $\sqrt{p_i}\ \mu$ on the ith axis. This plane divides the n-space into two regions. The origin lies in region I, and the region, II, is specified by (B.7). Now it is clear geometrically that we want the square of the radius of the smallest sphere with center at the origin that has at least one point in region II. This is obviously the sphere that is tangent to the plane. Hence we want

$$\frac{r_1}{\sqrt{p_1}} + \frac{r_2}{\sqrt{p_2}} + \ldots + \frac{r_n}{\sqrt{p_n}} = \mu, \text{ i.e., } \mu_1 + \mu_2 + \ldots + \mu_n = \mu. \tag{B.8}$$

This condition clearly satisfies all of the polygon conditions, since a polygon (degenerate, of course) can always be made from lengths μ, μ_i obeying (B.8).

To minimize (B.6), i.e., determine the size of the sphere, we use the method of Lagrange multipliers. Thus we minimize

$$Q \equiv r_1^2 + r_2^2 + \ldots + r_n^2 + 2\lambda \left[\mu - \frac{r_1}{\sqrt{p_1}} - \frac{r_2}{\sqrt{p_2}} \ldots \frac{r_n}{\sqrt{p_n}}\right]$$

Setting $\partial Q/\partial r_i = 0$ we get $r_i = \lambda/\sqrt{p_i}$. Then putting these values into (B.8) we get

$$\mu = \lambda \left(\frac{1}{p_1} + \frac{1}{p_2} + \ldots + \frac{1}{p_n}\right) = \frac{\lambda}{p}$$

where

$$p \equiv \left[\frac{1}{p_1} + \frac{1}{p_2} + \ldots + \frac{1}{p_n}\right]^{-1} \equiv \langle p_1 p_2 \ldots p_n \rangle_{\substack{\text{harmonic} \\ \text{sum}}} .$$

Thus we have

$$r_i = \frac{\mu p}{\sqrt{p_i}}, \text{or } \sqrt{|t_i|} \equiv \mu_i \equiv \frac{r_i}{\sqrt{p_i}} = \mu \frac{p}{p_i} = \frac{p}{p_i}\sqrt{|t|} . \qquad (B.9)$$

Then

$$Q_{min} = \left(\frac{\mu p}{\sqrt{p_1}}\right)^2 + \left(\frac{\mu p}{\sqrt{p_2}}\right)^2 + \ldots + \left(\frac{\mu p}{\sqrt{p_n}}\right)^2 = \mu^2 p^2 \left(\frac{1}{p_1} + \frac{1}{p_2} + \ldots + \frac{1}{p_n}\right) =$$

$$= \mu^2 p . \qquad (B.10)$$

Incidentally, we have found that the radius of the tangent sphere is the square root of the harmonic sum of the squares of the intercepts of the plane.

Now, taking (B.10) and returning to (B.1) we have the result

$$\text{Top of cut} = \text{Max}\left\{\alpha_1(t_1) + \alpha_2(t_2) + \ldots + \alpha_n(t_n) - (n-1) \;\middle|\; \begin{matrix}\text{polygon} \\ \text{condition}\end{matrix}\right\} =$$

$$= [a_1 + a_2 + \ldots + a_n - (n-1)] + pt , \qquad (B.11)$$

where $p \equiv \langle p_1 p_2 \ldots p_n \rangle_{\text{harmonic sum}}$.

This is the result (II.20) of the text.

We may notice from (B.9) that the maximum is obtained with

$$|t_i| = \left(\frac{p}{p_i}\right)^2 |t| < |t| ,$$

since the harmonic sum of a set of positive numbers is always less than the smallest number in the set. This fact is to be compared with the statements made in the section on polygon conditions in Appendix A concerning the validity of the asymptotic unitarity condition. In this light Eq. (B.11) gives the form of the top of the cut in the limit of large s.

B. Top of the Cut for Trajectories of Arbitrary Shape

We now show that, regardless of the shape of the Regge trajectories, it is true that the top of the highest cut approaches a constant value (horizontal line) over the whole range from any fixed t to zero as more and more Pomeranchons are exchanged, provided

1. $\alpha'_{Pom}(0)$ is finite (or at least $\alpha'_{Pom}(t)$ does not diverge too strongly as $t \to 0$) and
2. for each trajectory $\alpha_i(t) \leqslant \alpha_i(0)$ for all $t < 0$.

Consider a diagram for the exchange of n Pomeranchons and m other Reggeons, R_1, R_2, ..., R_m. Then to find the top of the cut we must maximize

$$\alpha(t_1) + \alpha(t_2) + \ldots + \alpha(t_n) + \alpha_1(h_1) + \alpha_2(h_2) + \ldots + \alpha_m(h_m) + \\ - (n + m - 1) , \qquad (B.12)$$

subject to polygon* conditions on the $\sqrt{|t_i|}$, $\sqrt{|h_i|}$, and $\sqrt{|t|}$. We obtain a lower bound for this maximum by taking all $h_i \equiv 0$ and by taking all of the t_i equal to each other. We satisfy all of the polygon conditions

* The polygon conditions are discussed in Appendix A.

by setting

$$n\sqrt{|t_1|} = \sqrt{|t|}\,.$$

Thus, we take, for each i,

$$t_i = \frac{t}{n^2}$$

and obtain as a lower bound for the top of the cut

$$\left[n\,\alpha\left(\frac{t}{n^2}\right) - (n-1)\right] + [\alpha_1(0) + \alpha_2(0) + \ldots + \alpha_m(0) - m]. \quad \text{(B.13)}$$

Now, for any value of t, say t_0, we may consider this lower bound in the region from t_0 to zero, as the number, n, of Pomeranchons increases. We have $\alpha(0)= 1$ and we have presumed $\alpha'(0)$ is finite. When n is large enough that $\alpha(t_0/n^2) \approx 1 + (t_0/n^2)\,\alpha'(0)$, it is clear that (B.13) may be written in the form

$$\text{const} + \frac{t}{n}\,\text{const}'$$

where $t_0 \leqslant t \leqslant 0$. It is clear, therefore, that as $n \to \infty$, the bound for the top of the highest cut approaches a constant value over the range from t_0 to zero. For exchange of Pomeranchons only, this bound is at $\alpha = 1$. One now can show, using lines of positive slope for upper bounds for the trajectories, that for trajectories satisfying the condition

$$\alpha_i(t) < \alpha_i(0) \text{ for all } t < 0,$$

then $\alpha_{max}(t)$ can be no higher than a horizontal line. This gives the conclusion that as $n \to \infty$, the top of the highest cut approaches a

constant value over the entire range from t_0 to zero.

As a matter of fact, the condition that the Pomeranchuk trajectory have finite slope at t = 0 could even be relaxed somewhat and still allow the conclusion that the top of the highest cut approaches a horizontal line. We only need

$$n\left[\alpha\left(\frac{t}{n^2}\right) - 1\right] \to 0 \text{ as } n \to \infty \qquad \text{(B.14)}$$

which is true as long as

$$\frac{1}{\sqrt{|t|}}\left[\alpha(t) - 1\right] \to 0 \text{ as } t \to 0 .$$

For example, if for small $|t|$, $\alpha(t)$ goes like

$$\alpha(t) \sim 1 + (\text{const})|t|^{2/3}$$

then

$$\frac{1}{\sqrt{|t|}}\left[\alpha(t) - 1\right] \sim (\text{const})|t|^{1/6} \to 0 \text{ as } t \to 0$$

so that (B.14) holds. The critical power law is that for small $|t|$

$$\alpha(t) \sim 1 - (\text{const})|t|^{1/2} .$$

If the slope goes infinite more strongly than $1/\sqrt{|t|}$ at t = 0, then the conclusion that the top of the highest cut approaches a horizontal line no longer follows. In fact, the location of the top of the cut may not move at all as more and more Pomeranchons are exchanged. However, the result obtained should be strong enough since we do not believe $\alpha'(0)$ is infinite for the Pomeranchon.

APPENDIX C

NUMBER OF WAYS TO MAKE TWO PARTICLE UNITARITY CUTS

The function Q_n, used in Section II, is the number of times that a given unitarity diagram occurs in the iteration of (II.5). The order of the Reggeon rungs is fixed, but it is a familiar fact that the same diagram occurs more than once because it must be evaluated for all possible ways to make two particle cuts.

The subscript n denotes the number of rungs and Q_n denotes the weight with which that Feynman diagram contributes to the amplitude. For the pole term itself:

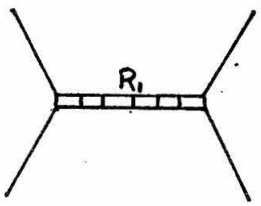

we have $Q_1 = 1$ since this diagram occurs only once in the iteration. Similarly the diagram

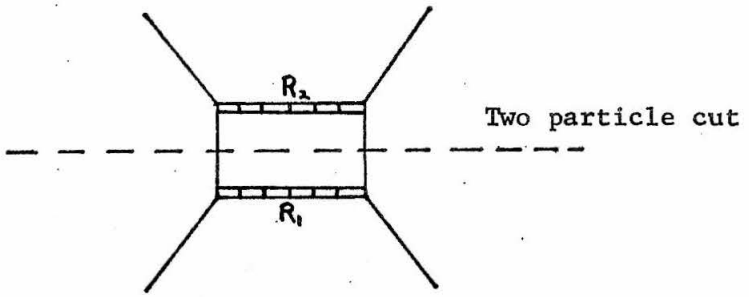

has only one two particle cut, so $Q_2 = 1$. The next diagram

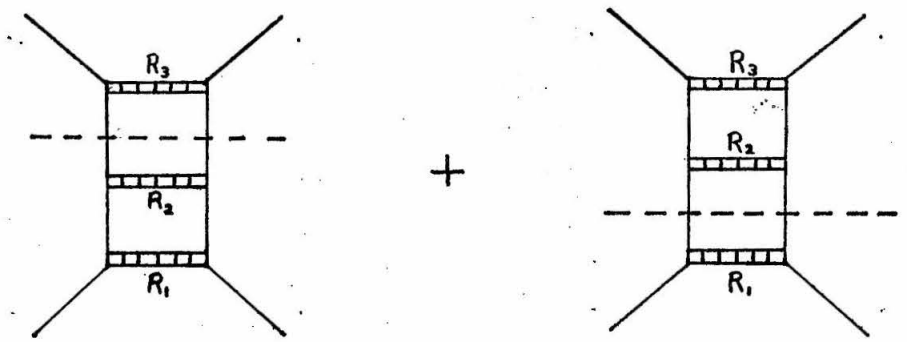

however, may be cut two different ways, so $Q_3 = 2$.

In general the number of ways a diagram can be cut is conveniently counted by summing all possible ways of cutting the subdiagrams. For example

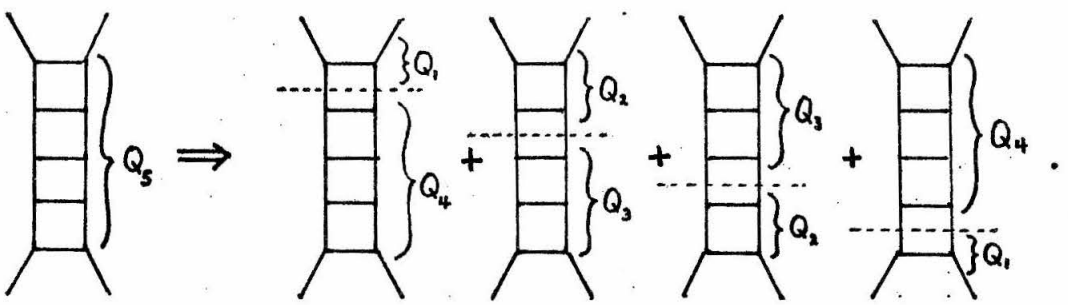

We see that $Q_5 = Q_1Q_4 + Q_2Q_3 + Q_3Q_2 + Q_4Q_1$. To make the pattern very clear, observe the following list

$$Q_1 = 1$$
$$Q_2 = Q_1Q_1 = 1$$
$$Q_3 = Q_1Q_2 + Q_2Q_1 = 2$$
$$Q_4 = Q_1Q_3 + Q_2Q_2 + Q_3Q_1 = 5$$
$$Q_5 = Q_1Q_4 + Q_2Q_3 + Q_3Q_2 + Q_4Q_1 = 14$$
$$- \quad -- \quad -- \quad -- \quad -- \quad -- \quad --$$

For convenience define

$$Q_0 \equiv -\frac{1}{2}, \text{ so that } 1 = -2Q_0.$$

We then have the boundary conditions

$$\begin{aligned} Q_0Q_0 &= \frac{1}{4} \\ Q_0Q_1 + Q_1Q_0 &= -1 \end{aligned} \tag{C.1}$$

for the difference equations:

$$\begin{aligned} &Q_0Q_2 + Q_1Q_1 + Q_2Q_0 = 0 \\ &Q_0Q_3 + Q_1Q_2 + Q_2Q_1 + Q_3Q_0 = 0 \\ &Q_0Q_4 + Q_1Q_3 + Q_2Q_2 + Q_3Q_1 + Q_4Q_0 = 0 \\ &\text{--} \quad \text{--} \quad \text{--} \quad \text{--} \quad \text{--} \quad \text{--} \end{aligned}$$

$$\sum_{i=0}^{n} Q_i Q_{n-i} = 0 \quad . \tag{C.2}$$

This situation is easily resolved by letting

$$H \equiv Q_0 + Q_1x + Q_2x^2 + Q_3x^3 + \ldots \quad . \tag{C.3}$$

Then

$$H^2 = Q_0Q_0 + (Q_0Q_1 + Q_1Q_0)x + (Q_0Q_2 + Q_1Q_1 + Q_2Q_0)x^2 + \ldots . .$$

Now, using Eqs. (C.1) and (C.2), we find

$$H^2 = \frac{1}{4} - x \quad \text{or} \quad H = -\frac{1}{2}\sqrt{1 - 4x}\,.$$

This H is a generating function for the Q_n by virtue of the series

expansion (C.3). Using the binomial expansion for H we obtain

$$Q_n = \frac{1}{2}\,(4)^n\,\frac{(2n-3)!!}{(2n)!!} = \frac{(2n-2)!}{(n-1)!\,n!}$$

or

$$Q_{n+1} = \frac{(2n)!}{n!(n+1)!} = \frac{1}{n+1}\binom{2n}{n}\,.$$

APPENDIX D

VALIDITY OF THE ITERATION PROCEDURE : REAL PART OF THE SCATTERING AMPLITUDE

Our procedure for iterating Eq. (II.5) is based upon the fact that the scattering amplitude is almost purely imaginary for large s. We verify now that it is consistent, therefore, to iterate only the absorptive part of the scattering amplitude.

First, we examine the real part[15] corresponding to each term in Eq. (III.12) to see if it is permissible to neglect the real part at each separate step in the iteration. We then sum all of the real parts so determined and compare this sum with the final absorptive contribution.

To determine $D_n(s,t)$ we use (II.7), except that we must make one subtraction because the nth term in (III.12) goes like the first power of s. Thus we use

$$D_n(s,t) = d_0(t)s^0 + \frac{s}{\pi} \mathcal{P} \int_{\text{threshold}}^{\infty} \frac{A_n(x,t)}{x(x-s)}\, dx - \tau \frac{s}{\pi} \int_{\text{threshold}}^{\infty} \frac{A_n(x,t)}{x(x+s)}\, dx \qquad (D.1)$$

where τ is the signature factor and equals + 1 for the Pomeranchon. It is possible to neglect the term $d_0(t)$ and to extend the lower limits of integration to zero, because these corrections are of order 1 in s and cannot modify the value that we obtain below for $D_n(s,t)$ for large s.

With these modifications we obtain

$$D_n(s,t) \approx \frac{2s^2}{\pi} \mathop{P}\int_0^\infty \frac{A_n(x,t)}{x(x^2 - s^2)}\, dx \,. \qquad (D.2)$$

Then taking A_n from Eq. (III.12) we encounter

$$D_n(s,t) = \left(\frac{2s^2}{\pi}\right)\sqrt{16\pi}\,\Gamma\,\frac{Q_{n+1}}{n+1}\left(\frac{\log\frac{s}{\sigma}}{R}\right)^n \frac{1}{\pi} \mathop{P}\int_0^\infty \frac{\left(\frac{x}{\sigma}\right)^{\frac{pt}{n+1}}}{[\log\frac{x}{\sigma}]^n(x^2 - s^2)}\, dx \,. \qquad (D.3)$$

Then, taking $x = (\sqrt{\nu}\, s)$, we get

$$D_n(s,t) \approx \sqrt{16\pi}\,\Gamma\, s\,\frac{Q_{n+1}}{n+1}\left(\frac{\log\frac{s}{\sigma}}{R}\right)^n \frac{1}{\pi} \mathop{P}\int_0^\infty \frac{[\sqrt{\nu}]^{\frac{pt}{n+1}} - 1}{[\log\frac{s}{\sigma} + \frac{1}{2}\log\nu]^n(\nu - 1)}\, d\nu$$

$$\approx \sqrt{16\pi}\,\Gamma\, s\,\frac{Q_{n+1}}{n+1}\,\frac{1}{R^n}\,\frac{1}{\pi} \mathop{P}\int_0^\infty \frac{[\sqrt{\nu}]^{\frac{pt}{n+1}} - 1}{\nu - 1}\, d\nu \left[1 + O\left(\frac{n}{\log\frac{s}{\sigma}}\right)\right]$$

$$\approx - A_n(s,t) \cdot \cot\left[\frac{\pi}{2}\left(1 + \frac{pt}{n+1}\right)\right] \cdot \left[1 + O\left(\frac{n}{\log\frac{s}{\sigma}}\right)\right] \cdot \qquad (D.4)$$

We ignore the part of $O(n/\log s/\sigma)$ because the cotangent removes the effect of this term for large n, and because we see from (III.18), that for very large s the largest correction tends to be of order $\sqrt{z}/\log(s/\sigma) \backsim 1/\sqrt{\log s/\sigma}$. We have therefore approximated

$$D_n(s,t) \approx - A_n(s,t) \cdot \cot\left[\frac{\pi}{2}\left(1 + \frac{pt}{n+1}\right)\right] = A_n(s,t) \cdot \tan\frac{\pi pt}{2(n+1)} \cdot \qquad (D.5)$$

Keeping in mind that, in order to avoid the famous "ghost" poles where pt vanishes, our model is only appropriate for $|pt| < 1$, we may interpret equation (D.5). Due to the fact that the tangent term goes monotonically to zero as n increases, we readily observe that for $|pt|$ such that the pole term itself is essentially imaginary, it is true that the succeeding terms are even more predominantly imaginary. Thus, at each stage of the iteration it is consistent to neglect the dispersive part of the amplitude.

For $|pt|$ small enough that the pole term is essentially imaginary, it is accurate to replace $[\tan \pi pt/2(n+1)]$ by $\pi pt/2(n+1)$. This gives

$$D(s,t) = \sum_{n=0}^{\infty} D_n(s,t) = \sum_{n=0}^{\infty} \frac{\pi pt}{2(n+1)} A_n(s,t). \qquad (D.6)$$

Then, since

$$A(s,t) = \sqrt{16\pi}\, \Gamma\, s \sum_{n=0}^{\infty} \frac{(2n)!}{[(n+1)!]^2} \frac{1}{R^n} e^{\frac{zt}{n+1}}$$

we readily find

$$D(s,t) = \frac{\pi pt}{2z} \frac{dA(s,t)}{dt} . \qquad (D.7)$$

One may now use Eq. (D.7) for $t \approx 0$, i.e., for the case when the pole term dominates to find

$$\left.\frac{D(s,t)}{A(s,t)}\right|_{t \approx 0} \approx \frac{\pi}{2} pt .$$

Similarly, when condition (III.19) is satisfied, one may put (III.20) into (D.7) to obtain

$$\left.\frac{D(s,t)}{A(s,t)}\right|_{s\to\infty} \approx \frac{\pi p t}{2z}\left[-\frac{3}{2t}+\frac{2z\,\log\frac{R}{4}}{1+2\sqrt{z|t|\,\log\frac{R}{4}}}\right] \xrightarrow[s\to\infty]{} -\frac{\pi p}{2}\cdot$$

$$\cdot\sqrt{\frac{|t|\,\log\frac{R}{4}}{z}} \to 0\ .$$

APPENDIX E.

ITERATION WITH THE ω-POLE

We consider here the terms arising from the iteration of the ω-pole with various numbers of Pomeranchons. In our notation the pole terms are

$$A_{in}^{Pom}(s,t) = \sqrt{16\pi}\,\Gamma\, s\, e^{zt} \qquad (E.1)$$

$$A_{in}^{\omega}(s,t) = -\sqrt{16\pi}\,\bar{\Gamma}\, s \left(\frac{s}{\bar{\sigma}}\right)^{a-1} e^{\bar{z}t}\,(1 + \frac{t}{t_0}) \qquad (E.2)$$

$$\equiv A_{\omega p}^{(1)}(s,t) \equiv G_1\, e^{\bar{z}t}(1 + \frac{t}{t_0})\ .$$

Then

$$A_{\omega p}^{(2)}(s,t) = \frac{1}{64\pi^2\sqrt{r}}\ \frac{4}{s_0} \iint_{-\infty}^{0} \tau(t_1,t_2,t)\ A_{in}^{Pom}(s,t_1)\ A_{in}^{\omega}(s,t_2)\ dt_1 dt_2\ . \qquad (E.3)$$

Putting (E.1) and (E.2) in (E.3) and performing the necessary integrations we obtain

$$A_{\omega p}^{(2)}(s,t) = \frac{\Gamma\sqrt{r}G_1}{\sqrt{16\pi K}}\, e^{-\frac{s_0}{2}(z_1 + z_2)} \left\{\left(2 - \frac{s_0}{t_0}\right) \sinh\frac{s_0 K}{2} + \frac{s_0}{t_0 K}\left[(z_2 + z_1) + \right.\right.$$

$$\left.\left. + \frac{2z_1 t}{s_0}\right]\left[\cosh\frac{s_0 K}{2} - \frac{2}{s_0 K}\ \sinh\frac{s_0 K}{2}\right]\right\}, \qquad (E.4)$$

where $z_1 \equiv z$ and $z_2 \equiv \bar{z}$,

$$K = \sqrt{(z_2 + z_1)^2 + \frac{4z_1 z_2 t}{s_0}}$$

and

$$G_1 = -\sqrt{16\pi}\ \bar{\Gamma}\ s \left(\frac{s}{\bar{\sigma}}\right)^{a-1} .$$

We now approximate (E.4) for large s_0 to obtain

$$A^{(2)}_{\omega p}(s,t) \approx G_2\ e^{z_3 t} \left(1 + \frac{t}{t_1}\right), \qquad \text{(E.5)}$$

where

$$z_3 \equiv \langle z_1, z_2 \rangle_{HS}$$

$$t_1 \equiv \frac{z_1 + z_2}{z_1^2} \left[t_0(z_1 + z_2) - 1\right]$$

and

$$G_2 = \frac{\Gamma\sqrt{r}}{\sqrt{16\pi}\ (z_1 + z_2)} \left[1 - \frac{1}{t_0(z_1 + z_2)}\right] G_1 .$$

We observe that (E.5) is of the same form as (E.2), so that upon iterating another Pomeranchon a similar expression will again be obtained. Recalling that we must collect terms according to (III.10) we may obtain

$$A_{\omega P}(s,t) = \sum_{n=1}^{\infty} n\ Q_n\ G_n\ e^{z_{n+1} t} \left(1 + \frac{t}{t_{n-1}}\right), \qquad \text{(E.6)}$$

where

$$G_n = \frac{\Gamma\sqrt{r}}{\sqrt{16\pi}(z_1 + z_n)}\, G_{n-1} \tag{E.7}$$

$$t_{n-1} = \frac{(z_1 + z_n)}{z_1^2}\left[t_{n-2}(z_1 + z_n) - 1\right] \tag{E.8}$$

$$z_1 + z_n = z\left[\frac{1 + (n-1)\frac{\bar{z}}{z}}{1 + (n-2)\frac{\bar{z}}{z}}\right]. \tag{E.9}$$

After a certain amount of algebra we finally obtain

$$A_{\omega p}(s,t) = -\sqrt{16\pi}\; s\; \bar{\Gamma}\left(\frac{s}{\sigma}\right)^{a-1} \sum_{n=0}^{\infty} \frac{(2n)!}{n!\,n!}\, \frac{1}{(1 + n\frac{\bar{z}}{z})^3}\, \frac{1}{R^n}\, e^{z_{n+2}\, t} \cdot \left(\frac{t_n}{t_0} + \frac{t}{t_0}\right), \tag{E.10}$$

where R is the same quantity defined in Section III*. Examination of (E.10) reveals that the sum diverges unless $R > 4$. This is the same condition, (III.15), which must be satisfied in order that series (III.12) converge. The physical meaning of this condition is discussed in Section VI.

---

* As a check for (E.10) we might set $z_1 = z_2 = \bar{z} = z$, take $a = 1$ and $\bar{\Gamma} = \Gamma$, let $t_0 \to \infty$, and remove the minus sign which arises because the ω has negative signature. We also remove the factor $(n + 1)$ which distinguishes (III.10) from (III.9). Under these conditions, one can show from (E.8) that $t_n/t_0 = (n + 1)^2$ and, from (E.9), $z_{n+2} = z/(n+1)$. These changes turn the ω-pole into a Pomeranchon so that we would expect to recover (III.12), and indeed we do!

The real parts corresponding to the terms in (E.10) may be found by a procedure similar to that in (D.1) - (D.5). We end this discussion with one further remark. The first several terms in this series were found to be the largest for the parameters used in the data fitting attempts described in Section VI. These first several terms have the same behavior as the ω-pole term, i.e., they change sign near $t \approx -0.15$. We took $t_0 = 0.15$ and succeeding values of t_n were typically: 0.152, 0.118, 0.049, -0.055, -0.195, -0.371, -0.582, and so forth, monotonically down to, say, $t_{30} \approx -15.25$. All terms with $t_n < 0$ do not have the sign change as a function of t. They oppose the pole contribution for $|t| < 0.15$ BeV^2 and support it for $|t| > 0.15$ BeV^2.

REFERENCES

1. D. Amati, A. Stanghellini, and S. Fubini, Nuovo Cimento 26, 897 (1962).
2. S. Mandelstam, Nuovo Cimento, 30, 1127 and 1148 (1963).
3. J.C. Polkinghorne, J. Math. Phys. 4, 1396 (1963).
4. J.C. Polkinghorne, J. Math. Phys. 4, 503 (1963).
5. B. Lee and R. Sawyer, Phys. Rev. 127, 2266 (1962).
6. V.N. Gribov, I. Ya. Pomeranchuk, Phys. Letters 2, 239 (1962).
7. M. Froissart, Phys. Rev. 123, 1053 (1961).
8. I.R. Gatland and J.W. Moffat, Phys. Rev. 129, 2812 (1963) and 132, 442 (1963).
9. P.G.O. Freund and R. Oehme, Phys. Rev. Letters 10, 450 (1963).
10. A. Stanghellini, report delivered at the Siena Conference (Oct. 1963).
11. K. Igi, Phys. Rev. 113, 820 (1963); also S.D. Drell, Rapporteur's talk to the 11th International High-Energy Physics Conference at CERN (1962).
12. K. Igi and V.L. Teplitz, Phys. Letters 6, 73 (1963).
13. T. Regge, Nuovo Cimento 14, 951 (1959); 18 947 (1960); also A. Bottino, A. Longoni and T. Regge, Nuovo Cimento 23, 954 (1962).
14. A. Pignotti, Phys. Rev. Letters 10, 416 (1963).
15. D. Amati, M. Cini, and A. Stanghellini, Phys. Letters 4, 270 (1963), and Nuovo Cimento 30, 193 (1963).
16. K.J. Foley, S.J. Lindenbaum, W.A. Love, S. Ozaki, J.J. Russell and L.C.L. Yuan, Phys. Rev. Letters 11, 425 and 503 (1963).
17. T. Binford and B. Desai, Phys. Rev. 138 , B1167 (1965).
18. R. Serber, Phys. Rev. Letters 10, 357 (1963).
19. W. Rarita and V.L. Teplitz, Phys. Rev. Letters 12, 206 (1964).
20. B. Desai, Phys. Rev. 138, B1167 (1965).

21. For example, refer to any of the Regge pole fits, such as that of Reference 17.

22. S.C. Frautschi, M. Gell-Mann and F. Zachariasen, Phys. Rev. 126, 2204 (1962);
V.N. Gribov and I. Pomeranchuk, Phys. Rev. Letters 8, 343, 412 (1962).
See also Reference 23.

23. W.G. Wagner and D.H. Sharp, Phys. Rev. 128, 2899 (1962).

24. M. Gell-Mann, Phys. Rev. Letters 8, 263 (1962); also
V.N. Gribov and I. Pomeranchuk, Phys. Rev. Letters 8, 343, 412 (1962).

25. L. Van Hove, Phys. Letters 5, 252 (1963).

26. L. Bertocchi, S. Fubini and M. Tonin, Nuovo Cimento 25, 626 (1962).

27. F. Hadjioannow, R.J.N. Phillips and W. Rarita, Phys. Rev. Letters 9, 183 (1963).

28. A. Ahmadzadeh and I.A. Sakmar, Phys. Rev. Letters 11, 439 (1963).

29. D.H. Sharp and W.G. Wagner, Phys. Rev. 131, 2226 (1963).

30. M. Jacob and G.C. Wick, Ann. Phys. 7, 404 (1959).